CubeSat Development for Identification of Space Debris

A Major Qualifying Project Report

Submitted to the Faculty of the

WORCESTER POLYTECHNIC INSTITUTE

in Partial Fulfillment of the Requirements for the

Degree of Bachelor of Science

in Aerospace Engineering

by

Dev Gujarathi

Kaitlyn Smith

Ben Workinger

March 24th, 2023

Approved by: ________________________

Zachary R. Taillefer, Advisor

Assistant Teaching Professor, Aerospace Engineering Program

WPI

Abstract

This project presents the design and analysis of a 12U CubeSat that could be used to detect orbital debris. The CubeSat has a 700 km sun-synchronous orbit and 98.19° inclination with the Collapsible Space Telescope as the payload. The mechanical subsystem analyzed the structure and layout of the satellite, managing the volume and mass constraints. Analysis was also done for equal weight distribution. The propulsion subsystem selected Busek's BGT-X5 thruster for the mission. Orbital analysis was done to understand the lifetime of the system and analyze station-keeping maneuvers. The power subsystem managed the power budget of each subsystem, ensuring solar panels and batteries would generate enough power for the components. This report also discusses an ADC Testbed and work done to it.

Acknowledgements

We would like to thank the following individuals and groups for their help and support throughout the duration of this project. Our primary and secondary advisors, Professors Taillefer, Gatsonis, and Demetriou have been instrumental in the success of this MQP. We would also like to thank the significant support received from Dr. Adriana Hera in training us in the proper use of the ANSYS and COMSOL software. Finally, we appreciate the IT support provided by Ed Burnham in regard to the low friction table and Helmholtz cage.

Table of Authorship

Section Title	Authors (initials, if applicable)
1. Introduction	All
2. Mission Payload	BW
3. Mechanical Subsystem Analysis and Design	BW
4. Propulsion Subsystem Analysis and Design	DG
5. Power Subsystem Analysis and Design	KS
6. ADC Testbed	ALL
7. Conclusions and Social Impacts	KS, DG

Table of Contents

List of Figures

List of Tables

1. Introduction

Humanity is on the verge of becoming a space-faring civilization, however every year of progression results in the creation of new debris added to the space environment. Orbital debris is considered as any man-made object in orbit around the Earth that no longer serves a useful purpose such as old separation rings, defunct spacecraft, and scrap metal. An increasing number of objects in geocentric orbit inherently increases the probability of collisions with other Resident Space Objects (RSOs), leading to the creation of more debris. As humans populate the space around earth the risk of a cascade event increases. If this cascade begins, Earth will be surrounded by a shell of debris preventing any type of further space endeavors. This phenomenon is known as Kessler Syndrome [1]. To prevent the Kessler Syndrome from becoming a reality, orbital debris identification and tracking is of the utmost importance. As of January 2022, the National Aeronautics and Space Administration (NASA) actively tracks more than 25,000 pieces of orbital debris with diameters greater than 10 cm. However, the population of debris is inversely proportional to the diameter. It is estimated that there are 500,000 pieces of debris with a diameter between 1 to 10 cm and over 100 million pieces of debris smaller than 1mm [2]. Fortunately, RSOs and debris of diameter 10 cm or greater are actively tracked by ground stations using either radar-based or optical systems [3] and most collisions with debris smaller than 1mm can be mitigated through shielding practices [4]. Therefore, the population of RSOs of greatest concern is that of a diameter between 1 and 10 cm as these objects are large enough to cause considerable damage, yet too small to be accurately tracked from the ground [5]. It is evident that a space-based observing system is best suited for tracking this sized RSO.

Like ground-based systems, space-based observing systems take one of two forms: optical systems and radar-based systems [7]. Spaceborne radar systems come at the cost of large power requirements and low measurement precision from low-frequency band operation [10]. This, coupled with the fact that space-based optical imaging systems have seen success in the past, makes an optical imaging system worthy of research for debris detection missions.

Since their first launch in 2003, CubeSats have been gaining popularity for scientific space missions. Due to their small size and weight, these satellites have become a low-cost option for demonstrating new technologies, carrying out scientific studies, and as imaging system platforms.

This Major Qualifying Project (MQP) details the structure, propulsion, and power subsystems of a 12 Unit volume (henceforth denoted as 12U) small form satellite, commonly referred to as CubeSat [11]. The team will be working on both the CubeSat and the testbed with two other MQP teams. The CubeSat designed by this team will be referred to as the Orbital Debris Detection Satellite, or ODDSat. These teams will oversee the attitude determination and controls subsystem, guidance and navigation, telemetry and communications, space environments mitigation, and thermal control subsystems.

1.1 Background and Literature Review

In 1999, two professors at the California Polytechnic State University and a professor from Stanford University wanted to give students the opportunity to gain engineering experience working on satellites. The initial CubeSat configuration consisted of a 10cm cube, known as 1U, that had a maximum mass of 1.33 kg [13]. To accommodate missions that require more volume or mass, further configurations based on the initial 1U satellite were developed. These standard configurations include 1U, 2U, 3U, 6U, 12U, and 27U. Because of their small size and low mass, CubeSats could be deployed as secondary payloads for a fraction of the cost for a dedicated launch.

Cost was further reduced by the introduction of standardized deployment methods made possible by the predefined CubeSat size and weight limits.

In 2010, NASA embraced the CubeSat program by starting the CubeSat Launch Initiative. This program allows U.S. institutions and educational non-profits low-cost access to space by providing rideshare opportunities on most launches. Since 2010, NASA has selected over 200 CubeSat missions, 140 of which have been launched [13]. In addition to NASA, private companies such as SpaceX and Rocket Lab also provide rideshare options for CubeSats.

The first MQP involving designs of a CubeSat took place in the year 2010. The design revolved around a 3U CubeSat carrying a Sphinx-NG X-Ray spectrometer as a collaboration effort between WPI, NASA, and the Polish Space Research Center. The design behind this CubeSat involved multiple years of projects as an iterative process to develop more sophisticated hardware and control methods. This project ended in 2017 with a refined parts list and a comprehensive list of algorithms and simulations for the utilization of a spectrometer on a satellite [14].

Further MQP feasibility studies on CubeSats involved the utilization of a Micro Pulsed Plasma Thruster (μPPT) on a 3U CubeSat, which outlined methods for controlling a satellite utilizing this propulsion method and conventional CubeSat control systems [18]. The next two years of projects on CubeSats involved extreme Low Earth Orbit (eLEO) missions which utilized a 4U CubeSat at an approximate 210 km altitude paired with a 16U CubeSat at an approximate 500 km altitude in a formation flight to study high altitude atmospheric parameters [19]. The latest project was the development of a 6U CubeSat to deliver a small form factor Ion Neutral Mass Spectrometer (INMS) payload to survey the ionosphere in an elliptical orbit with a perigee of 180 km. This CubeSat, named Appleton, was developed over two projects which generated a comprehensive analysis of the controls, guidance, and communications systems along with their challenges. The last project in this endeavor was also accompanied by a parts list of modern CubeSat components, many of which were utilized in this project [21].

1.2 Project Goals

- Design and analyze the base model of a 12U CubeSat for use in an orbital debris detection constellation. The CubeSat will operate at an altitude of 700-800 km and carry the Collapsible Space Telescope (CST) developed by NASA AMES [24] to optically monitor a range of altitudes from 800-850 km where orbital debris is most prevalent
- Continue previous MQP efforts to build and test an ADC testbed, using a Helmholtz cage and a low-friction air bearing table. This testbed will create a dynamic magnetic field that replicates Earth’s magnetic environment, in which the performance of the CubeSats magnetorquers can be tested

1.3 Mission Design Requirements, Constraints, and Considerations

1.3.1 Requirements

Payload

- Payload should have the ability to detect 1 cm objects up to a range of 1200 km
- Payload should always point away from the sun to reduce the collection of stray light and to minimize the phase angle between debris and sun
- At 1,200 km, the relative velocity between debris and spacecraft shall not exceed 11.5 km/s

Mechanical

- Must interface with deployment mechanism without exceeding weight and volume allowances
- Structure must withstand launch and vibration loads
- No debris can be generated by the CubeSat during deployment or operation

Power

- Must provide enough power for subsystem needs throughout mission duration
- Spacecraft shall be powered from onboard solar cells and batteries
- Power shall be reserved for end-of-life deorbiting
- No electronics shall be active during launch
- Solar panels must generate ~2x the nominal requirement for risk mitigation and deorbit
- Battery packs must provide enough power to support mission during detumbling and eclipse periods

Propulsion

- The propulsion subsystem must be able to counteract orbital perturbations to extend mission duration
- The propulsion subsystem is responsible for de-orbiting the spacecraft within the required time

ADC

- Subsystem must counteract orbital perturbations caused by atmospheric drag, magnetic field, and thrust vector misalignment.
- The spacecraft must achieve a pointing accuracy of payload and communications with a maximum error of 0.5 degrees.

- The CubeSat must be able to detumble from initial angular velocities due to ejection from the launch vehicle without reaction wheel saturation and within time constraints set by the power system.

Telemetry and Comms

- Subsystem must be able to fully receive command uplink
- Subsystem shall have the ability to fully transfer scientific data during downlink
- Subsystem must be able to communicate with its satellite group during crosslink

Space Environments

- Spacecraft shall be designed to operate for mission duration considering electromagnetic conditions at operational altitudes
- Spacecraft shall be designed to operate for mission duration in expected radiation conditions at operational altitudes
- Spacecraft shall be designed to operate for mission duration considering the micrometeorite and orbital debris concentrations at operational altitudes

Thermal

- Spacecraft must be able to operate in an ambient and self-induced thermal environment
- Thermal design shall provide temperatures within survivability and operating range of components

1.3.2 Constraints

Mechanical

- Anodized aluminum tabs shall run the entire length of the spacecraft

- Tabs must be an aluminum alloy with a minimum yield strength of 56ksi and a maximum surface roughness of N7
- No holes or protruding features may exist along the tabs
- Tabs must conform to the dimensions provided by the CSD datasheet
- The face that contacts the CSD ejection plate must be a uniform surface or discrete contact points and envelope the center of mass
- CubeSat must remain within a maximum dynamic volume provided by the CSD
- The center of mass must remain within a defined rectangular area provided by the CSD datasheet
- Static and dynamic loads applied to the tabs must not be greater than 3559 Newtons
- Deformation due to launch vibrations must be analyzed using the provided vibration spectrum
- Structural deformation cannot exceed the CSD dynamic volume

Power

- Solar panel size cannot exceed 3U $\times$ 2U due to surface area constraints
- Solar panels must fold on the $\pm y$ faces so the other faces are open for launch vehicle connection

Propulsion

- The propulsion system should be able to provide the necessary ΔV, I_{sp}, and T set forth by the orbital and mission requirements
- The propulsion system should be able to operate under limitations set by the power and mechanical subsystems

ADC

- The spacecraft must be able to detumble from ~15 deg/s angular velocities over ~1-2 orbit time span without reaction wheel saturation or excessive power draw
- The control law development for the spacecraft must allow for a pointing accuracy of 0.5 degrees while accommodating for reaction wheel limitations of 0.1 Nm-s of momentum and 0.07 Nm of torque
- Noise in measurements and torquers must be accounted for by an Extended Kalman Filter, see the components list for noise amounts

Telemetry and Comms

- The antenna shall be able to receive S-Band Radio Frequencies.
- The receiver shall be able to uplink GPS and ADC data
- The transmitter shall be able to downlink pictures collected from the payload of approximately 10 Mbps
- The onboard computer shall be able to connect each of the subsystems, as well as process and store images captured by the payload

Space Environments

- The minimum thickness of the aluminum shell and the aluminized mylar must be at least 1.27 cm or 50 mils thick to prevent radiation damage to the internal components

Thermal

- The components most sensitive to temperature must be kept in the most temperate areas of the spacecraft

1.3.3 Optimal Orbit

The orbit will be a sun-synchronous one so that the satellite is in sunlight for the majority of the orbit. This maximizes power generation from the solar panels. To continue optimizing the power generation, the solar panels face directly against the sun vector at optimal orbit, resulting in an incidence angle of 0^o. The payload focuses in the opposite direction away from the sun and has a range of around 1200 km. The highest concentration of orbital debris occurs at an altitude of ~800 km, so to optimize the number of objects in the payload's field of view, the CubeSat will remain at a constant altitude of 700km. Since the highest concentration of debris also exists around the North and South Poles, the optimal orbit for the payload's field of view occurs when the power generation is not optimal.

1.4 Project Management and System Engineering

For this project, the following subsystems were held:

1. Mechanical Design and Structures (Ben Workinger)
2. Propulsion (Dev Gujarathi)
3. Power (Kaitlyn Smith)
4. Thermal (Ben Brady)
5. Space Environments (Ryan Weeks)
6. Telemetry and Communications (Matt Liliedahl)
7. Attitude Determination (Di Abdimash)
8. Attitude Control (Connor Moriarty)

Bi-weekly meetings were held in person to facilitate communication between the subsystems. Furthermore, the team used Slack to communicate outside of meetings. Ben Workinger, Ben

Brady, and Connor Moriarty acted as team leads, while Dev Gujarathi was the purchasing liaison. Ben Brady was the Air Bearing Table Lead and Cage Development was led by Matt Liliedahl and Dev Gujarathi.

1.5 Launch Vehicle

The Rocket Lab Electron Rocket was chosen as the launch vehicle for this mission. The Electron uses it has the capability to go directly to a sun-synchronous orbit from 400 to 1200 km as shown in Figure 1. This will allow ODDSat to share the inclination of the desired orbit, with a value of 98.1929°. With this capability, the CubeSat can eject into the 700 km parking orbit without the need for an orbit raising maneuver to get to a higher altitude. Furthermore, the Electron has over 30 launches to date with over 150 satellites successfully deployed, making it a reliable choice to be the launch vehicle for this mission [23].

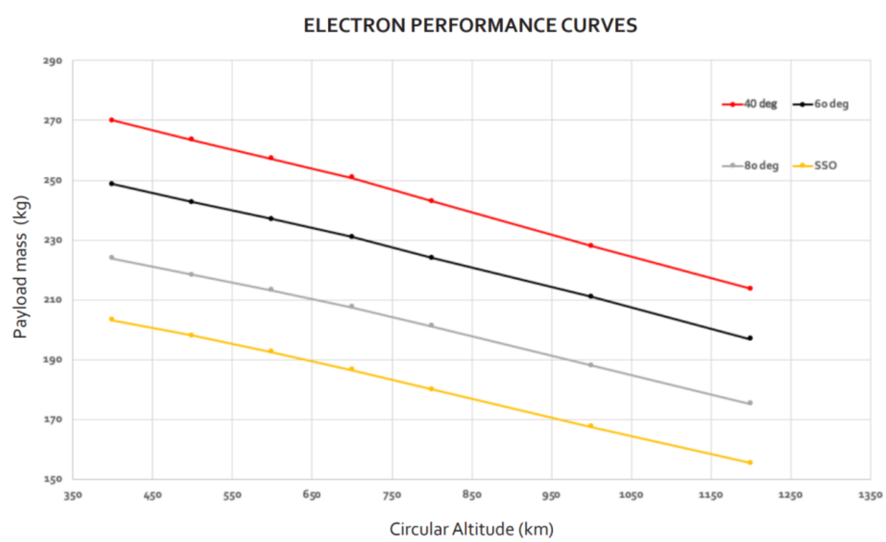

Figure 1: Electron performance curves at various inclinations [23]

2. Mission Payload

2.1 Payload Overview

Detecting and tracking orbital debris is a task that has been almost completely done from earth. The primary method of detection for ground-based systems is by using a large radar. However, due to power and size constraints, this is not a feasible solution for a CubeSat. The second method of detecting orbital debris is by taking one or more exposures using an optical sensor. Streaks in the images, left by debris, can be analyzed to find the right ascension and declination of the object at its initial and final location. This data can be packaged as a tracklet and sent to a third party such as the Unified Data Library, who will match the tracklet with similar detections and attempt to create an orbital estimate of the object. While not as power intensive, an optical system can still occupy a large amount of space. Fortunately, NASA's AMES research center did initial research and development of a CubeSat-mountable collapsible telescope called the Collapsible Space Telescope (CST).

2.2 Collapsible Space Telescope

The CST is a low Technology Readiness Level (TRL) optical system developed by NASA for use on a 6U CubeSat. In its stowed configuration, the CST occupies a 20 cm × 20 cm × 10 cm volume and weighs 1.6 kg. With a focal length of 1250 mm and an aperture of 152 mm, this telescope's field of view is about 1.6 degrees × 1.1 degrees [24]. Due to the low TRL of the CST, very little information regarding the deployment of the telescope is available.

The performance of the telescope is dependent on the brightness of the target and the limiting magnitude of the telescope. The apparent magnitude of the target m_v can be calculated using Eq. (1), where A is the cross-sectional area in cm^2, ρ is the albedo coefficient, φ is the phase angle in degrees, and r is the distance from the object to the observer [25]. Because ODDSat faces opposition during operation, it can be assumed that the phase angle is zero. Albedo for space debris ranges from 0.01 to 0.18 [26], so to be conservative, a value of 0.1 was assumed.

$$m_v = -26.7 - 2.5\, log\left(A\rho\left(\frac{2}{3\pi^2}\right)\left((\pi - \varphi) + sin(\varphi)\right)\right) + 5log(r) \quad (1)$$

The limiting magnitude, V, of the CST can be roughly calculated to be 12.7 using Eq. (2), where D is the aperture diameter in inches [27].

$$V = 8.8 + 5log(D) \quad (2)$$

Substituting the limiting magnitude for the magnitude of the target results in a relationship between debris diameter and maximum range. At the minimum range of 500 km, the CST can detect objects as small as 5.13 cm in diameter and at the maximum range of 1400 km, the CST can detect objects as small as 14.4 cm.

3. Mechanical Subsystem Analysis and Design

This chapter reviews the mechanical design ODDSat, as well as the analysis performed to test the CubeSat's compliance with the design requirements and constraints.

3.1 Overview

The mechanical subsystem is responsible for the structural design and layout of ODDSat, making sure that the CubeSat complies with all requirements set forth by the launch vehicle and deployment system . Many of these requirements are physical limitations or design features such as maximum spacecraft size, center of mass positioning, and mounting tab dimensions. These requirements can be verified using the SolidWorks model. Other requirements, such as finding the maximum deflection of the structure, require further analysis and were conducted using ANSYS software. Off-the-shelf components were assumed to be qualified for launch to simplify the model and allow the focus of the analysis to be on the structure.

3.2 Mechanical Subsystem Requirements

The requirements for the mechanical subsystem have been broken down into three subsections: mechanical features, volume and mass properties, and structural limits. These requirements come from the Canisterized Satellite Dispenser (CSD), which is shown in Figure 2, as well as components from other subsystems.

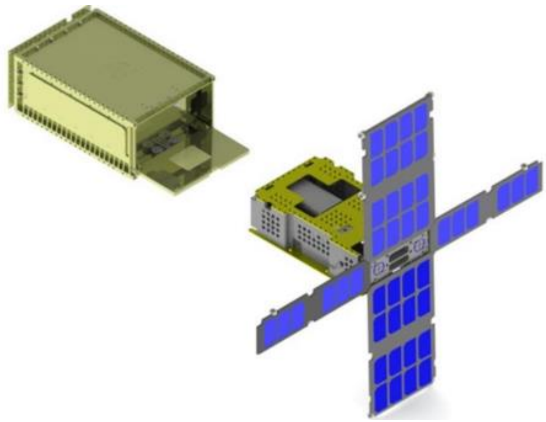

Figure 2: A 6U Canisterized Satellite Dispenser deploying a CubeSat [25]

- **Mechanical Features**
  - Anodized aluminum tabs shall run the entire length of the spacecraft
  - Tabs must be an aluminum alloy with a minimum yield strength of 56ksi and a maximum surface roughness of N7
  - No holes or protruding features may exist along the tabs
  - Tabs must conform to the dimensions provided by the CSD datasheet
  - The face that contacts the CSD ejection plate $(-Z)$ must be a uniform surface or discrete contact points and envelope the center of mass
  - All deployables must be verified with the CSD before flight
  - No debris can be generated by the CubeSat during deployment or operation
- **Volume and Mass Properties**
  - CubeSat must remain within a maximum dynamic volume provided by the CSD
  - The center of mass must remain within a defined rectangular area provided by the CSD datasheet
- **Structural Limits**
  - Static and dynamic loads applied to the tabs must not be greater than 3559 Newtons

    - Deformation due to launch vibrations must be analyzed using the provided vibration spectrum
    - Structural deformation cannot exceed the CSD dynamic volume
    - Modal analysis must be performed to identify dominant modes between 20 Hz and 2000 Hz
- **Component Requirements**
    - Sun sensors must be mounted with an unobstructed view of space on each of the six sides of the spacecraft
    - Reaction wheels must be positioned along each axis that passes through the center of mass of the spacecraft
    - The rate gyro, accelerometer, and magnetorquer must be located at the center of mass of the spacecraft
    - The laser transmitter must have an unobstructed view of space during operations
    - The thrust vector must pass through the center of mass

3.3 Canisterized Satellite Dispenser (CSD)

The CSD was originally designed by Planetary Systems Corp. and is now owned by Rocket Labs. This system offers a unique deployment method for 3U, 6U, and 12U satellites. The design features two clamps that run the length of the spacecraft's Z axis. When the deployment door is closed, these clamps apply pressure to mounting tabs on the CubeSat and ensure that it remains fixed inside the deployment unit. Per the requirements of the CSD, the total load on the tabs cannot exceed 3559 Newtons. When the deployment door on the CSD opens, an ejection plate pushes on the back panel ($-Z$ face) of the CubeSat to provide an even force which reduces tumbling from deployment. While inside the canister, the CubeSat must stay within a designated volume of 239 × 239 × 366 mm considering any thermal changes and vibrations that accompany the launch. Contact zones are available for deployable systems along the four faces that run perpendicular to the deployment plate ($\pm X$ and Y faces). Mechanisms such as roller bearings that contact these provided zones are allowed [28].

3.4 Structural Design

Although many CubeSat missions adapt off-the-shelf structures to meet their requirements, this option was unfeasible for ODDSat due to the size of the payload. Instead, the payload was incorporated into the structure by using the payload base as the $+Z$ structural element. Due to the low TRL level, the actual structural strength of the payload base is unknown and may require modifications to be used in this manner. The remaining structure was designed around the CSD requirements. Figure 3 shows the maximum dynamic volume compared to the size of the CubeSat.

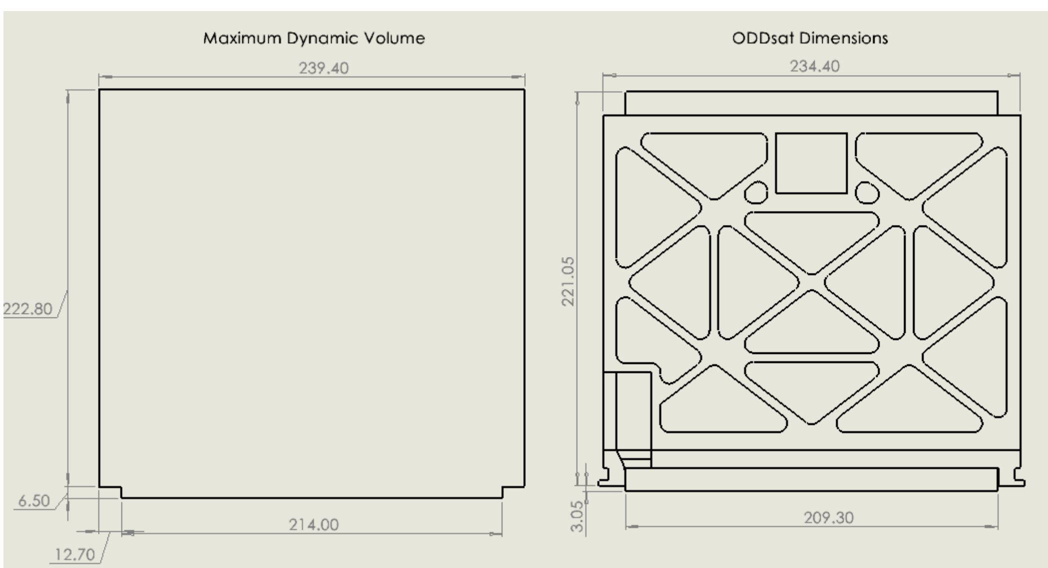

Figure 3: Comparison of the maximum dynamic volume and CubeSat dimensions.

The minimum difference between the CubeSat volume and the maximum dynamic volume is 1.75mm in the Y direction while static. Figure 3 also shows the contact surface that is pressed against the CSD ejection plate during deployment. The surface is flat to prevent uneven loading, with cutouts for the electrical interface and fine sun sensor.

Another mechanical feature visible in Figure 3 are the CSD mounting tabs that run the entire length of the spacecraft's Z axis. For proper securement of the CubeSat during launch, these tabs must be designed and manufactured based on dimensions provided by the CSD datasheet. Figure 4 shows a comparison between the provided dimensions and the modeled tabs.

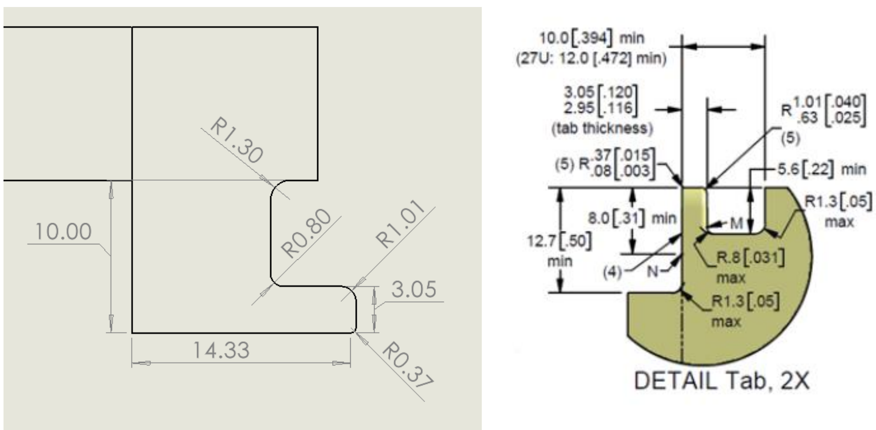

Figure 4: ODDSat's mounting tabs compared to the CSD dimensions [25].

To improve rigidity of the spacecraft, these tabs are manufactured as part of the bottom support plate and provide a recessed area for one of the solar arrays in the stowed configuration. Unlike the other support panels, the tab panel does not have any lightweighting cutout with the only through feature being for the laser transmitter.

3.4 Internal Layout

The internal layout of the spacecraft was dictated by individual component requirements and center of mass. As shown in Table 1, the heaviest components are the payload, propellant tanks, batteries, and solar panels.

Table 1: Mass Breakdown of Components

Component	**Total Mass (kg)**
Transceiver	0.19
Laser TXRX	0.40
Reaction Wheel (3)	0.99
Magnetorquer	0.20
Payload	1.60
Ops Battery (3)	2.45
EPS	0.14
Solar Array (2)	2.03
Detumbling Battery	0.46
Structure	3.39
Thruster	1.50
Propellant Tank (4)	5.00
Components < 0.1 kg	0.15

For ODDSat to maneuver correctly, the reaction wheels must be located precisely along one of the axes passing through the center of mass both before and after deployment. Similarly, the center of mass must be located along the vector of thrust after the detumbling process. To achieve these strict requirements, the ODDSat relies upon multiple design features seen in Figure 5.

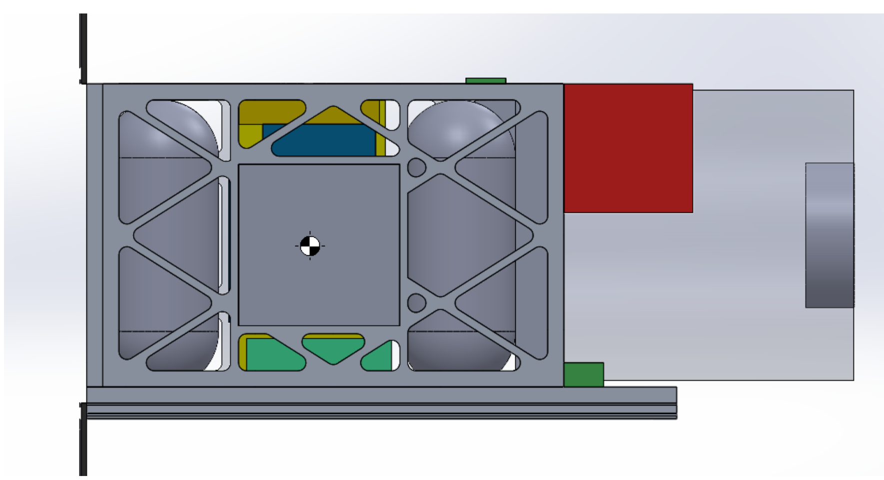

Figure 5: ODDSat in the deployed configuration, showing the center of mass.

First, the solar arrays and telescope were positioned to mitigate center of mass movement between stowed and deployed configuration. Large, heavy components such as the EPS system were placed in line with the thruster forming a central component block, further cementing the center of mass location. Finally, the four propellant tanks are spaced symmetrically around the central component block. This allows for adjustments in the center of mass around the X and Z axis, simply by using propellant. Another benefit of the central component block is that the layout naturally increases the structural integrity by connecting the center of the $\pm X$ and Y panels.

3.5 Mechanical Analysis

Throughout the project, modal and random vibration analysis were performed using ANSYS to see how the spacecraft structure would respond to launch vibrations. Per CSD requirements, all modes between 20-2000 Hz must be identified, structural deformation must not exceed the maximum dynamic volume, and the resultant static load and random vibration load must not exceed 3559N [28]. Before analysis was run, the CAD model was simplified. Small, low mass components such as the rate gyro, accelerometer, and course sun sensors were removed. Because the analysis is done on the stowed configuration, each set of solar panels was combined into a single mass/volume part. Once imported into ANSYS, each component's properties were redefined using custom Engineering Data entries. Each entry was created based on the mass and density of the respective part. The first analysis was performed to determine the frequencies at which the structure and components had compounding responses. Modal analysis revealed a total of eight modes ranging from 872.95 Hz to 1978 Hz as shown in Figure 6.

	Mode	Frequency [Hz]
1	1.	872.95
2	2.	938.95
3	3.	1098.3
4	4.	1241.5
5	5.	1578.1
6	6.	1728.7
7	7.	1759.6
8	8.	1923.

Figure 6: ODDSat mode frequencies

These modes were then used as an input for a random vibration analysis along with a power spectral density, provided by the CSD datasheet. The power spectral density describes the expected intensity of vibration at each frequency during launch, which allows for the calculation of deformation of the structure, as well as load on the CSD mounting tabs. Table 2 shows the resulting tab load and maximum X, Y, and Z deformation as random vibrations are applied along each axis of the model. In all three directions of vibration, the tab loading never exceeds the 3556N limit given by the CSD. The maximum deformation is also within the 1.75mm tolerance between the structure and the maximum dynamic volume envelope.

Table 2: Mechanical Analysis Results

Vibration Direction	Tab Loading (N)	X Deformation (mm)	Y Deformation (mm)	Z Deformation (mm)
X	1169	0.107	0.018	0.113
Y	2280	0.023	0.031	0.027
Z	3406	0.148	0.032	0.142

Furthermore, by looking closer at the ANSYS results for vibration in the Z direction as shown in Figure 7, the most deformed part is internal rather than the structure itself. These results show that the structural concept of ODDSat is valid, and that further development is feasible.

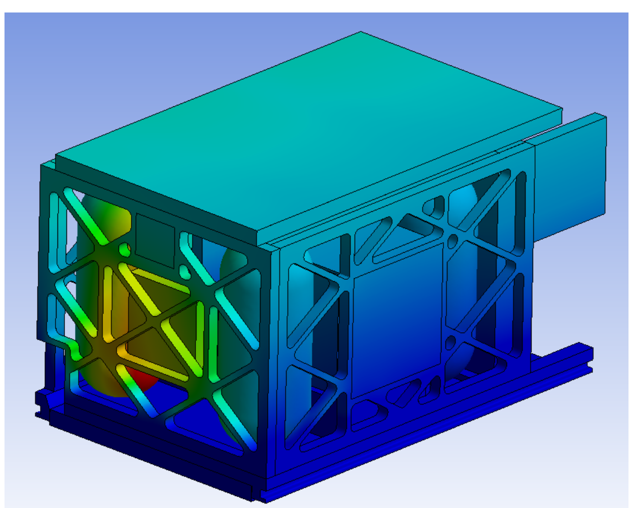

Figure 7: ANSYS simulation results for deformation when vibration is applied on the Z axis

4. Propulsion Subsystem Analysis and Design

The purpose of this chapter is to present information regarding the propulsion system for this MQP. The discussion will be focused on the design and analysis of the orbital maneuvers used for mission design, as well as a preliminary propulsion system selection process.

4.1 Propulsion Overview

The propulsion system is responsible for all orbital maneuvers and orbital maintenance required for the duration of the mission. The propulsion system must provide the necessary thrust and ΔV required for each orbital maneuver. In general, there are two types of thrusters commonly used on spacecraft, primary and secondary, for different classes of maneuvers. Primary thrusters are used for orbital maneuvers that require higher magnitude ΔV's. Secondary thrusters are used to reorient the spacecraft in the desired heading as determined by the mission requirements. Due to volume and mass constraints set forth by the power and mechanical subsystems, it was determined that a primary thruster would be the only source of propulsion for this mission. A magnetorquer is also being used for attitude control and reaction wheels are used for detumbling, further eliminating the need for a secondary thruster. Initial research was done to determine the different types of orbital maneuvers that may be needed throughout the duration of the mission. Once the required orbital maneuvers were determined, a thruster trade study was performed to refine a list of several thrusters that could be used for the mission.

4.2 Thruster Trade Study

Several different thrusters were considered for the propulsion system for the ODDSat. Any thruster considered had to be compact and low in total mass in order to fit the requirements set forth by the mechanical system. To fit the requirements of the power subsystem, the thruster should have a bus power requirement that is as low as possible.

The first thruster considered was the Scalable ion Electrospray Propulsion System (SiEPS) produced by MIT. One of the benefits of this system is its modular capability, allowing for it to be scaled according to the mission requirements. The specifications of the SiEPS thruster are presented in Table 3.

Table 3: SiEPS thruster characteristics [29]

Nominal Thrust	74 μN
Specific Impulse	1150 s
System Power	1.5 W
System Volume	9 × 9.6 × 2.1 cm

The second thruster considered was the BET-1mN produced by Busek Co. Inc. One benefit of this thruster is its ability to have a customizable tank. The specifications of the BET-1mN thruster are presented in Table 4.

Table 4: BET-1mN thruster characteristics [29]

Nominal Thrust	0.7 mN
Specific Impulse	800 s
System Power	15 W
System Volume	8.5 × 8.5 × 6 cm

Both the SiEPS and BET-1mN thrusters are examples of electrospray thrusters. Electrospray thrusters are a form of electric propulsion in which an electrostatic field is applied to the surface of an ionic liquid propellant, which in turn accelerates droplets or ions of the propellant. Field emission electric propulsion (FEEP) thrusters such as the SiEPS rely on ion emission to generate thrust, whereas colloid thrusters such as the BET-1mN rely on droplet emission through a Taylor cone to generate thrust [29]. Electrospray thrusters have high specific impulse specifications and relatively low thrust specifications, making them perfect for fine attitude control or for primary propulsion for nanosatellites, such as CubeSats [30].

The third thruster and the only chemical propulsion system considered was the BGT-X5, also produced by Busek Co. Inc. This monopropellant thruster uses a more environmentally friendly propellant compared to the more commonly used hydrazine, allows for start-stop procedures, and supports customized tanks. Monopropellant thrusters are a type of chemical propulsion systems in which chemical energy stored within the propellant is used to propel the spacecraft. As the propellant burns, molecular bonds break and release energy in the form of heat. The products of the reaction are then accelerated through a nozzle to produce thrust [30]. Monopropellant thrusters are simple since they contain the oxidizing agent and combustible matter in a single substance. Monopropellants decompose and yield combustion gases either when heated or catalyzed in a catalyst bed [31]. Green monopropellants, such as the one used in the BGT-X5, offer higher density, thrust, and performance as opposed to hydrazine [29]. The specifications of the BGT-X5 thruster are presented in Table 5.

Table 5: BGT-X5 thruster characteristics [32]

Nominal Thrust	0.5 N
Specific Impulse	225 s
System Power	20 W
System Volume	10 × 10 × 10 cm

ThrustMe's NPT-30 I2 Smart Iodine Electric Propulsion System was also considered as a possible option. Like the SiEPS system, the NPT-30 I2 also has a modular design which is useful in terms of scaling the propulsion system. The NPT-30 I2 thruster is an example of an ion engine, which adds or removes electrons from easily ionized and high atomic mass propellants. This results in positively charged ions, which are then accelerated out of the thruster in a beam along with an equal amount of electrons, to produce thrust that has a total neutral charge [33]. Table 6 presents the specifications of the NPT-30 I2 thruster.

Table 6: NPT-30 I2 thruster characteristics [34]

Nominal Thrust	1.1 mN
Specific Impulse	2400 s
System Power	65 W
System Volume	9.6 × 9.6 × 11.3 cm

The last thruster considered was the Busek BHT-100 Hall Thruster. This thruster has a high thrust, allowing for the capability to perform maneuvers requiring a high ΔV. The BHT-100 thruster is an example of a Hall thruster. Hall thrusters use electrons circulating in a Hall current channel and eventually ionize the propellant, creating ionized plasma. This plasma is then accelerated by the electric field created by the electrons to exhaust velocities up to 65,000 miles per hour, producing thrust [35]. Table 7 presents the specifications of the Busek BHT-100 Hall Thruster.

Table 7: Busek BHT-100 Hall Thruster characteristics [37]

Nominal Thrust	7.0 mN
Specific Impulse	1000 s
System Power	100 W
System Diameter	8.0 cm
System Length	5.5 cm

4.3 Initial Thruster Analysis and Propulsion System Selection

To determine what thruster would be used as the primary propulsion system for the ODDSat, initial estimates were made using a combination of the MATLAB script in Appendix A and STK's Lifetime Tool. These estimates would help to understand the capabilities and performance of each thruster. The MATLAB script uses the initial and final altitudes and models a Hohmann transfer between the two to determine the total ΔV required for the Hohmann transfer. Once the ΔV was found, it can be plugged in to the Rocket Equation:

$$\Delta V = -gI_{sp}\, ln\left(\frac{m_f}{m_i}\right) \tag{3}$$

where ΔV is the required change in velocity during a burn in meters per second, m_f the final mass of the ODDSat after the burn in kilograms, m_i is the initial mass of the ODDSat before the burn in kilograms, and g is the acceleration of gravity. The I_{sp} is given by the manufacturer of the thruster. From Eq. (3), the mass of propellant consumed per burn can be found using:

$$m_p = \left(1 - \frac{m_f}{m_i}\right) m_i \tag{4}$$

where m_p is the mass of propellant consumed per burn in kilograms. For the initial thruster analysis, an initial mass of 24 kg, which is the maximum allowable mass for a 12U CubeSat, was assumed.

The burn time required for each maneuver can be found using:

$$t_b = \frac{m_p g I_{sp}}{T} \tag{5}$$

where t_b is the burn time per maneuver in seconds and T is the thrust of each thruster in Newtons.

However, in the case of low-thrust thrusters such as the electric propulsion systems above, the Edelbaum equation must be used to determine the ΔV needed to follow a spiral trajectory between the two orbit altitudes:

$$\Delta V = \sqrt{V_i^2 + V_f^2 - 2V_iV_f \cos\left(\frac{\pi}{2}\Delta i\right)} \tag{6}$$

where ΔV is the required change in velocity during a burn in meters per second, V_i and V_f are the velocities on the initial and final circular orbits in meters per second, and Δi is the inclination change between the two orbits in radians. The velocity on any circular orbit is given by:

$$V_c(r) = \sqrt{\frac{\mu}{r}} \tag{7}$$

where μ is the standard gravitational parameter of Earth (approximately $3.986 \times 10^{14} \frac{m^3}{s^2}$) and r is the radius of the circular orbit in meters. Once the ΔV is found using Eqs. (6) and (7), it can be plugged into Eqs. (3) and (4) to find the spacecraft mass ratio after the orbit transfer, as well as the propellant mass needed for the transfer. To find the burn time, the below equation can be used:

$$t_b = \frac{m_p}{\dot{m}} \tag{8}$$

where t_b is the burn time per maneuver in seconds, m_p is the mass of propellant consumed per burn in kilograms, and $\dot{m}$ is the mass flow rate of the thruster given by:

$$\dot{m} = \frac{T}{gI_{sp}} \tag{9}$$

where T is the thrust of the thruster in Newtons, g is the acceleration of gravity, and I_{sp} is the given specific impulse of the thruster in seconds.

This analysis was performed for every phase of the mission where a burn would be needed.

4.3.1 Initial State and Parking Orbit

As mentioned in Section 1.5, the Rocket Lab Electron will be used as the launch vehicle for the mission. Since the Electron can eject satellites over the 400 to 1200 km range in a sun-synchronous orbit, there is no need to account for an orbit raise maneuver to bring the ODDSat to the 700 km orbit. Furthermore, the ability for the Electron rocket to launch to a sun-synchronous orbit means that a maneuver will not be required to change the inclination of the ODDSat.

4.3.2 Station-Keeping Maneuvers

One of the goals of the propulsion system is to choose a thruster that can extend the mission lifetime. For this, the propulsion system must be able to counteract orbital perturbations, mainly caused by drag. The first step in this analysis was to determine how long the ODDSat would take to decrease in altitude due to drag. Using STK's Lifetime Tool with an iterative process with a Drag Area of 0.06 m^2 and an Area Exposed to Sun of 0.04 m^2, it was determined that the ODDSat would take roughly 3.7 years to go from 700 km to 683 km without any burn being performed by the propulsion system, as shown in Figure 8. For the purposes of this initial analysis, an inclination change of 0 was assumed.

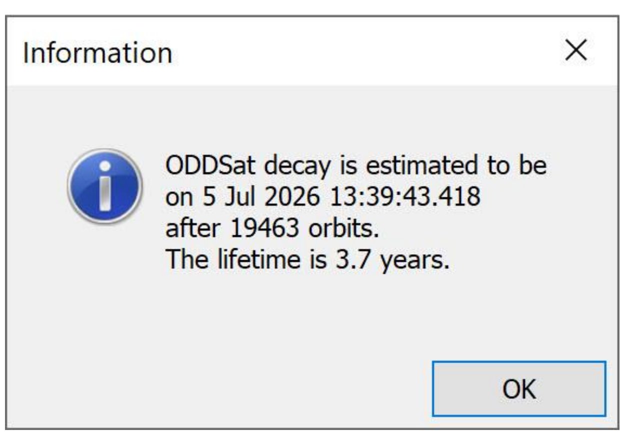

Figure 8: STK Lifetime Analysis Tool estimate for station-keeping

Using Eqs. (6) and (7) for the electric propulsion systems and the MATLAB script for the monopropellant thruster, it was determined that for the propulsion system to bring the ODDSat back to the desired 700 km, a total ΔV of roughly 9.028 $\frac{m}{s}$ would be required. For each of the aforementioned five thrusters, Eqs. (5)-(9) were used to determine the amount of propellant required, as well as the burn time, for one station-keeping maneuver. Table 8 summarizes the results.

Table 8: Thruster characteristics for one station-keeping maneuver

Thruster	Thrust (N)	I_{sp} (s)	Power (W)	m_p used (kg)	Burn Time (days)
SiEPS	0.00074	1200	1.5	0.0184	33.876
BET-1mN	0.0007	800	15	0.02759	3.580
BGT-X5	0.5	225	20	0.09796	0.005
NPT-30 I2	0.0011	2400	65	0.00920	2.279
BHT-100	0.007	1000	100	0.02208	0.358

4.3.3 Deorbiting Maneuver

An additional maneuver that the propulsion subsystem must perform is deorbiting. Currently, there is a rule set by the FCC which states that a satellite in a low-Earth orbit must deorbit within 5 years of completing its mission in space [38]. For de-orbiting, only the first burn is needed to lower the altitude of periapsis of the ODDSat's orbit for the chemical propulsion system. For the electric propulsion systems, the entire ΔV must be accounted for. So, using Eqs. (6) and (7) for the electric propulsion systems and the MATLAB script for the monopropellant thruster, it was determined that a ΔV of 134.231 $\frac{m}{s}$ would be needed for the monopropellant thruster and ΔV of 270.947 $\frac{m}{s}$ would be needed from the chemical propulsion systems to lower the

ODDSat's altitude from 683 km to 200 km. Eqs. (5)-(9) were again used to determine the amount of propellant required, as well as the burn time, for the de-orbiting maneuver. Table 9 summarizes the results. Again, an inclination change of 0 was assumed for this analysis.

Table 9: Thruster performance for a de-orbiting burn from 683 to 200 km

Thruster	Thrust (N)	I_{sp} (s)	Power (W)	m_p used (kg)	Burn Time (days)
SiEPS	0.00074	1200	1.5	0.546	1005.453
BET-1mN	0.0007	800	15	0.814	105.684
BGT-X5	0.5	225	20	1.078	0.055
NPT-30 I2	0.0011	2400	65	0.217	53.856
BHT-100	0.007	1000	100	0.654	10.605

Using STK's Lifetime Analysis Tool, it was determined that due to the effect of drag at low altitudes, the ODDSat would take roughly 7 days for it to get to 75 km, as shown in Figure 9. The 75 km altitude is a recognized altitude at which peak heat fluxes and mechanical loads result in satellite break up [39]. Using the results from the table above, all five of the thrusters would be capable of having the CubeSat de-orbit within the previously mentioned 5-year limit.

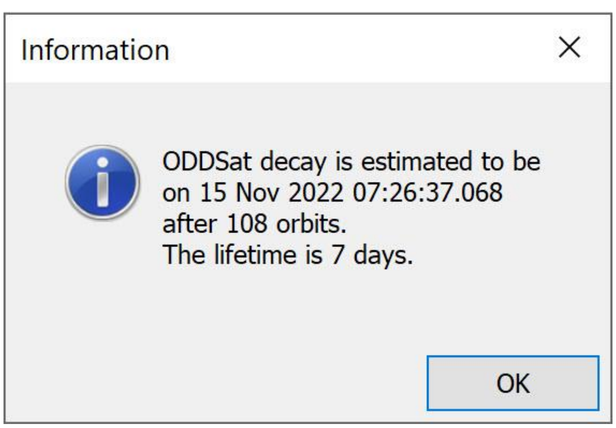

Figure 9: STK Lifetime Analysis Tool estimate for orbit-lowering from 200 to 75 km

4.3.4 Propulsion System Selection

Based on the initial analysis presented in Sections 4.3.2 and 4.3.3, Busek's BGT-X5 monopropellant thruster was chosen as the primary and only propulsion system for the ODDSat. Due to its high thrust specification, the BGT-X5 has a significantly lower burn time than any of the other four thrusters that were considered. Although the thruster has a low specific impulse, leading to a larger amount of propellant needed for the mission, the thruster still fit within the mass and volume constraints set forth by the mechanical subsystem. The maximum 20W of power needed also fit the constraints set forth by the power subsystem. The ability to integrate with customized tanks and the use of a more environmentally friendly propellant were also a deciding factor in choosing the thruster.

4.4 Orbital Analysis

Once the thruster for the ODDSat was chosen, the total amount of propellant that the ODDSat carried was determined. Based on that amount of propellant, propellant tanks were sized accordingly. Additionally, STK's Astrogator was used to perform in-depth orbital analysis to create a propulsion system timeline for two cases: with station-keeping and without station-keeping.

4.4.1 Total Propellant Carried and Tank Sizing

To determine the amount of propellant that the ODDSat would carry, a maximum duration of 15 years was assumed for the time the ODDSat could remain in space. Using Tables 8 and 9, it was determined that four station-keeping maneuvers could be performed, along with the one de-orbiting burn at the end. The total amount of propellant required was roughly 1.4698 kg. A maximum limit of 4.5 kg of propellant, roughly three times greater than what was required, was set, with the extra propellant accounting for redundancy. Based on this 4.5 kg limit, a cylindrical Ti-6Al-4V tank with spherical endcaps was sized according to the following equation:

$$V_{int} = \frac{4}{3}\pi r_{int}^3 + (AR r_{int})\pi r_{int}^2 \tag{10}$$

where V_{int} is the internal volume of the tank in m^3, r_{int} is the internal radius of the tank in m, and AR is the aspect ratio of the tank. For the tank sizing, an aspect ratio of 4 was assumed. The internal radius of the tank was found by setting V_{int} equal to the volume V_p of the propellant, which can be found using:

$$V_p = \frac{m_p}{\rho_p} \tag{11}$$

where m_p is the mass of propellant in kilograms and ρ_p is the density of the propellant in $\frac{kg}{m^3}$. V_p was calculated to be around 0.0031 m^3 using Eq. (11) This value was then substituted into Eq. (10) for V_{int} to determine that a single tank with an internal radius of 0.057 would be needed to store all propellant. Since this did not fit within the model of the ODDSat created by the mechanical subsystem, it was decided to instead use four smaller tanks. Each tank would have an internal radius of 0.0359 m. The combined mass of all four tanks, assuming a mass factor of 1.25, was calculated to be just under 0.5 kg. This meant that the mass of the entire propulsion system including the propellant, the propellant tanks, and the BGT-X5 thruster was 6.5 kg, bringing the initial wet mass of the ODDSat to 18.5 kg.

4.4.2 Orbital Analysis with Station-Keeping

Orbital analysis was first performed with the assumption of performing station-keeping maneuvers as mentioned in Section 4.3.2. However, the Lifetime Analysis estimate from above was performed with an initial wet mass of 24 kg. With the new updated wet mass of 18.5 kg and updated estimates for the Drag Area and Area Exposed to Sun provided by the mechanical subsystem, the Lifetime Analysis Tool was used to determine that the ODDSat would take 2.1 years to go from 700 km to 683 km because of drag. Figure 10 shows the results from the Lifetime Tool with the settings mentioned above. An analysis start time of 1 Feb 2023 17:00:00.000 UTCG was used for the Lifetime estimate in Figure 10.

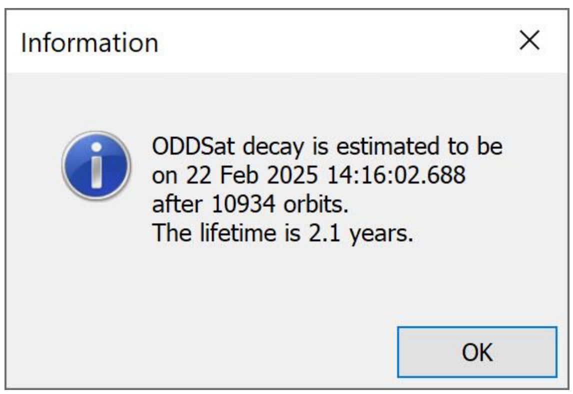

Figure 10: STK Lifetime Analysis Tool updated estimate for station-keeping

To obtain more accurate estimates for the ΔV and m_p needed to raise the ODDSat's orbit to 700 km from 683 km, a Hohmann transfer as was modeled using the Targeter within STK's Astrogator. Figure 11 shows the Mission Control Sequence (MCS) for the Hohmann transfer mentioned above.

Figure 11: Hohmann transfer modeled using the Targeter

Once the full MCS was run, the ΔV required for one station-keeping maneuver was determined to be roughly 9.028 $\frac{m}{s}$, while the m_p required was determined to be 0.07554 kg. The total time taken for the ODDSat to go from 683 km to 700 km was estimated to be 3921.2 seconds. With these values in mind, the decision was made to perform three station-keeping maneuvers. The MCS was run two more times, each with a more refined estimate of the mass of the ODDSat based on the propellant consumed for the previous station-keeping maneuvers. Once three station-keeping maneuvers were performed, an additional 2.1 years was accounted to bring the ODDSat back down to 683 km. Then, the Targeter sequence as shown in Figure 12 was used to determine the ΔV and m_p required to bring the ODDSat's altitude to 250 km to begin the de-orbiting process.

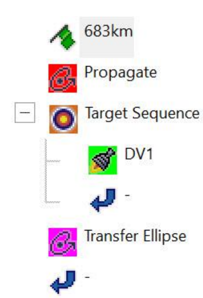

Figure 12: De-orbit burn modeled using the Targeter

The Targeter estimated that a ΔV of 119.781 $\frac{m}{s}$ and a m_p of 0.9656 kg would be needed to bring the ODDSat to 250 km. The total time taken was estimated to be 4261.1 seconds. After this point, the Lifetime Analysis Tool was used to estimate that the ODDSat would take 14 days to lower to 75 km, as shown in Figure 13.

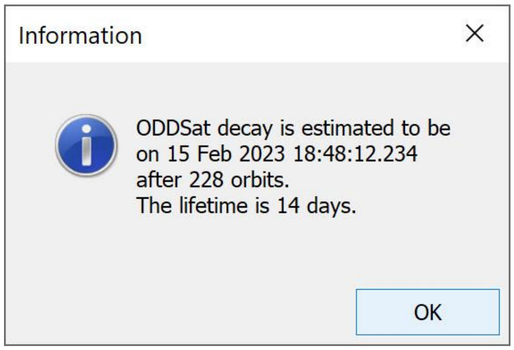

Figure 13: STK Lifetime Analysis Tool estimate for orbit lowering from 250 to 75 km

The propulsion system timeline including the three station-keeping maneuvers, the de-orbiting burn, and the time taken to decrease in altitude due to drag can be seen in Table 10. Also included is the ΔV and mass required for each maneuver/burn, the total ΔV and propellant mass, as well as the time taken.

Table 10: Propulsion system timeline with station-keeping

Phase/Maneuver/Burn	Initial Altitude (km)	Final Altitude (km)	ΔV Required $\left(\frac{m}{s}\right)$	m_p required (kg)	Time Taken (years)
Orbit-lowering #1	700	683	-	-	2.1
Station-keeping #1	683	700	9.028	0.07554	0.0001
Orbit-lowering #2	700	683	-	-	2.1
Station-keeping #2	683	700	9.028	0.07523	0.0001
Orbit-lowering #3	700	683	-	-	2.1
Station-keeping #3	683	700	9.028	0.07492	0.0001
Orbit-lowering #4	700	683	-	-	2.1
De-orbit	683	250	119.781	0.9656	0.00014
Orbit-lowering #5	250	75	-	-	0.0384
Total	**-**	**-**	**146.865**	**1.1913**	**8.44**

4.4.3 Orbital Analysis without Station-Keeping

To provide more insight on the capabilities of the BGT-X5 thruster, orbital analysis was also done for the case when no station-keeping maneuvers would be necessary throughout the duration of the mission. With the wet mass of 18.5 kg and updated estimates for the Drag Area and Area Exposed to Sun provided by the mechanical subsystem, the Lifetime Analysis Tool was used to determine that the ODDSat would take 10.6 years to go from 700 km to 680 km because of drag, as shown in Figure 14 below. An analysis start time of 1 Feb 2023 17:00:00.000 UTCG was used for the Lifetime estimate in Figure 14.

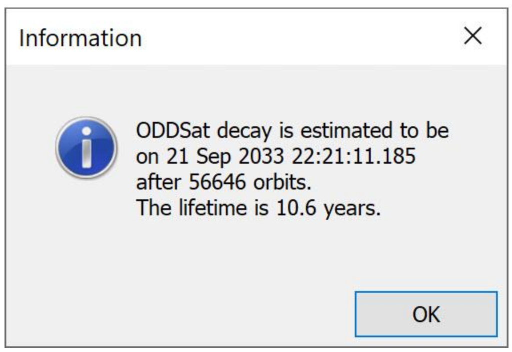

Figure 14: STK Lifetime Analysis Tool estimate for orbit-lowering from 700 to 680 km

It was noticed that there was a large gap in time to descend an additional 3 km. In Section 4.4.2, it was estimated that the ODDSat would take 2.1 years to get from 700 km to 683 km because of drag. However, as presented in Figure 14, it would take the ODDSat 10.6 years to get from 700 km to 680 km due to the effects of drag. After doing research why there is such a large time gap between the two estimates, it was determined that solar variation over the course of a solar cycle has a large effect on the lifetime of a satellite [40]. A solar cycle is an 11-year period during which the Sun's magnetic field completely flips [41]. The atmospheric density varies by roughly two orders of magnitude between solar maximum, when there is the highest amount of solar activity, and solar minimum, when there is the lowest amount of solar activity. Due to the large variations in the density, satellites decay faster during solar maximum and slower during solar minimum [40]. Figure 15 shows the latest forecast for the current solar cycle, Solar Cycle 25, provided by the National Oceanic and Atmospheric Administration (NOAA) [42].

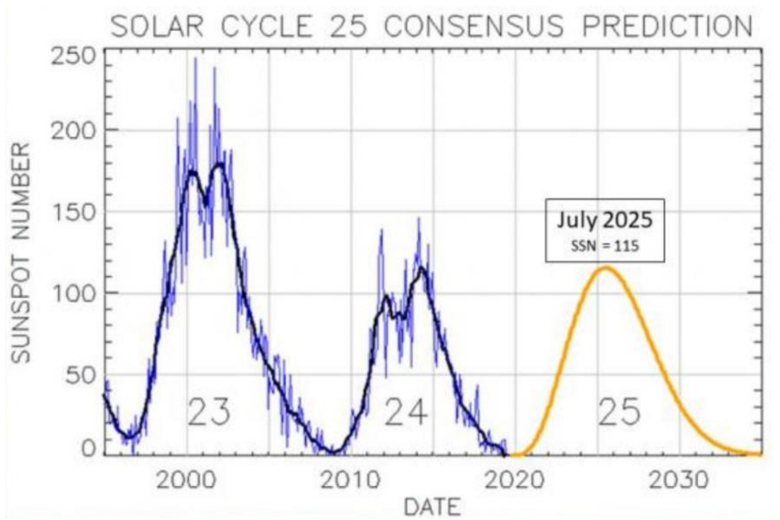

Figure 15: NOAA's latest prediction for Solar Cycle 25 [42]

An analysis start time of 1 Feb 2023 17:00:00.000 UTCG was used for the Lifetime estimate in Figure 14. The estimated decay date of 22 February 2025 from Figure 10 is very close to the estimated solar maximum of July 2025 in Solar Cycle 25, while the estimated decay date of 21 September 2033 from Figure 14 is relatively close to the estimated solar minimum of sometime in 2034. Figure 16 below shows the ODDSat's height of perigee when plotted against the time.

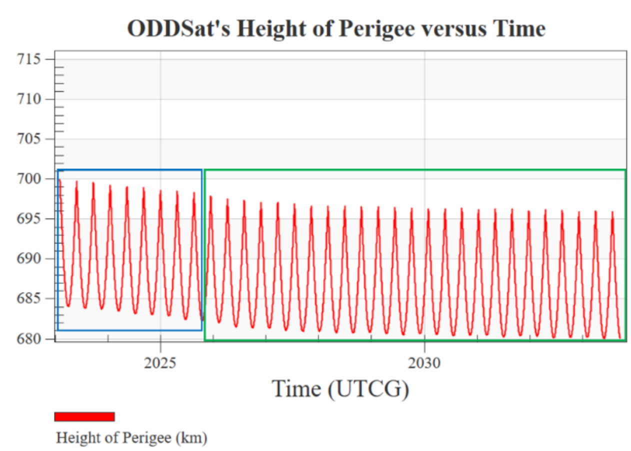

Figure 16: STK generated graph of the ODDSat's height of perigee versus time

The area in the blue box in Figure 16 proves that the height of perigee decreases at a faster rate as solar maximum approaches, as opposed to the area in the green box, where the height of perigee decreases at a much lower rate as the time slowly approaches solar minimum.

Even though the altitude of the ODDSat would eventually reach 680 km as opposed to the 683 km altitude used in Section 4.4.2, analysis was still performed for this situation since the 3 km difference was considered negligible when comparing it to the 1400 km maximum range of the CST mentioned in Section 2.2.

After the ODDSat reaches an altitude of 680 km, a de-orbiting burn can be performed to lower the altitude to 250 km. The MCS shown in Figure 12 was set up with an initial altitude of 680 km to estimate that a ΔV of 118.996 $\frac{m}{s}$ and a m_p of 0.9713 kg would be needed to bring the ODDSat down to 250 km. The time taken to get to 680 km was estimated to be 4286.2 seconds. From that point, drag could take over and take the ODDSat to 75 km in 14 days, as shown in Figure 13.

The propulsion system timeline including the three station-keeping maneuvers, the de-orbiting burn, and the time taken to decrease in altitude due to drag can be seen in Table 11. Also included is the ΔV and mass required for each maneuver/burn, the total ΔV and propellant mass, as well as the time taken.

Table 11: Propulsion system timeline without station-keeping

Phase/Maneuver/Burn	Initial Altitude (km)	Final Altitude (km)	ΔV Required $\left(\frac{m}{s}\right)$	m_p required (kg)	Time Taken (years)
Orbit-lowering #1	700	680	-	-	10.6
De-orbit	680	250	118.996	0.9713	0.00014
Orbit-lowering #2	250	75	-	-	0.0384
Total	**-**	**-**	**118.996**	**0.9713**	**10.638**

5. Power Subsystem Analysis and Design

This chapter reviews the power subsystem design and components on the ODDSat, as well as the analysis performed to ensure enough power generation and distribution for the other subsystems on the ODDSat with the given requirements and constraints.

5.1 Power Overview

The power system is responsible for managing the collection and distribution of power to the spacecraft and all the subsystems. It is also responsible for storing power so that the satellite has power for eclipses. The power subsystem must ensure that there is enough power to meet the mission requirements. Like most spacecraft, CubeSats typically use solar panels for their power generation. Solar panels consist of photovoltaic solar cells that convert solar radiation to electrical energy [43]. This energy is then stored or distributed to the spacecraft so that the spacecraft can operate and perform mission objectives. Other power generation methods were researched, but the mission is using a sun-synchronous orbit that can maximize the power received from the panels since the panels will be in the sunlight for most of their orbit.

Solar cells have p-n junctions, which are boundaries between two semiconductor materials, a p and n-type. These can be divided into two regions, the p and n regions. P regions have a low electron concentration, and the n-region has a high concentration. Photons from solar radiation remove an electron from the n region and it moves to the p region [43]. The electron flow generates electrical power that can then be distributed through the Electrical Power System (EPS) to the instrumentation on board. Along with the EPS is a battery pack consisting of batteries that will store power for when the satellite requires a higher power output or during eclipses.

5.2 Hardware Selection

5.2.1 Solar Panels

To generate the most amount of power during the mission, the cells must have high efficiency. Since the distance from the sun is nearly constant throughout the CubeSat's orbit, higher-efficiency cells will produce more power than low-efficiency cells. Single junction cells only have one p-n junction where electrons flow, while multi-junction cells have more than one junction. These extra junctions make the panels more efficient overall since there can be more electrons flowing from region to region. Additional junctions also can receive different wavelengths so there is a higher amount of flow occurring. Since the goal is to have the highest efficiency, multi-junction cells were chosen.

After understanding the type of panel needed, the selection of cells came next. Although the choice will be focused on having the cells with the highest efficiency, the subsystem must ensure that the panels fit the size and weight constraints for the satellite. The CubeSat size selected was 12U using a 3U × 2U × 2U configuration. This meant that the largest possible solar panel was 3U × 2U based on the surface area where the panels would be placed. The research was conducted on solar array sizes and their efficiency by different manufacturers. The highest power generation came from the solar cells used by EnduroSat, a manufacturing company that focuses its products on small satellites such as CubeSats. EnduroSat's 6U solar panels have ~30% efficiency using a triple junction cell (3 p-n regions in the cell for 3 wavelengths) [44]. This efficiency is one of the highest that exists for nanosatellite solar panels and therefore is the chosen panel to maximize power generation. A 6U solar panel was analyzed since the solar panel size is 3U × 2U, the size needed for the ODDSat without the need for additional configuration. A single solar panel from EnduroSat has 16 solar cells and can generate around 19.2W of power at 19.2V and 1A [44].

Once these cells were selected, the power subsystem focused on maximizing the solar array size as well to generate the most power. To find the optimal array size at the optimal orbit, the following equations were used:

$$P_0 = ns \tag{12}$$

$$P_{BOL} = P_o I_d \, cos(\theta) \tag{13}$$

$$A_a = \frac{Psa}{P_{BOL}} \tag{14}$$

Equation (12) solves for P_0 (panel output power) by using the solar cell efficiency (n) and the solar flux at Earth's distance from the sun (s). Equation (13) (P_{BOL}) is the beginning of life power, which is determined from the panel output power, the nominal inherent degradation I_d, and the solar incidence angle θ (which was assumed to be 0° at optimal and 10° at non-optimal based on mission parameters). Equation (14) is the optimal array size, which is simply the needed power divided by the beginning of life power. The efficiency of the EnduroSat panels is 30%, and the nominal inherent degradation is assumed to be 77% [44],[45]. Dividing the optimal array size by the size of one panel (0.06 m^2) gives the number of panels to create the optimal array.

To determine the power needed, the subsystem created a budget to manage what each other subsystem would require for mission operations. The budget, shown in Table 12, is based on four different parts of the mission. The first two columns, the nominal wattage and the eclipse needs, both occur for most of the mission while the detections occur. Detumbling needs are the power used before the solar panels are deployed after detaching from the launch vehicle, and the final column measures what is needed while the spacecraft deorbits to a burnup altitude. All of these are conservative estimates of the power needed during the mission, to ensure the panels and EPS can support the maximum necessary amount of power.

Table 12: Power Budget

Subsystem	Nominal Wattage (W)	Eclipse Needs (W)	Detumbling Needs (W)	Deorbiting Needs (W)
Attitude Determination	2	2	0	0
Attitude Control	6	4.235	4	0
Propulsion	0	0	0	20
Comms	10	10*	5	0
Payload	12	12	0	0
Total	30	28.235	9	20

*Comms would need 10W only if downlink occurs during an eclipse period (38min total), otherwise 0W is used

Based on the nominal wattage, the optimal solar array size would be 0.19 m^2 for optimal orbit and 0.1929 m^2 for 10° incidence angle, meaning that the number of panels is around 3.2 and rounds up to 4 total panels. Based on the maximum wattage, the optimal array size is 0.3167 m^2 for optimal orbit and 0.3217 m^2 for 10° incidence angle, meaning the number of panels is 5.3 rounding up to 6 total panels. Though this is the optimal array size, it must still fit onto the satellite and fit the size and mass constraints. Assuming the worst-case scenario (6 total panels needed for operating), there is not enough room to fit only body-fixed panels on the CubeSat. The team decided to instead use 6 deployable panels that would fold on top of each other on the CubeSat faces. The configuration chosen was 3 panels on opposite faces of the CubeSat folded, and then extending in the $\pm y$ direction when deployed.

5.2.2 Electrical Power System and Batteries

The EPS is the system that distributes power throughout the satellite. To choose the proper EPS, research was performed to ensure that the system is compatible with the solar panel connections and the instrumentation selected. Based on the different subsystems' instrumentation selections, the payload is the instrument with the highest power draw during one orbit, needing about 12W. This means the EPS must have an output converter that generates more than 12W. Additionally, the physical connections of each instrument must be compatible with the EPS. Another condition that would be beneficial for the system is Maximum Power Point Tracking (MPPT). MPPT is a technology that ensures the power output is as close to the input as possible. The system will measure the solar panel generation and looks at the voltage of the instruments and batteries [46]. It then can adjust the current through the EPS so that there is no power lost from start to finish. It does this by taking the DC input of the solar panels and converting it to AC, then back to DC with the adjusted current and correct voltage [46].

An EPS has multiple different components that help take the solar energy and convert it into power for the instruments. The process can be seen in the schematic in Figure 17.

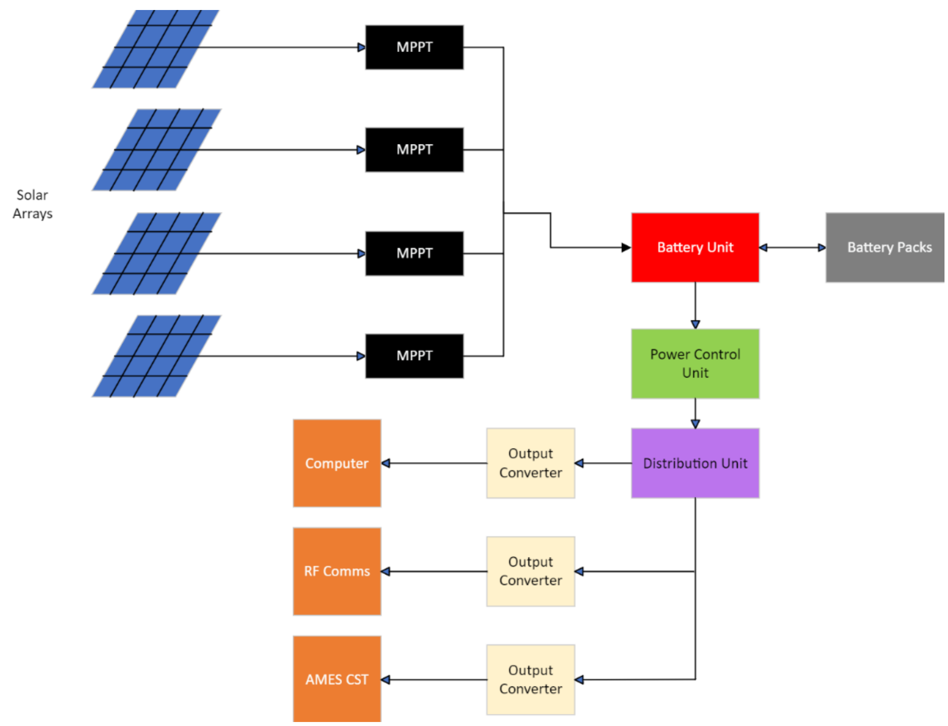

Figure 17: Schematic of general EPS internal workings and connections

The solar arrays connect directly to the MPPTs, which convert the input to the proper battery voltage. The battery unit then distributes to the battery packs and the power control unit. From the power control unit, the distribution unit sends the voltage to the output converters, which connect to the instruments onboard.

When selecting an EPS system, some with batteries on board were considered, meaning that battery packs were included with the EPS. However, this on-board battery pack would sometimes limit additional or external battery packs being added, and the charging time would not be enough between the eclipse periods measured and discussed in Section 5.3. Other EPS systems had connection options for battery packs to attach to it, leaving more flexibility for the types of batteries. After considering different manufacturers and types of EPS', the Ibeos SmallSat EPS was the selected system with the 28V configuration. The EPS has 4 different output options which can be varied [47]. To find which outputs should be used, the following equation was used to find how much power would be generated for each option. Table 13 shows the numbers for each output.

$$P = VI - RI^2 \tag{15}$$

Table 13: Voltage regulator options for the Ibeos 28V EPS

	Voltage, volts (V)	Current, amperes (I)	Resistance, ohms (R)	Power Output, watts (P)
3.3V Regulated	3.3	3	0.015	9.765
5V Regulated	5	6	0.015	29.46
12V Regulated	12	4	0.015	119.76
Unregulated	28	10	0.015	278.5

Using the results from Table 13 and the power budget from Table 12, the 3.3V and 5V options are the best for the different subsystems. Attitude Control and Attitude Determination, the subsystems under the 9.765W threshold, will use the 3.3V regulated bus. Comms, Propulsion, and Payload, the subsystems over the 9.765W but below the 29.46W threshold, will use the 5V regulated bus.

Having no batteries included on the EPS allows for flexibility in selection, since the batteries would need a discharge time of over or 200 minutes to cover all detumbling but also need an 18-minute discharge for eclipse periods where mission operations are taking place. The EPS itself only consumes 1.5W, a small amount compared to the generation that comes from the solar panels [43]. The high efficiency allows for very little power to be lost while being converted in and out of the system. Ibeos also produces 28V compatible batteries that pair well with the system, which perform well with the chosen EPS. A discharge rate of 10A allows for rapid power distribution to the subsystems during eclipse periods [48]. The charging rate of 2.5A allows for a slower but still efficient recharge time. The BOL capacity is around 135 Wh, higher than many of its competitors [48]. Voltages accepted do not necessarily need to be at 28V, as the batteries can handle 22 –33.6V, but a 28V rail is selected since that is the most compatible with the EPS [48]. There are also built-in protection systems in the batteries, such as an over-current charge or discharge, remove-before-flight (a CubeSat requirement), and more [48]. Three of these batteries were added to the system to support recharging periods and not falling below the DOD of 80% for lithium-ion batteries [49]. While these specs fit the eclipse needs well, the detumbling needs would not be met.

For detumbling, the conservative estimate is that the ADC subsystem needs 2 orbits to have the satellite pointing and positioned correctly with a smaller amount of power needed over the 200-minute period. The 28V batteries could not be configured to give a small amount of power initially and then adjust later on in the mission to support mission operations with a higher power draw. Instead, a detumbling battery was added to the satellite. A detumbling battery would have the primary purpose of operating the system while detumbling is occurring and the solar panels are not deployed. This battery would require different specs: a lower discharge rate and a smaller volume that would fit in the internal system. This battery would not need as high of power storage since it would only be used once during the mission lifetime. For all of these reasons, the EaglePicher Technologies 12Ah Space Cell was chosen to be the detumbling battery. The discharge rate is C/5, meaning that it takes around 5 hours for the battery to be fully discharged at maximum usage [50]. The battery is also small and narrow to fit well within the internal structure of the CubeSat [50].

5.3 STK Simulations and Analysis

To understand how the selected components would work over the mission duration, STK was used to model the mission's orbit in LEO. STK generates solar panel power reports which can be used to ensure that the model is working and that the panels are configured correctly.

5.3.1 Model and Scenario Building

STK provides many satellite models to upload into the simulated orbit, some with solar panels and some without. However, the only CubeSat models STK generates are 1U-6U. Since the satellite is 12U, this would not be the right sizing. Additionally, none of the models had solar panels that fit the 12U configuration. Blender was used to create a model of the spacecraft so the correct sizing of the body and panels could be uploaded into the system. The initial model is shown in Figure 18 below, where the rectangular prism is the size of the main body, and the extruding parts are the solar panels.

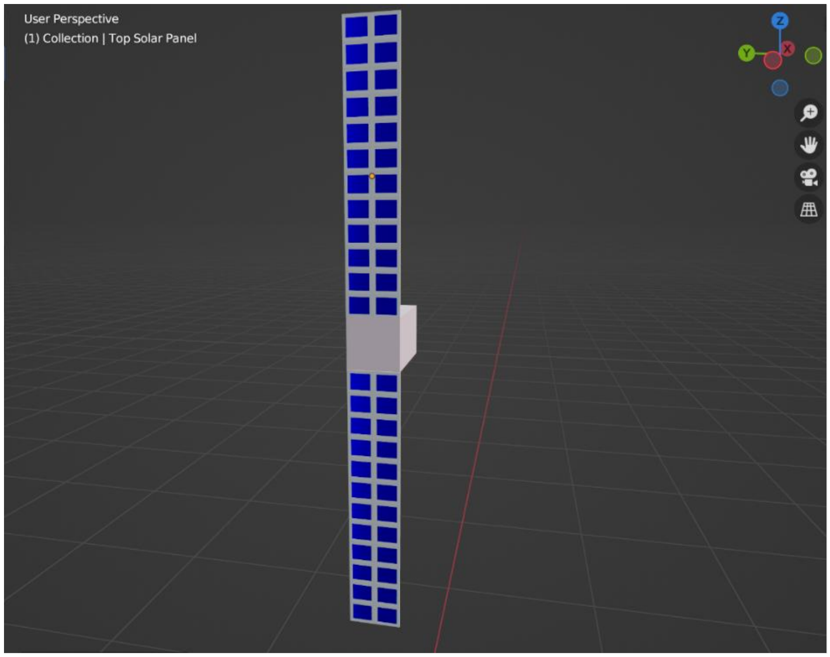

Figure 18: Snapshot of the initial Blender model of the deployed configuration

To create the model in Blender, the initial cube given by the system was narrowed into the rectangular prism with the dimensions of the ODDSat. To create the solar panels, another object was added and adjusted to be the dimensions of three solar arrays deployed, the total top solar panels. To add a grid to the external face, 'Mesh' followed by 'Grid' were selected. The number of subdivisions could be adjusted and were done to create the number of solar cells for the top set of panels. To create the divisions between each cell, a 'Modifier' was added. The modifier selected was 'Wireframe', and the thickness was lowered until the solar cells were visible and equal to the dimensions given by EnduroSat. The material of the solar cells also needed to be edited in the modeling software, and was done by selected 'Material' for each of the cells and adjusting the features such as 'Metallic', 'Roughness', and 'Subsurface' so that it was a metallic, blue color to bring attention to the cells that would be generating the power. Once these steps were completed, the shape was duplicated so that there was a bottom set of solar panels.

It was important while modeling to ensure that the solar panels were separate components from the body and each other. This needed to be done so that the power output in STK would show each of the panel's outputs and the overall output. However, to export the model into a working COLLADA file, the components needed to be connected to one another. This was done by moving the top and bottom solar panels to line up with on face of the ODDSat's body so that they were aligned on the same plane. To add the solar panels, the process was done one set of panels at a time. The body was selected, then 'Properties' was clicked and a 'Boolean' modifier was added. After naming the modifier, the button 'Object' was selected and the top panel component was chosen from the list. To finally merge the objects, 'Operation' followed by 'Union' was selected. The process was repeated for the bottom solar panel set. This creates a single moving piece with three components.

The model was exported from Blender into a COLLADA file so that it could be uploaded to STK. Initially, there was no power generation reported because the COLLADA file did not have the code needed to identify which components were the solar panels. In order to target certain parts of the CubeSat, code was taken from the 6U CubeSat COLLADA file provided by STK. The 6U file had code written to target certain parts and to give those parts the necessary efficiency. The editing was done in the Notepad app, then saved as a COLLADA file again. The COLLADA file was reuploaded to STK with the corrected efficiency can be found in Appendix B.

5.3.2 Beginning of Life Analysis

To ensure the model correctly shows the power generation of the panels, a single orbit analysis was done for each solar panel and the total of both panels. Two dates were analyzed, the spring equinox and the summer solstice of the first year in orbit. Figure 19 shows the power generation over one orbit on June 21st, 2023, while Figure 20 shows the power generation over one orbit on March 21st, 2024. The green line is the $+y$ panel, the dark blue line is the $-y$ panel, and the light blue line is both panels' output combined.

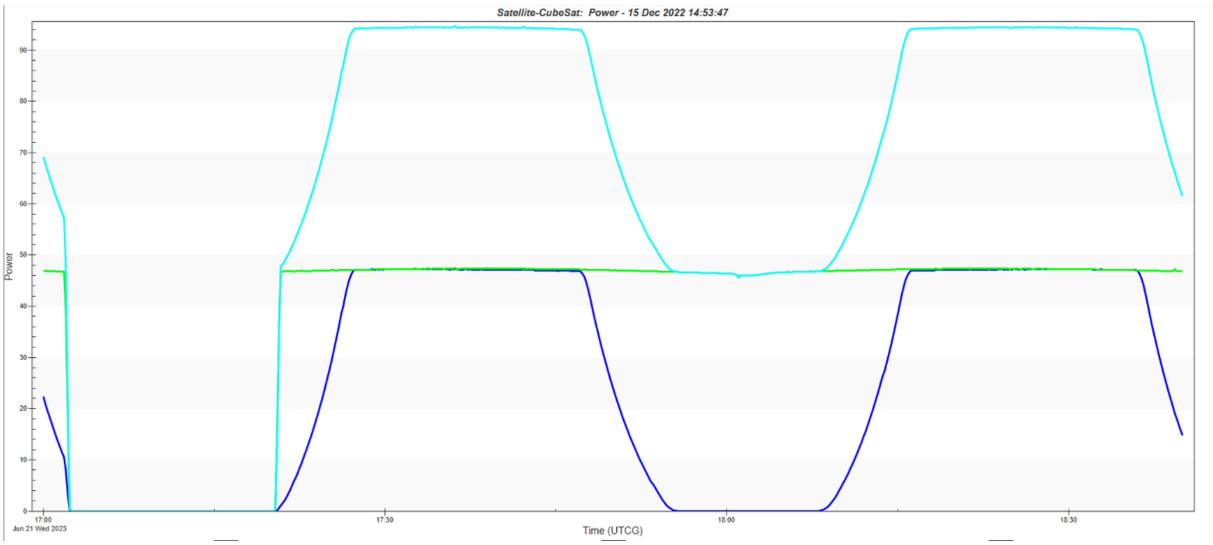

Figure 19: Solar panel power output for one orbit on June 21st, 2023

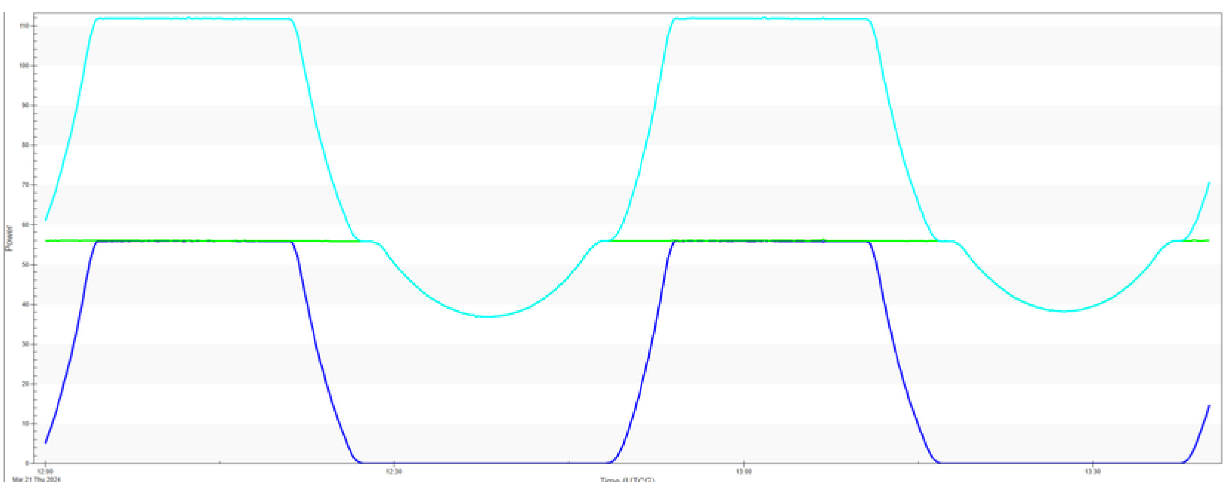

Figure 20: Solar panel power output for one orbit on March 21st, 2024

June 21st shows that at the beginning of the orbit, there is a full eclipse period that lasts around 18 minutes. Both solar panels are in total shadow for that time. The power increases quickly once the $+y$ panel is back in full sunlight and generates 47W of power. The $-y$ panel takes a few minutes to go from total shadow to total sunlight. Both panels in full sunlight generate around 94W, which lasts for 20 minutes. The $-y$ panel then drops into partial and then total shadow again after this period and stays in total shadow for around 14 minutes before returning to total sunlight. The $+y$ panel stays in full sunlight for the remainder of the orbit. The cycle repeats itself during the orbit and based on the beginning of the graph, a full eclipse can be expected shortly after. Further analysis will need to be done on this part of the orbit to ensure that the subsystems have enough power at all points and the batteries can recharge fully between eclipse periods.

In contrast, March 21st shows the highest power output of the panels over the two days, around 56W per panel (112W total). There is no full eclipse period at this point in the mission, but the $-y$ panel does have periods of full shadow that last around 30 minutes, with 3.5 minutes on either side for the transition from partial to full shadow/sunlight. During the periods where the $-y$ panel is in total shadow, the $+y$ has a smaller period of partial shadow. The power generation goes no lower than 36.5W, but this amount is not enough to fully support the subsystems, and battery support will be needed. To fully understand how the power will change throughout the mission, a longer analysis needed to be done. A one-year analysis (March 21st, 2023 to March 21st, 2024) was completed to understand when eclipse periods occur and how partial shadow changes. Figure 21 shows the full results.

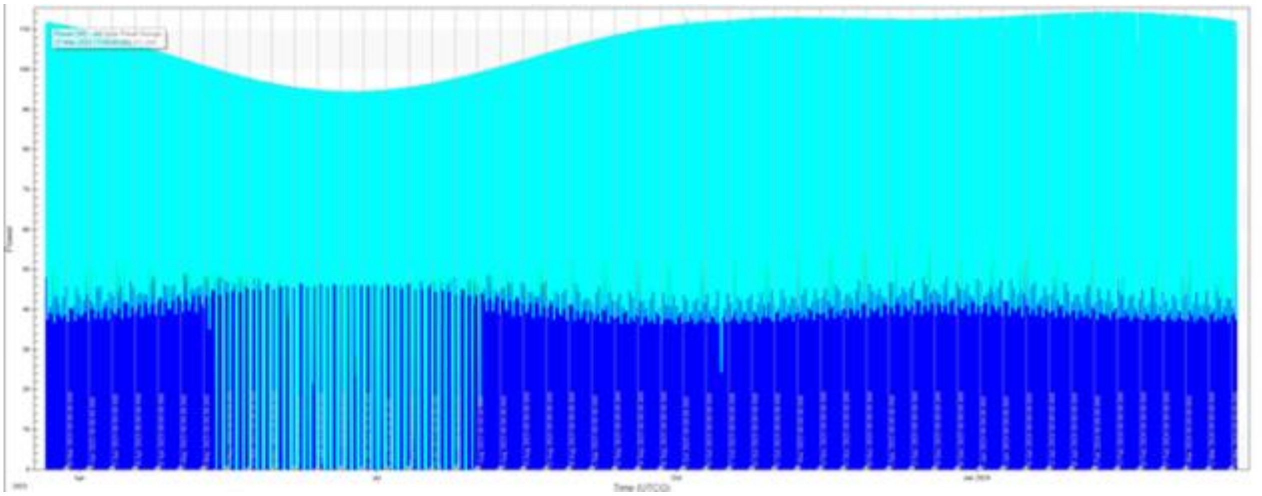

Figure 21: Solar panel power output for one year, March 21st, 2023 to March 21st, 2024

The graph shows that there are periods of total eclipse beginning in late May and continuing until late July. The peak eclipse period occurs on the summer solstice, June 21st, and lasts a maximum of 18 minutes. In contrast, the highest amount of power is generated on February 10th, generating about 114W. Outside of the months that have a full eclipse period, the power generation is steady and stays above 110W. A second full-year analysis, from March 21st, 2024 to March 21st, 2025, was done to ensure the pattern was the same from year to year. Figure 22 shows the results, proving that this pattern will stay consistent throughout the mission.

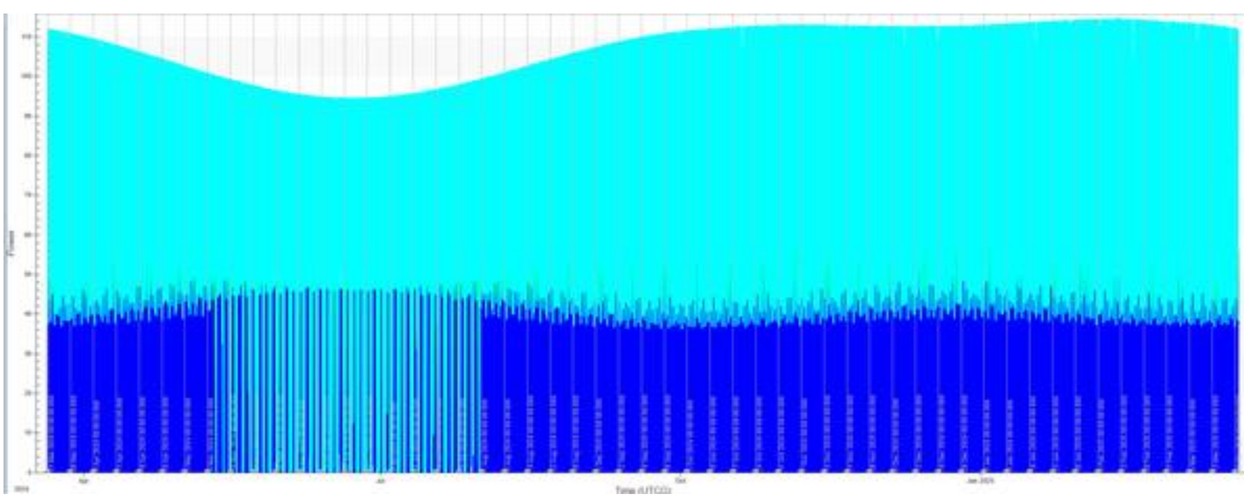

Figure 22: Solar panel power output for one year, March 21st, 2024 to March 21st, 2025

5.3.3 End of Life Analysis

The End of Life (EOL) analysis also needed to be done to measure the performance of the hardware after the 10-year lifetime. The propulsion subsystem does not require station-keeping maneuvers since the satellite will still operate at 680km, the altitude after around 10 years in LEO. This will be the EOL altitude, which was adjusted in STK. Additionally, most solar panels typically degrade over time during the mission. However, according to the EnduroSat 6U data, the EOL efficiency should remain above 29%. To do a worst-case scenario analysis, the lifetime degradation equation was done using the following equation:

$$Ld = (1 - Yd)^t \tag{16}$$

Assuming the annual environmental degradation rate (Yd) is 0.017 and using t as the full mission lifetime, the lifetime degradation Ld is about 0.834. Putting this into the EOL power generation, and assuming no cosine loss angle, the highest power generation should come at about 100W. This is still enough power to support the nominal wattage.

Using this analysis, the COLLADA file was adjusted to account for this degradation, and the STK scenario reflected the EOL altitude. The scenario was re-run as it was for the BOL analysis to ensure the power generation was similar to what was calculated. The initial analysis was a full year power generation graph at an estimated EOL timeline shown in Figure 23.

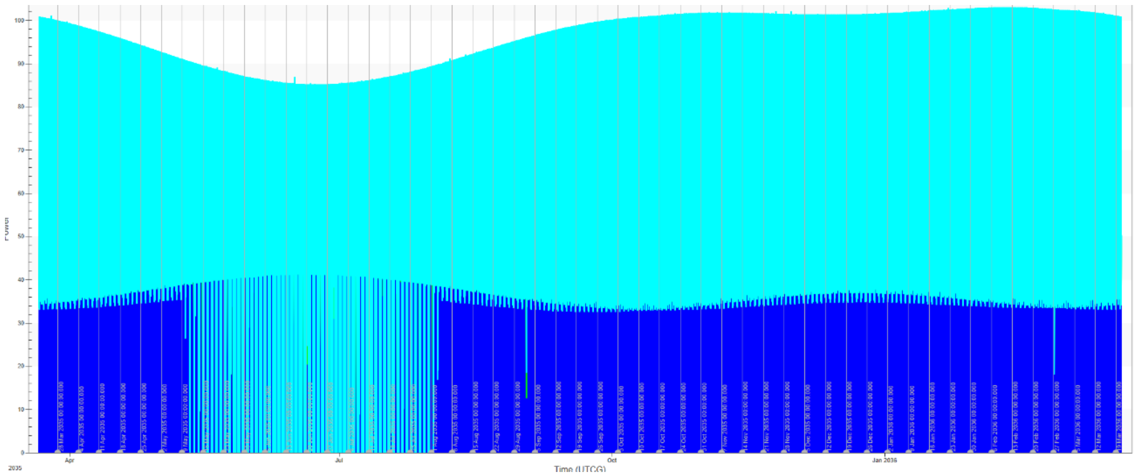

Figure 23: Solar panel power output for one year, March 21st, 2035 to March 21st, 2036

The above figure shows that the power generation has a similar pattern to what was seen in the BOL analysis, but there appears to be two anomalies due to solar eclipses. Additionally, the estimate of 100W appears to be correct from the initial analysis. To fully understand the power generation and the effect of eclipse periods at the new altitude, a three-orbit analysis was conducted on the same dates as the BOL analysis, March 21st and June 21st. The results can be seen in Figure 24.

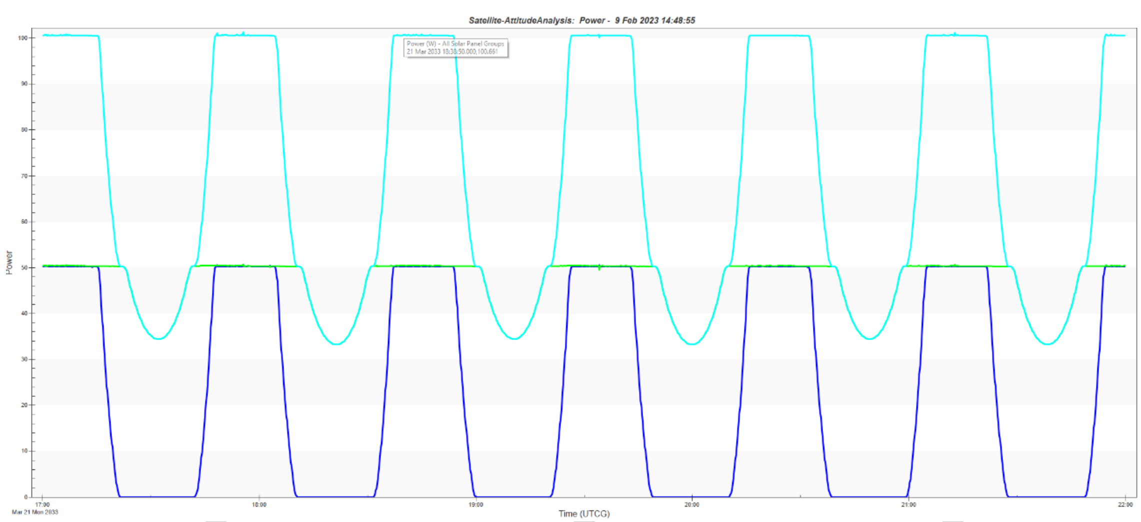

Figure 24: Solar panel power output for three orbits on March 21st, 2035

Similar to the BOL conditions, two partial eclipse periods occur during one orbit. The full shadow for the $-y$ panel is still around 30min, while the top panel's shadow period lasts for about 20 minutes. As seen in the full year power EOL analysis, Figure 24 proves that the highest power generation occurs at just around 100W. The minimum amount of power generated is 33.4W, slightly under the lowest generation on March 21st with the BOL conditions. The partial shadow period is still enough to support the system, meaning battery support is not needed during these months. Figure 25 is another 3-orbit analysis done, but on June 21st, 2035 instead to compare what a total eclipse period generates with the EOL conditions.

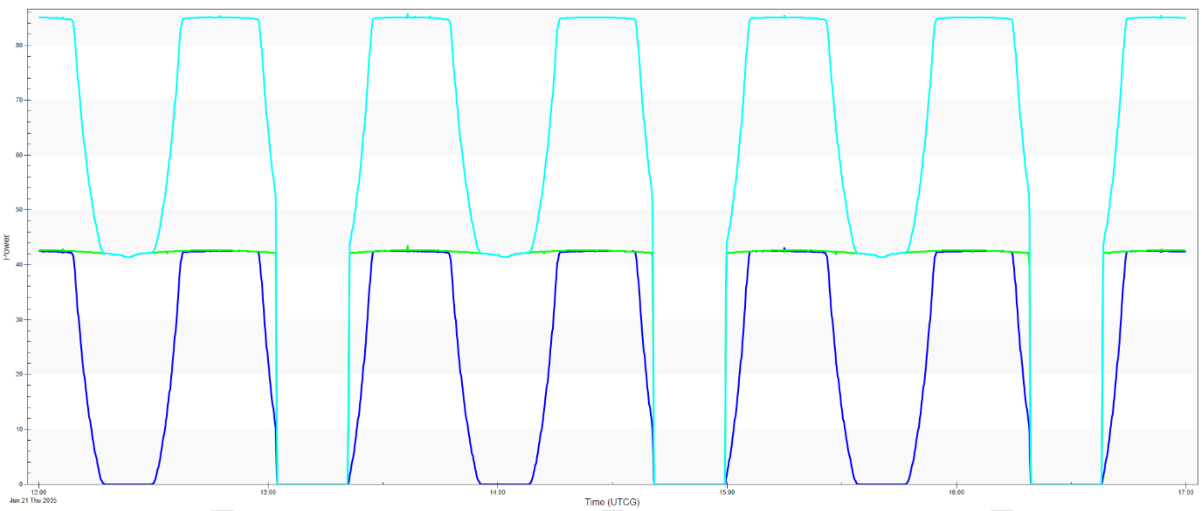

Figure 25: Solar panel power output for three orbits on June 21st, 2035

The EOL conditions prove that the pattern is the same as the BOL generation, with an eclipse period length of 18 minutes maximum, and a rapid increase back up to full power generation. The highest generation shown in Figure 25 is around 85W. The periods of full shadow for the bottom panel generate 42W, still enough to support the system at nominal wattage. Despite the lower wattage generation at EOL, there is still enough time for the batteries to recharge before the next eclipse period. Since eclipse periods happen often, and the partial shadow periods might not allow for a full recharge of one battery, two additional mission operations batteries were added to the system to ensure that none of the batteries will fall past the DOD.

The EOL analysis demonstrates that the altitude has minimal effect on the mission operations and power generation. Since the degradation is intendent of altitude, a lower output was expected if eclipse periods were longer or partial shadows were more frequent. However, it seems that only the lifetime degradation of the panels will affect the power generation. This is good for the mission since it means transitioning into deorbiting will be a simple task.

Since 680km is the altitude that the science period will cease and the deorbiting maneuvers will begin, the EOL analysis also shows that the thruster can be supported for any burns needed to reach a burnup altitude. Based on the thruster need as well as the information presented in Figures 19 and 20, there will be more than enough power for the thruster if the solar panels remain deployed. Alternatively, if the panels become stowed and are not deployed, the mission operations batteries will be activated to support the burn. Unlike detumbling, the deorbiting will only be a finite burn that will not take as long, so the detumbling battery will not be needed. To find the time that it takes for the battery to fully discharge, the following equations were used:

$$Ah = \frac{Wh}{V} \tag{17}$$

$$h = \frac{Ah}{A} \tag{18}$$

In the case of the Ibeos 28V battery pack, an unregulated bus is used with a 10A current as seen in Table 13. The Wh is given as 135Wh, meaning it takes around 28.926min for one battery to fully discharge. Assuming all three batteries are fully charged, this allows for a maximum of 86.778 min to discharge. Since these support times are much longer than the finite burn at 680km, the batteries will be able to support the deorbiting if there is any issue with the solar panels during the deorbiting burn.

6. ADC Testbed

6.1 Overview

The ADC Testbed is a system designed to simulate the Earth’s magnetic field. This allows for testing of the ADC subsystem in an environment that mimics that which the CubeSat will be operating under in orbit. The testbed is divided into two different subsystems: the Helmholtz cage and the low friction table. The Helmholtz cage is the portion of the testbed that creates a magnetic field, while the low friction table allows for the ADC system to be tested with minimal friction.

6.2 Helmholtz Cage

The Helmholtz Cage is used to simulate the magnetic field that the CubeSat will face during its mission in space. The cage consists of three orthogonal coil pairs with a current passing through them. The three pairs represent the three axes of motion. Each coil has several windings, so when the current passes through the coils, the magnetic field generation is created and amplified at the midpoint of the cage. The power is supplied to the coils through programmable power supplies so that the current, and eventually the magnetic field, can be adjusted manually. There are several current sensors and magnetometers that measure the current and magnetic field passing through the cage. The magnetic field data obtained by the magnetometers is plotted against the theoretical magnetic field that should be generated by the cage.

To read the magnetic field values created by the cage, a software called LabVIEW was downloaded to record the magnetic field of the cage. The B-field was to be recorded and mapped to verify results. This software’s implementation was made after a few attempts, but progress was halted due to time constraints.

In terms of improvements, programmable power supplies were bought, as well as a Gauss Meter to measure the magnetic field physically. The eventual goal of the cage is to use LabView with a DAQ to automate the entire process such that the magnetic field can be automatically adjusted based on the current magnetic field measured by the magnetometer. The schematic seen in Figure 26 below shows what the theoretical wiring of the LabJack, board, and power supplies would be.

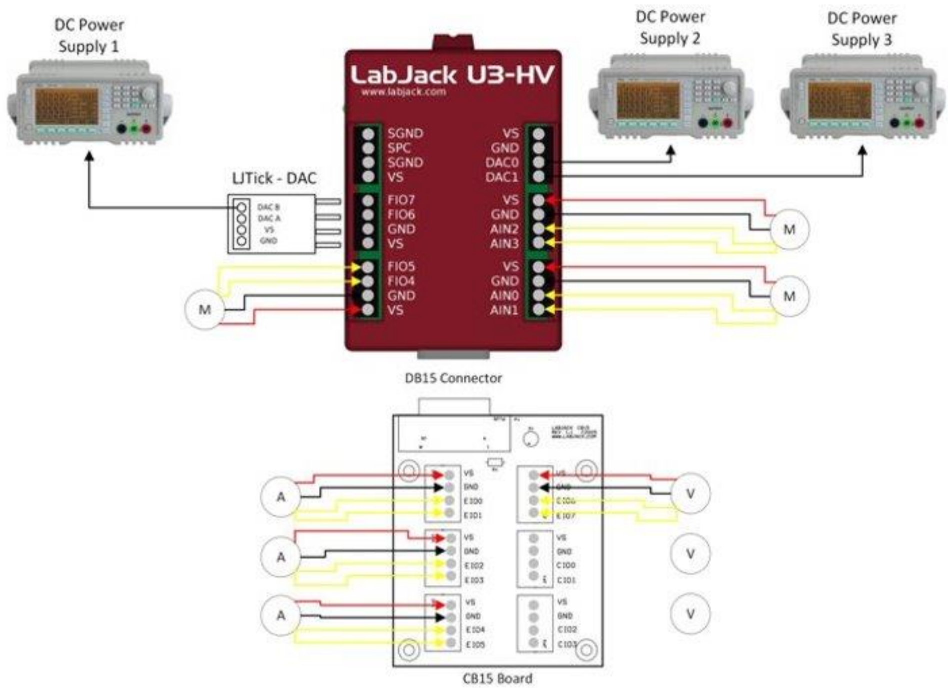

Figure 26: Wiring of LabJack, CB15 Board, and power supplies for Helmholtz cage

6.3 Air Bearing Table

The air bearing table consists of two major parts: the table and the socket. The table is made up of an instrumentation platform containing a battery, reaction control wheels, and a Raspberry Pi that can be remotely accessed. On the underside of the table is a large bearing. When in use, this bearing is placed on top of the socket. Pressurized air is routed into the bottom of the socket, forming a cushion of air that the table rides on top of. Figure 27 shows the socket part of the air bearing table. Also seen is a pressurized air hose and adapter used to route air from an air compressor into the bottom of the socket. According to previous MQP’s, the table is balanced via weights and once balanced is controlled by the reaction control wheels. The system is currently non-functional due to an incident with the lithium-ion battery from the previous year, however work is underway to identify and procure a replacement.

Figure 27: The socket part of the air bearing table

6.4 Future Recommendations

For the Helmholtz cage and Air bearing table, the components we compiled will save time for future teams. We suggest testing all of the components and their connections within the first few weeks of the project to understand what is working, if any extra components are needed, and if anything needs to be replaced. The schematic above shows how everything should be connected, so we suggest beginning with the wiring and using the Gauss meter to measure the magnetic field. Cross-reference the reading on the gauss meter with the magnetometers to ensure that the data is the same. This recommendation will help save time and progress the cage more steadily in the future.

7. Conclusions and Social Impacts

7.1 Conclusions

For the main portion of this project, a team of 8 students were responsible for designing and analyzing a CubeSat in LEO. This report presents the work done by the mechanical design and structures, propulsion, and power subsystems. The other critical subsystems were discussed in detail in separate reports. Each subsystem was able to select components and design their section to fit the mission parameters best while collaborating with the other subsystems to ensure that the mission was successful.

The ODDSat is a 12U CubeSat utilizing the NASA AMES Collapsible Space Telescope (CST) in order to identify and track space debris. The ODDSat was designed to operate in a 700 km Sun-synchronous orbit.

The mechanical design and structures subsystem was limited by the selection of the Rocket Lab Electron rocket as the launch vehicle and a Canisterized Satellite Dispenser used to deploy the ODDSat from the Electron rocket. The use of the CST also limited the volume that the other necessary components of the ODDSat had to fit into. The CAD model of the ODDSat was then analyzed using ANSYS software to conduct vibrational analysis. The results of the analysis confirmed that the satellite met all the requirements that the mechanical subsystem had to meet.

The propulsion system was focused on any orbital maneuvers that were needed to extend the lifetime of the mission. The Busek BGT-X5 monopropellant thruster was chosen as the sole propulsion system. STK was an invaluable resource to model the necessary burns and/or maneuvers that were deemed necessary. The propulsion system was within the constraints set forth by the mechanical and power subsystems.

The power subsystem focused on any power needs that any of the other subsystems required. 6 deployable solar panels were chosen to generate all of the required power, with the power being stored in 4 batteries. An on-board EPS was also selected to distribute the power throughout the ODDSat.

The secondary objective of this project was to understand the ADC Testbed, including the Helmholtz Cage and the Air Bearing Table, and continue creating it so that magnetorquers can be used on it to better understand the effects if a magnetic field. While shipping parts and time constraints prevented us from progressing as much as originally hoped, we were able to understand the workings of the testbed and compile tools and components that will save time for future teams working on this project.

7.2 Societal Impacts

All spacecraft launched into space have the potential to leave debris behind. Debris left at a high enough altitude will not re-enter the atmosphere and instead stays in orbit, potentially in the path of other spacecraft or satellites. As LEO becomes polluted with debris, the chance of debris impact increases, and so does the likelihood of a cascade event known as the Kessler Syndrome, discussed in Section 1. LEO could potentially be rendered unusable and would have lasting societal impacts.

There are thousands of satellites currently in LEO. A few well-known satellites in LEO are the Hubble Telescope, SpaceX's StarLink, and the International Space Station. As debris stays in orbit at high altitudes, a collision could occur with these satellites. Even small debris can have catastrophic effects on the satellite it damages. One study specifically studies space debris colliding with solar arrays. While it is not currently possible to measure the impacts in space, experiments were conducted in a lab to understand the consequences. The study found that when debris impacts at a higher velocity, the electrons discharged will increase in temperature and density. The results hypothesize that the faster the object moves, the more detrimental the collision [51]. Satellites in orbit may become operationally unstable and useless. Satellites with a shorter lifetime than expected become an economic problem. Funding is put into the building and upkeep of the satellite over many years. If the satellite's mission ends early, some of the money will go to waste.

Additionally, future missions will become increasingly difficult. Launch windows will be much more complicated to navigate, making missions scarcer. Like the previous economic impact, it may become more challenging to fund LEO missions since the chance of early shut down is increasingly evident. Without these satellites in orbit, space research would become much more complicated, and there would be little to no way to advance our knowledge.

Having missions become scarcer due to funding and the current debris will also limit missions beyond LEO. Satellites would eventually reach the end of their mission lifetime. Replacing the necessary satellites in Geostationary Operational Environmental (GEO) orbit would become impossible, meaning those satellites would be decommissioned as well. GEO satellites include weather satellites (such as National Oceanic and Atmospheric Administration (NOAA)) and communication satellites for telemetry. Scientific research and knowledge would regress if these were not operational since we would not have access to any information generated by these satellites.

Another issue with space debris is that no active governing body regulates it. Since space is not part of any one country, continent, or governing body on Earth, there are many varying regulations about putting space debris into LEO. One country's government may not have any rules for protecting LEO, while another organization may have specific rules to follow once a mission is complete. Not having a single set of regulations for all space forces, both private and public sector, can create issues in relationships with other governing bodies. It also means that while an organization is fighting against space debris, its efforts are negated by another organization that is less careful. Showing how much debris is in LEO and that it is an increasing issue would push governing bodies to find a united resolution.

References

[1] Kessler, D. J., and Cour-Palais, B. G., *Collision Frequency of Artificial Satellites: The Creation of a Debris Belt,* Journal of Geophysical Research, Vol. 83, No. A6, 1978, pp. 2637–2646. doi:10.1029/JA083iA06p02637.

[2] National Aeronautics and Space Administration. (2022, September 29). *Ares: Orbital Debris Program Office: Frequently asked questions*. ARES | Orbital Debris Program Office | Frequently Asked Questions. Retrieved October 13, 2022, from https://www.orbitaldebris.jsc.nasa.gov/faq/.

[3] Morton, M., and Roberts, T., *Joint Space Operations Center (JSPOC) Mission System (JMS)*, AMOS Technologies Conference, Maui Economic Development Board, Inc., Maui, HI, 2011, p 6.

[4] Shannon Ryan, Eric L. Christiansen, *Hypervelocity impact testing of advanced materials and structures for micrometeoroid and orbital debris shielding*, Acta Astronautica, Volume 83, 2013, Pages 216-231, ISSN 0094-5765, https://doi.org/10.1016/j.actaastro.2012.09.012.

[5] Shoots, D., *Update on 3 Major Debris Clouds*, Orbital Debris Quarterly, Vol. 14, No.2, 2010, pp. 1–3.

[6] Christiansen, E., Hyde, J., and Bernhard, R., *Space Shuttle Debris and Meteoroid Impacts*, Advances in Space Research, Vol. 34, No. 5, 2004, pp. 1097–1103.

[7] J. R. Carl, G. D. Arndt, B. A. Bourgoise and I. Paz, "Space-borne radar detection of orbital debris," *Proceedings of GLOBECOM '93. IEEE Global Telecommunications Conference*, 1993, pp. 939-943 vol.2, doi: 10.1109/GLOCOM.1993.318216.

[8] Creed, Lewis & Graham, Julie & Jenkins, Ciaran & Diaz Riofrio, Sebastian & Wilson, Andrew & Vasile, Massimiliano. (2021*). STRATHcube: The Design of a CubeSat for Space Debris Detection Using In-Orbit Passive Bistatic Radar.*

[9] P. S. Baranov, R. S. Siryi and A. S. Sahnyuk, *A Wide-field Optical System for Detecting Space Debris Based on a Cubesat-Type Spacecraft*, 2021 IEEE Conference of Russian Young Researchers in Electrical and Electronic Engineering (ElConRus), 2021, pp. 94-97, doi: 10.1109/ElConRus51938.2021.9396409.

[10] Xiongjun. Fu, Guoman. Liu and Meiguo. Gao, *Overview of orbital debris detection using spaceborne radar*, 2008 3rd IEEE Conference on Industrial Electronics and Applications, 2008, pp. 1071-1074, doi: 10.1109/ICIEA.2008.4582681.

[11] Johnstone, Alicia et al., *CubeSat Design Specification*, California Polytechnic State University

[12] Howell, Elizabeth. "Cubesats: Tiny Payloads, Huge Benefits for Space Research." Space.com. Space, June 19, 2018. https://www.space.com/34324-cubesats.html#:~:text=The%20cubesat%20design%20was%20first,expensive%20to%20build%20and%20launch.

[13] Jackson, Shanessa. "NASA's CubeSat Launch Initiative." NASA. NASA, February 17, 2017. https://www.nasa.gov/directorates/heo/home/CubeSats_initiative.

[14] Bigelow, Andrew Timothy, and Cyle Anthony Hawkins. 2011. Attitude Determination and Control, On Board Computing & Communication Subsystem Design for a Cubesat Mission.: Worcester Polytechnic Institute.

[15] Dawson, Elizabeth I, Dianna M Velez, and Nell Elizabeth Nassiff. 2012. Attitude Determination and Control Subsystem Design for a Cubesat. : Worcester Polytechnic Institute.
[16] Lu, Ye, Assaad T Farhat, Alan Thomas Snapp, and Jighjigh Tersoo Ivase. 2013. Attitude Determination and Control System for Cubesat. Greenbelt: Worcester Polytechnic Institute.
[17] Gadoury, James, Jack Arnis Agolli, and Andrew M Rathbun. 2017. Design and Analysis of the Sphinx-Ng Cubesat. : Worcester Polytechnic Institute.
[18] Lu, Ye. 2015. Cubesat Design and Attitude Control with Micro Pulsed Plasma Thrusters.: Worcester Polytechnic Institute.
[19] Maki, Colin, Adam M Koubeck, Tristam Winship, and Matthew T Sanchy. 2018. Design of Cubesats for Formation Flying & for Extreme Low Earth Orbit.: Worcester Polytechnic Institute.
[20] Galliath, Robaire C. 2020. Design and Analysis of a Cubesat.: Worcester Polytechnic Institute.
[21] Mileti, John M., Allison L Robatzek, Alia R Brown, Matthew St Jean, William R Cooley, Sydney E Messey, and Alexander D Klenk. 2021. Magnetospheric Nanosat Design.: Worcester Polytechnic Institute.
[22] Gagnon, Jeremy, Drake Tierney, and Christopher Ritter. 2022. Design of a Cubesat for an Ionospheric Science Mission-2.: Worcester Polytechnic Institute.
[23] Rocket Lab USA, Inc. (2022, November 1). *Payload User's Guide*. rocketlabusa.com. Retrieved March 6, 2023, from https://www.rocketlabusa.com/assets/Uploads/Electron-Payload-User-Guide-7.0.pdf
[24] Agasid, Elwood, Kimberly Ennico-Smith, and Abraham Rademacher. "Collapsible Space Telescope for Nanosatellites." NASA Ames Research Center, August 2013.
[25] Henize, K. G., O'Neill, C. A., Mulrooney, M. K., & Anz-Meador, P. (1994). Optical properties of orbital debris. *Journal of Spacecraft and Rockets*, *31*(4), 671–677. https://doi.org/10.2514/3.26494.
[26] J. G. Williams and G. A. McCue, "An Analysis of Satellite Optical Characteristics Data," Planetary and Space Science Vol. 14 (1966) pp. 839-847.
[27] Bowen, I. S. "Limiting Visual Magnitude." *Publications of the Astronomical Society of the Pacific* 59 (1947): 253. https://doi.org/10.1086/125960.
[28] "Canisterized Satellite Dispenser." Planetary Systems Corporation, August 2018.
[29] Kristina Lemmer, Propulsion for CubeSats, Acta Astronautica, Volume 134, 2017, Pages 231-243, ISSN 0094-5765, https://doi.org/10.1016/j.actaastro.2017.01.048.
[30] NASA. (2016). *Electrospray thrusters boost efficiency, precision*. NASA. Retrieved March 1, 2023, from https://spinoff.nasa.gov/Spinoff2016/ip_9.html
[31] Sutton, G. P., & Biblarz, O. (2017). *Rocket Propulsion Elements*. John Wiley & Sons, Inc.
[32] *BGT-X5 monoprop*. Busek. (n.d.). Retrieved December 18, 2022, from https://www.busek.com/bgtx5
[33] Dunbar, B. (2016, January 11). *Ion Propulsion*. NASA. Retrieved March 1, 2023, from https://www.nasa.gov/centers/glenn/about/fs21grc.html
[34] *Thrustme*. ThrustMe. (n.d.). Retrieved December 18, 2022, from https://www.thrustme.fr/
[35] National Aeronautics and Space Administration. (n.d.). *Hall Effect Thruster Technologies*. NASA Transfer Technology Program. Retrieved March 1, 2023, from https://technology.nasa.gov/patent/LEW-TOPS-34

[36] Busek Co. Inc. (n.d.). *Hall thrusters*. Busek. Retrieved March 1, 2023, from https://www.busek.com/hall-thrusters
[37] *BHT-100 - static1.squarespace.com*. (n.d.). Retrieved December 18, 2022, from https://static1.squarespace.com/static/60df2bfb6db9752ed1d79d44/t/6154811d7ac4036af765f736/1632928031263/BHT_100_v1.0.pdf
[38] Federal Communications Commission. (2022, September 29). FCC Adopts New '5-Year Rule' For Deorbiting Satellites To Address Growing Risk Of Orbital Debris. *FCC Adopts New '5-Year Rule' for Deorbiting Satellites*. Retrieved from https://www.fcc.gov/document/fcc-adopts-new-5-year-rule-deorbiting-satellites.
[39] *Space debris: Feel the burn*. ESA. (2021, April 28). Retrieved February 24, 2023, from https://www.esa.int/Space_Safety/Clean_Space/Space_debris_feel_the_burn#.Y_j2QJRRAL8.link
[40] Wertz, J. R., Everett, D. F., & Puschell, J. J. (2011). *Space Mission Engineering: The New SMAD*. Microcosm Press.
[41] Erickson, K. (2021, July 22). *What is the solar cycle?* NASA. Retrieved March 20, 2023, from https://spaceplace.nasa.gov/solar-cycles/en/
[42] *Solar cycle 25 forecast update*. Solar Cycle 25 Forecast Update | NOAA / NWS Space Weather Prediction Center. (2019, December 9). Retrieved March 20, 2023, from https://www.swpc.noaa.gov/news/solar-cycle-25-forecast-update
[43] "U.S. Energy Information Administration - EIA - Independent Statistics and Analysis." Photovoltaics and electricity - U.S. Energy Information Administration (EIA). Accessed December 18, 2022. https://www.eia.gov/energyexplained/solar/photovoltaics-and-electricity.php.
[44] "6U Deployable Solar Array CubeSat Solar Panel." CubeSat by EnduroSat, October 13, 2022. https://www.endurosat.com/cubesat-store/cubesat-solar-panels/6u-deployable-solar-array/.
[45] Wertz, J. R., & Larson, W. J. (1999). 11.4.1 Power Sources. In *Space mission analysis and design* (3rd ed., pp. 414–414). essay, Microcosm Press.
[46] Posted in Batteries & Charging. "What Is Maximum Power Point Tracking (MPPT)." Northern Arizona Wind & Sun. Accessed December 18, 2022. https://www.solar-electric.com/learning-center/mppt-solar-charge-controllers.html/.
[47] *28V/250W Electrical Power Subsystem (EPS) / datasheet*. Ibeos. (2021, July). Retrieved March 3, 2023, from https://www.ibeos.com/28v-eps-datasheet
[48] *28V / 135 WHR Battery / Datasheet*. Ibeos. (2021, September). Retrieved March 3, 2023, from https://www.ibeos.com/28v-battery-datasheet
[49] Ning, G., & Popov, B. N. (2004). Cycle life modeling of lithium-ion batteries. *Journal of The Electrochemical Society*, *151*(10). https://doi.org/10.1149/1.1787631
[50] *High energy, long cycle life and low maintenance lithium- ion cell for ...* EaglePicher Technologies. (2019). Retrieved March 3, 2023, from https://www.eaglepicher.com/sites/default/files/LP32975%2012%20Ah%20Space%20Cell%200123.pdf
[51] Akahoshi, Y., Nakamura, T., Fukushige, S., Furusawa, N., Kusunoki, S., Machida, Y., Koura, T., Watanabe, K., Hosoda, S., Fujita, T., & Cho, M. (2008). Influence of space debris impact on solar array under power generation. *International Journal of Impact Engineering*, *35*(12), 1678–1682. https://doi.org/10.1016/j.ijimpeng.2008.07.048

Appendices

Appendix A: Hohmann Transfer MATLAB Code

```
alt_i = 683*10^3; %initial altitude (m)
alt_f = 700*10^3; %final altitude (m)
r_E = 6.37814*10^6; %(m)
mu_E = 3.986*10^14; % standard gravitational parameter (m^3/s^2);
r_t_1 = r_E + alt_i;
r_t_p = r_t_1;
r_n_1 = r_t_p;
r_t_a = r_E + alt_f;
a_t = (r_t_a+r_t_p)/2;
eps_t = -mu_E/(2*a_t);
v_t_1 = sqrt(2*(eps_t+((mu_E)/r_t_1)));
v_i_1 = sqrt(mu_E/r_n_1);
v_f_1 = v_t_1;
v_n_1 = v_i_1;
DelV_1 = v_f_1 - v_i_1;
r_t_2 = r_t_a;
v_i_2 = sqrt(2*(eps_t+((mu_E)/r_t_2)));
v_t_2 = v_i_2;
r_0_2 = r_t_a;
v_f_2 = sqrt(mu_E/r_0_2);
DelV_2 = v_f_2 - v_i_2;
DelVTot = DelV_1 + DelV_2;
```

Appendix B: Blender and STK COLLADA File


```
<?xml version="1.0" encoding="utf-8"?>

<COLLADA xmlns="http://www.collada.org/2005/11/COLLADASchema" version="1.4.1"
xmlns:xsi="http://www.w3.org/2001/XMLSchema-instance">

  <asset>

    <contributor>

      <author>Blender User</author>

      <authoring_tool>Blender 3.3.1 commit date:2022-10-04, commit time:18:35, hash:b292cfe5a936</authoring_tool>

    </contributor>

    <created>2022-12-14T17:29:45</created>

    <modified>2022-12-14T17:29:45</modified>

    <unit name="meter" meter="1"/>

    <up_axis>Z_UP</up_axis>

  </asset>

  <library_effects>

    <effect id="Material-effect">

      <profile_COMMON>

        <technique sid="common">

          <lambert>

            <emission>

              <color sid="emission">0 0 0 1</color>

            </emission>

            <diffuse>

              <color sid="diffuse">1 0.7678673 0.8189839 1</color>

            </diffuse>

            <index_of_refraction>
```

```
          <float sid="ior">1.45</float>
        </index_of_refraction>
      </lambert>
    </technique>
  </profile_COMMON>
</effect>
<effect id="Material_001-effect">
  <profile_COMMON>
    <technique sid="common">
      <lambert>
        <emission>
          <color sid="emission">0 0 0 1</color>
        </emission>
        <diffuse>
          <color sid="diffuse">0.1402947 0.2311604 0.8000001 1</color>
        </diffuse>
        <index_of_refraction>
          <float sid="ior">1.45</float>
        </index_of_refraction>
      </lambert>
    </technique>
  </profile_COMMON>
</effect>
<effect id="Material_002-effect">
  <profile_COMMON>
    <technique sid="common">
      <lambert>
```

```
          <emission>
            <color sid="emission">0 0 0 1</color>
          </emission>
          <diffuse>
            <color sid="diffuse">0.8 0.8 0.8 1</color>
          </diffuse>
          <index_of_refraction>
            <float sid="ior">1.45</float>
          </index_of_refraction>
        </lambert>
      </technique>
    </profile_COMMON>
  </effect>
</library_effects>
<library_images/>
<library_materials>
  <material id="Material-material" name="Material">
    <instance_effect url="#Material-effect"/>
  </material>
  <material id="Material_001-material" name="Material.001">
    <instance_effect url="#Material_001-effect"/>
  </material>
  <material id="Material_002-material" name="Material.002">
    <instance_effect url="#Material_002-effect"/>
  </material>
</library_materials>
<library_geometries>
```

<geometry id="Cube_013-mesh" name="Cube.013">

<mesh>

<source id="Cube_013-mesh-positions">

<float_array id="Cube_013-mesh-positions-array" count="639">-0.002881348 -0.1549686 -0.1 0.3392321 -0.6950884 -0.09900003 -0.002881348 -0.4969686 -0.1 -0.002881348 -0.1549686 0.1 0.3392321 -0.6950884 0.101 -0.002881348 0.5290315 -0.1 -0.002881348 -0.1549685 -0.1 -0.00426793 -0.6950884 -0.09900003 -0.002881348 -0.1549685 0.1 -0.00426793 -0.6950884 0.101 -0.002881348 0.1870314 -0.1 0.005818665 -0.4969686 -0.1 -0.002881348 0.1870314 0.1 -0.00426793 -0.6941379 0.1009999 -0.002881348 0.5290315 0.1 -0.00426793 -0.4941379 -0.09900015 -0.00426793 -0.6941379 -0.09900015 0.005818665 -0.1549685 -0.1 0.005818665 -0.1549686 -0.1 0.005818665 -0.1549685 0.1 0.004432022 -0.4970884 -0.09899991 0.005818665 -0.1549686 0.1 0.004432022 -0.4970884 0.1010001 -0.00426793 -0.4970884 0.001000106 -0.002881348 -0.2404685 -0.1 0.005818665 0.1870314 -0.1 0.005818665 0.5290315 -0.1 -0.00426793 -0.6910884 -0.09899997 -0.002881348 -0.3259686 -0.1 -0.00426793 -0.6910884 0.1010001 0.005818665 0.5290315 0.1 0.004432022 -0.6910884 -0.09899997 0.004432022 -0.6910884 0.1010001 -0.002881348 -0.4114686 -0.1 0.005818665 0.1870314 0.1 -0.00426793 -0.6910884 0.001000046 0.004432022 -0.6910884 0.001000046 -0.002881348 -0.4114686 0.1 -0.002881348 -0.3259686 0.1 -0.002881348 0.4435315 -0.1 -0.002881348 -0.2404686 0.1 -0.002881348 0.1015314 -0.1 -0.002881348 0.01603144 -0.1 0.005818665 -0.4114686 -0.1 -0.002881348 0.3580315 -0.1 0.005818665 -0.3259686 -0.1 -0.002881348 -0.06946861 -0.1 0.005818665 -0.2404686 -0.1 0.005818665 -0.2404685 0.1 -0.002881348 0.2725315 -0.1 0.005818665 -0.3259686 0.1 -0.002881348 0.2725315 0.1 0.005818665 -0.4114686 0.1 -0.002881348 -0.06946861 0.1 -0.002881348 0.01603138 0.1 -0.002881348 -0.1549685 0 -0.002881348 0.3580315 0.1 -0.002881348 0.1015313 0.1 0.005818665 -0.1549685 0 -0.002881348 0.4435314 0.1 0.005818665 -0.2404686 0 0.005818665 0.2725315 -0.1 0.005818665 -0.06946861 -0.1 0.005818665 -0.3259686 0 0.005818665 -0.4114686 0 0.005818665 0.3580315 -0.1 0.005818665 0.01603138 -0.1 -0.002881348 -0.4114686 0 -0.002881348 -0.3259686 0 0.005818665 0.4435314 -0.1 0.005818665 0.1015313 -0.1 -0.002881348 -0.2404686 0 -9.21667e-4 -0.2284685 0.01200002 0.005818665 0.1015314 0.1 0.005818665 0.4435315 0.1 -9.21667e-4 -0.2284685 0.08799999 -9.21667e-4 -0.1669685 0.08799999 0.005818665 0.3580315 0.1 -9.21667e-4 -0.1669685 0.01200002 0.005818665 0.01603144 0.1 -9.21667e-4 -0.4849686 0.01200002 0.005818665 -0.06946861 0.1 -9.21667e-4 -0.4849686 0.08799999 0.005818665 0.2725315 0.1 -0.002881348 -0.1549686 0 -9.21667e-4 -0.4234687 0.08799999 -9.21667e-4 -0.4234687 0.01200002 -0.002881348 0.1870314 0 -9.21667e-4 -0.3994686 0.01200002 -0.002881348 0.5290315 0 -9.21667e-4 -0.3994686 0.08799999 0.005818665 0.1870314 0 -9.21667e-4 -0.3379687 0.08799999 0.005818665 0.5290315 0 -9.21667e-4 -0.3379687 0.01200002 0.005818665 -0.1549686 0 -9.21667e-4 -0.3139686 0.01200002 0.005818665 0.4435314 0 -9.21667e-4 -0.3139686 0.08799999 0.005818665 0.1015313 0 -9.21667e-4 -0.2524687 0.08799999 0.005818665 0.01603138 0 0.005818665 0.3580315 0 -9.21667e-4 -0.2524687 0.01200002 0.005818665 -0.06946861 0 -9.21667e-4 -0.3139686 -0.08799999 0.005818665 0.2725315 0 -9.21667e-4 -0.3139686 -0.01200002 -0.002881348 0.2725315 0 -9.21667e-4 -0.2524686 -0.01200002 -9.21667e-4 -0.2524686 -0.08799999 -0.002881348 -0.06946861 0 -9.21667e-4 -0.3994686 -0.08799999 -0.002881348 0.3580315 0 -0.002881348 0.01603138 0 -9.21667e-4 -0.3994686 -0.01200002 -0.002881348 0.1015313 0 -9.21667e-4 -0.3379686 -0.01200002 -0.002881348 0.4435314 0 -9.21667e-4 -0.3379686 -0.08799999 -9.21667e-4 -0.4849686 -0.08799999 -9.21667e-4 0.1135314 0.01200002 -9.21667e-4 -0.4849686 -0.01200002 -9.21667e-4 0.4555315 0.01200002 -9.21667e-4 0.1135314 0.08799999 -9.21667e-4 -0.4234687 -0.01200002 -9.21667e-4 0.4555315 0.08799999 -9.21667e-4 -0.4234687 -0.08799999 -9.21667e-4 0.1750314 0.08799999 -9.21667e-4 -0.2284685 -0.08799999 -9.21667e-4 0.5170316 0.08799999 -9.21667e-4 -0.2284685 -0.01200002 -9.21667e-4 0.1750314 0.01200002 -9.21667e-4 -0.1669685 -0.01200002 -9.21667e-4 0.5170316 0.01200002 -9.21667e-4 -0.1669685 -0.08799999 -9.21667e-4 -0.1429686 0.01200002 -9.21667e-4 0.1990314 0.01200002 -9.21667e-4 -0.1429686 0.08799999 -9.21667e-4 0.1990314 0.08799999 -9.21667e-4 -0.08146864 0.08799999 -9.21667e-4 0.2605314 0.08799999 -9.21667e-4 -0.08146864 0.01200002 -9.21667e-4 0.2605314 0.01200002 -9.21667e-4 0.2845315 0.01200002 -9.21667e-4 -0.05746859 0.01200002 -9.21667e-4 -0.05746859 0.08799999 -9.21667e-4 0.2845315 0.08799999 -9.21667e-4 0.00403136 0.08799999 -9.21667e-4 0.3460314 0.08799999 -9.21667e-4 0.3460314 0.01200002 -9.21667e-4 0.00403136 0.01200002 -9.21667e-4 0.0280314 0.01200002 -9.21667e-4 0.3700315 0.01200002 -9.21667e-4 0.0280314 0.08799999 -9.21667e-4 0.3700315 0.08799999 -9.21667e-4 0.08953136 0.08799999 -9.21667e-4 0.4315314 0.08799999 -9.21667e-4 0.08953136 0.01200002 -9.21667e-4 0.4315314 0.01200002 -9.21667e-4 0.3700315 -0.08799999 -9.21667e-4 0.0280314 -0.08799999 -9.21667e-4 0.0280314 -0.01200002 -9.21667e-4 0.3700315 -0.01200002 -9.21667e-4 0.4315316 -0.01200002 -9.21667e-4 0.08953142 -0.01200002 -9.21667e-4 0.4315316 -0.08799999 -9.21667e-4 0.08953142 -0.08799999 -9.21667e-4 -0.05746859 -0.08799999 -9.21667e-4 0.2845315 -0.08799999 -9.21667e-4 -0.05746859 -0.01200002 -9.21667e-4 0.2845315 -0.01200002 -9.21667e-4 0.004031419 -0.01200002 -9.21667e-4 0.3460315 -0.01200002 -9.21667e-4 0.004031419 -0.08799999 -9.21667e-4 0.3460315 -0.08799999 -9.21667e-4 -0.1429686 -0.08799999 -9.21667e-4 0.1990314 -0.08799999 -9.21667e-4 -0.1429686 -0.01200002 -9.21667e-4 0.1990314 -0.01200002 -9.21667e-4 -0.08146864 -0.01200002 -9.21667e-4 0.2605314 -0.01200002 -9.21667e-4 0.2605314 -0.08799999 -9.21667e-4 -0.08146864 -0.08799999 -9.21667e-4 0.4555315 -0.08799999 -9.21667e-4 0.1135314 -0.08799999 -9.21667e-4 0.1135314 -0.01200002 -9.21667e-4 0.4555315 -0.01200002 -9.21667e-4 0.1750314 -0.01200002 -9.21667e-4 0.5170316 -0.01200002 -9.21667e-4 0.1750314 -0.08799999 -9.21667e-4 0.5170316 -0.08799999 -0.002881348 -0.1549686 0.09999996 -0.002881348 -0.1549686 0 -0.002881348 -0.1549686 0 -0.002881348 -0.1549686 -0.09999996 -0.002881348 -0.1549685 0.09999996 -0.002881348 -0.1549685 0 -0.002881348 -0.1549685 0 -0.002881348 -0.1549685 -

0.09999996 0.005818665 -0.4950883 0.1 0.005818665 -0.4950883 0 -0.002881348 -0.4950883 0.1 0.005818665 -0.4969686 -0.09900003 -0.002881348 -0.4969686 -0.09900003 0.005818665 -0.4950883 -0.09900003 -0.002574265 -0.4950883 0.09811973 -0.002574265 -0.4950883 0.001880288 -0.002881348 -0.4950883 0 -0.002574265 -0.4950883 -0.001880288 -0.002718031 -0.4959686 -0.09900003 -0.002574265 -0.4950883 -0.09811973 -0.002718031 -0.4950883 -0.09900003</float_array>

<technique_common>

<accessor source="#Cube_013-mesh-positions-array" count="213" stride="3">

<param name="X" type="float"/>

<param name="Y" type="float"/>

<param name="Z" type="float"/>

</accessor>

</technique_common>

</source>

<source id="Cube_013-mesh-normals">

<float_array id="Cube_013-mesh-normals-array" count="309">-1 0 0 1 0 0 0 0 -1 0 0 1 -0.9869264 0.1611714 0 -0.9869264 0 -0.1611716 -0.9869264 -0.1611714 0 -0.9869265 0 0.1611714 -0.9869263 0.1611726 0 -0.9869265 0 -0.1611714 -0.9869264 0 0.1611714 -0.9869265 0 -0.1611714 -0.9869265 0 0.1611714 -0.9869265 0 -0.1611714 -0.9869265 0 0.1611714 -0.9869263 0.1611722 0 -0.9869264 -0.1611722 0 -0.9869264 0.1611714 0 -0.9869265 0 -0.1611714 -0.9869264 0 0.1611716 -0.9869263 0.1611726 0 -0.9869264 0 -0.1611714 -0.9869264 -0.1611714 0 -0.9869265 0 0.1611713 0 1 0 -0.9869266 0.1611707 0 -0.9869264 0 -0.1611714 -0.9869263 -0.1611722 0 -0.9869264 0 0.1611713 -0.9869265 0 -0.1611714 -0.9869265 0 0.1611715 -0.9869265 0 -0.1611713 -0.9869264 0 0.1611714 -0.9869265 0 -0.1611714 -0.9869261 -0.1611738 0 -0.9869265 0 0.1611715 -0.9869265 0 -0.1611714 -0.9869264 0 0.1611716 -0.9869265 0 -0.1611715 -0.9869264 -0.1611722 0 -0.9865978 -0.1631712 0 -0.9869264 0.1611718 0 -0.9869264 0 -0.1611715 -0.9869264 0 0.1611714 -0.9869265 0 0.1611714 -0.9869267 0.1611705 0 -0.9869264 0.1611718 0 -0.9869261 0 0.1611731 -0.9869264 0 -0.1611714 -0.9869263 -0.1611722 0 -0.9869265 0 0.1611714 -1.00163e-6 0 1 -1.00163e-6 0 1 1.00163e-6 0 -1 1.00163e-6 0 -1 -0.9869265 -0.1611714 0 -0.9869264 0 0.1611714 -0.9869263 0.1611726 0 -0.9869263 0 -0.1611722 -0.9996877 0.02499216 0 -0.9869329 0.1611319 0 -0.9869264 0.1611716 0 -0.9869264 0 -0.1611714 -0.9869265 -0.1611715 0 -0.9869265 0 0.1611715 -0.9869265 0.1611714 0 -0.9869263 0 -0.1611722 -0.999654 0.02630668 0 -0.9863939 0.164399 0 -0.9869264 0 -0.1611715 -0.9869265 0 0.1611715 5.00803e-7 0 1 1.50243e-6 0 1 -5.00803e-7 0 -1 -1.50243e-6 0 -1 -0.9869266 0.1611707 0 -0.9869264 0 -0.1611713 -0.9869264 0 -0.1611715 -0.9869265 0 0.1611714 -0.9869264 0 -0.1611716 -0.9869265 0 0.1611713 -0.9869263 -0.1611724 -1.9149e-7 -0.9869265 0 0.1611714 -0.9869264 0 0.1611715 -0.9869266 0.1611708 1.91488e-7 -0.9869264 0 0.1611715 -1.00163e-6 0 1 1 0 0 -0.9863939 -0.164399 0 -0.9869264 0 0.1611714 -0.9869258 3.77383e-7 -0.1611757 -0.9869264 0 -0.1611712 -0.9869258 0 0.1611753 -0.9869264 0 0.1611715 -0.9869258 0 -0.1611753 -0.9869264 0 -0.1611714 -0.9869276 4.03041e-7 0.1611647 -0.9869264 0 0.1611713 -0.9869263 0 0.161172 -0.9869329 -0.1611319 0 -0.9869263 -0.1611722 0 -0.9869264 0 0.1611723 -0.9996877 -0.02499216 0</float_array>

<technique_common>

<accessor source="#Cube_013-mesh-normals-array" count="103" stride="3">

<param name="X" type="float"/>

<param name="Y" type="float"/>

<param name="Z" type="float"/>

</accessor>

</technique_common>

</source>

<source id="Cube_013-mesh-map-0">

<float_array id="Cube_013-mesh-map-0-array" count="2142">0.61 0.1962719 0.5150001 0.2412281 0.5150001 0.1962719 0.5 0.6875 0.625 0.75 0.5 0.75 0.375 0.6875 0.125 0.75 0.125 0.6875 0.625 0.6875 0.875 0.75 0.625 0.75 0.875 0.5 0.625 0.5625 0.625 0.5 0.875 0.5625 0.625 0.625 0.625 0.5625 0.875 0.625 0.625 0.6875 0.625 0.625 0.375 0.5 0.125 0.5625 0.125 0.5 0.375 0.5625 0.125 0.625 0.125 0.5625 0.375 0.625 0.125 0.6875 0.125 0.625 0.5 0.5 0.625 0.5625 0.5 0.5625 0.5 0.5625 0.625 0.625 0.5 0.625 0.5 0.625 0.625 0.6875 0.5 0.6875 0.61 0.008771896 0.515 0.05372804 0.515 0.008771896 0.6100001 0.07127195 0.515 0.116228 0.515 0.07127195 0.6100001 0.1337719 0.515 0.178728 0.515 0.1337719 0.485 0.1337719 0.39 0.178728 0.3900001 0.1337718 0.485 0.07127195 0.39 0.116228 0.3900001 0.07127189 0.485 0.008771896 0.39 0.05372804 0.39 0.008771896 0.5 0.625 0.375 0.6875 0.375 0.625 0.5 0.5625 0.375 0.625 0.375 0.5625 0.5 0.5 0.375 0.5625 0.375 0.5 0.375 0.6875 0.5 0.75 0.375 0.75 0.485 0.1962719 0.3900001 0.2412281 0.3900001 0.1962719 0.625 0.1875 0.5150001 0.1962719 0.5 0.1875 0.625 0.25 0.61 0.1962719 0.625 0.1875 0.5 0.25 0.61 0.2412281 0.625 0.25 0.5 0.1875 0.5150001 0.2412281 0.5 0.25 0.515 0.008771896 0.6249999 0 0.61 0.008771896 0.625 0 0.625 0.0625 0.61 0.05372804 0.5 0.0625 0.61 0.05372804 0.625 0.0625 0.515 0.05372804 0.5 0.0625 0.5 0 0.625 0.0625 0.515 0.07127195 0.5 0.0625 0.625 0.125 0.6100001 0.07127195 0.625 0.0625 0.5 0.125 0.61 0.1162281 0.625 0.125 0.5 0.0625 0.515 0.116228 0.5 0.125 0.625 0.125 0.515 0.1337719 0.5 0.125 0.625 0.1875 0.6100001 0.1337719 0.625 0.125 0.5 0.1875 0.61 0.178728 0.625 0.1875 0.5 0.125 0.515 0.178728 0.5 0.1875 0.375 0.125 0.485 0.1337719 0.3900001 0.1337718 0.5 0.1875 0.485 0.1337719 0.5 0.125 0.5 0.1875 0.39 0.178728 0.485 0.1787281 0.375 0.125 0.39 0.178728 0.375 0.1875 0.5 0.0625 0.3900001 0.07127189 0.375 0.0625 0.5 0.125 0.485 0.07127195 0.5 0.0625 0.5 0.125 0.39 0.116228 0.485 0.1162281 0.375 0.0625 0.39 0.116228 0.375 0.125 0.39 0.008771896 0.5 0 0.485 0.008771896 0.5 0 0.5 0.0625 0.485 0.05372804 0.375 0.0625 0.485 0.05372804 0.5 0.0625 0.39 0.05372804 0.375 0.0625 0.375 0 0.375 0.1875 0.485 0.1962719 0.3900001 0.1962719 0.5 0.25 0.485 0.1962719 0.5 0.1875 0.375 0.25 0.485 0.2412281 0.5 0.25 0.375 0.1875 0.3900001 0.2412281 0.375 0.25 0.61 0.1962719 0.5150001 0.2412281 0.5150001 0.1962719 0.625 0.25 0.5 0.5 0.5 0.25 0.625 0.6875 0.5 0.75 0.5 0.6875 0.375 0.6875 0.125 0.75 0.125 0.6875 0.875 0.6875 0.625 0.75 0.625 0.6875 0.875 0.5 0.625 0.5625 0.625 0.5 0.875 0.5625 0.625 0.625 0.625 0.5625 0.875 0.625 0.625 0.6875 0.625 0.625 0.375 0.5 0.125 0.5625 0.125 0.5 0.375 0.5625 0.125 0.625 0.125 0.5625 0.375 0.625 0.125 0.6875 0.125 0.625 0.5 0.5 0.625 0.5625 0.5 0.5625 0.5 0.5625 0.625 0.625 0.5 0.625 0.5 0.625 0.625 0.6875 0.5 0.6875 0.61 0.008771896 0.515 0.05372804 0.515 0.008771896 0.6100001 0.07127195 0.515 0.116228 0.515 0.07127195 0.6100001 0.1337719 0.515 0.178728 0.515 0.1337719 0.485 0.1337719 0.39 0.178728 0.3900001 0.1337718 0.485 0.07127195 0.39 0.116228 0.3900001 0.07127189 0.485 0.008771896 0.39 0.05372804 0.39 0.008771896 0.5 0.625 0.375 0.6875 0.375 0.625 0.5 0.5625 0.375 0.625 0.375 0.5625 0.5 0.5 0.375 0.5625 0.375 0.5 0.5 0.6875 0.375 0.75 0.375 0.6875 0.5 0.25 0.375 0.5 0.375 0.25 0.485 0.1962719 0.3900001 0.2412281 0.3900001 0.1962719 0.625 0.1875 0.5150001 0.1962719 0.5 0.1875 0.625 0.25 0.61 0.1962719 0.625 0.1875 0.5 0.25 0.61 0.2412281 0.625 0.25 0.5 0.25 0.5150001 0.1962719 0.5150001 0.2412281 0.625 0 0.515 0.008771896 0.5 0 0.625 0.0625 0.61 0.008771896 0.625 0 0.5 0.0625 0.61 0.05372804 0.625 0.0625 0.5 0 0.515 0.05372804 0.5 0.0625 0.625 0.0625 0.515 0.07127195 0.5 0.0625 0.625 0.125 0.6100001 0.07127195 0.625 0.0625 0.5 0.125 0.61 0.1162281 0.625 0.125 0.5 0.0625 0.515 0.116228 0.5 0.125 0.625 0.125 0.515 0.1337719 0.5 0.125 0.625 0.1875 0.6100001 0.1337719 0.625 0.125 0.5 0.1875 0.61 0.178728 0.625 0.1875 0.5 0.1875 0.515 0.1337719 0.515 0.178728 0.375 0.125 0.485 0.1337719 0.3900001 0.1337718 0.5 0.1875 0.485 0.1337719 0.5 0.125 0.5 0.1875 0.39 0.178728 0.485 0.1787281 0.375 0.125 0.39 0.178728 0.375 0.1875 0.5 0.0625 0.3900001 0.07127189 0.375 0.0625 0.5 0.125 0.485 0.07127195 0.5 0.0625 0.5 0.125 0.39 0.116228 0.485 0.1162281 0.375 0.0625 0.39 0.116228 0.375 0.125 0.5 0 0.39 0.008771896 0.375 0 0.5 0.0625 0.485 0.008771896 0.5 0 0.375 0.0625 0.485 0.05372804 0.5 0.0625 0.375 0 0.39 0.05372804 0.375 0.0625 0.375 0.1875 0.485 0.1962719 0.3900001 0.1962719 0.5 0.25 0.485 0.1962719 0.5 0.1875 0.375 0.25 0.485 0.2412281 0.5 0.25 0.375 0.1875 0.3900001 0.2412281 0.375 0.25 0.61 0.1962719 0.5150001 0.2412281 0.5150001 0.1962719 0.625 0.6875 0.5 0.7486255 0.5 0.6875 0.375 0.6875 0.125 0.75 0.125 0.6875 0.625 0.6875 0.875 0.7486255 0.625 0.7486255 0.875 0.5 0.625 0.5625 0.625 0.5000001 0.875 0.5625 0.625 0.625 0.625 0.5625 0.875 0.625 0.625 0.6875 0.625 0.625 0.125 0.5625 0.375 0.5 0.375 0.5625 0.375 0.5625 0.125 0.625 0.125 0.5625 0.375 0.625 0.125 0.6875 0.125 0.625 0.625 0.5625 0.5 0.5000001 0.625 0.5000001 0.5 0.5625 0.625 0.625 0.5 0.625 0.5 0.625 0.625 0.6875 0.5 0.6875 0.61 0.008771896 0.515 0.05372804 0.515 0.008771896 0.6100001 0.07127195 0.515 0.116228 0.515 0.07127195 0.6100001 0.1337719 0.515 0.178728 0.515 0.1337719 0.485 0.1337719 0.39 0.178728 0.3900001 0.1337718 0.485 0.07127195 0.39 0.116228 0.3900001 0.07127189 0.485 0.008771896 0.39 0.05372804 0.39 0.008771896 0.5 0.625 0.375 0.6875 0.375 0.625 0.5 0.5625 0.375 0.625 0.375 0.5625 0.375 0.5625 0.5 0.5000001 0.5 0.5625 0.37625 0.7486256 0.375 0.75 0.375 0.6875 0.485 0.1962719 0.3900001 0.2412281 0.3900001 0.1962719 0.625 0.1875 0.5150001 0.1962719 0.5 0.1875 0.625 0.25 0.61 0.2412281 0.61 0.1962719 0.61 0.2412281 0.5000001 0.25 0.5150001 0.2412281 0.5150001 0.2412281 0.5000001 0.25 0.5000001 0.25 0.61 0.008771896 0.5023503 0.001374423 0.6226497 0.001374423 0.61 0.008771896 0.625 0.001374423 0.61 0.05372804 0.5 0.0625 0.61 0.05372804 0.625 0.0625 0.515 0.05372804 0.5 0.0625 0.5 0.001374423 0.625 0.0625 0.515 0.07127195 0.5 0.0625 0.625 0.125 0.6100001 0.07127195 0.625 0.0625 0.5 0.125 0.61 0.1162281 0.625 0.125 0.5 0.0625 0.515 0.116228 0.5 0.125 0.625 0.125 0.515 0.1337719 0.5 0.125 0.625 0.1875 0.6100001 0.1337719 0.625 0.125 0.5 0.1875 0.61

0.178728 0.625 0.1875 0.5 0.125 0.515 0.178728 0.5 0.1875 0.375 0.125 0.485 0.1337719 0.3900001 0.1337718 0.5 0.1875
0.485 0.1337719 0.5 0.125 0.5 0.1875 0.39 0.178728 0.485 0.1787281 0.375 0.125 0.39 0.178728 0.375 0.1875 0.5 0.0625
0.3900001 0.07127189 0.375 0.0625 0.5 0.125 0.485 0.07127195 0.5 0.0625 0.5 0.125 0.39 0.116228 0.485 0.1162281 0.375
0.0625 0.39 0.116228 0.375 0.125 0.37625 7.30991e-4 0.375 0 0.37625 0 0.39 0.008771896 0.4976496 0.001374423 0.485
0.008771896 0.485 0.008771896 0.5 0.001374423 0.485 0.05372804 0.375 0.0625 0.485 0.05372804 0.5 0.0625 0.375 0 0.37625
7.30989e-4 0.37625 0.001374423 0.375 0.1875 0.485 0.1962719 0.3900001 0.1962719 0.5000001 0.25 0.485 0.2412281 0.485
0.1962719 0.485 0.2412281 0.3750001 0.25 0.3900001 0.2412281 0.375 0.25 0.375 0.1875 0.3900001 0.1962719 0.61
0.1962719 0.61 0.2412281 0.5150001 0.2412281 0.5 0.6875 0.625 0.6875 0.625 0.75 0.375 0.6875 0.375 0.75 0.125 0.75 0.625
0.6875 0.875 0.6875 0.875 0.75 0.875 0.5 0.875 0.5625 0.625 0.5625 0.875 0.5625 0.875 0.625 0.625 0.625 0.875 0.625 0.875
0.6875 0.625 0.6875 0.375 0.5 0.375 0.5625 0.125 0.5625 0.375 0.5625 0.375 0.625 0.125 0.625 0.375 0.625 0.375 0.6875 0.125
0.6875 0.5 0.5 0.625 0.5 0.625 0.5625 0.5 0.5625 0.625 0.5625 0.625 0.625 0.5 0.625 0.625 0.625 0.625 0.6875 0.61
0.008771896 0.61 0.05372804 0.515 0.05372804 0.6100001 0.07127195 0.61 0.1162281 0.515 0.116228 0.6100001 0.1337719
0.61 0.178728 0.515 0.178728 0.485 0.1337719 0.485 0.1787281 0.39 0.178728 0.485 0.07127195 0.485 0.1162281 0.39
0.116228 0.485 0.008771896 0.485 0.05372804 0.39 0.05372804 0.5 0.625 0.5 0.6875 0.375 0.6875 0.5 0.5625 0.5 0.625 0.375
0.625 0.5 0.5 0.5 0.5625 0.375 0.5625 0.375 0.6875 0.5 0.6875 0.5 0.75 0.485 0.1962719 0.485 0.2412281 0.3900001 0.2412281
0.625 0.1875 0.61 0.1962719 0.5150001 0.1962719 0.625 0.25 0.61 0.2412281 0.61 0.1962719 0.5 0.25 0.5150001 0.2412281
0.61 0.2412281 0.5 0.1875 0.5150001 0.1962719 0.5150001 0.2412281 0.515 0.008771896 0.5000001 0 0.6249999 0 0.61
0.05372804 0.61 0.008771896 0.625 0 0.625 0 0.625 0 0.61 0.05372804 0.5 0.0625 0.515 0.05372804 0.61 0.05372804 0.5 0 0.5
0 0.515 0.008771896 0.515 0.008771896 0.515 0.05372804 0.5 0 0.625 0.0625 0.6100001 0.07127195 0.515 0.07127195 0.625
0.125 0.61 0.1162281 0.6100001 0.07127195 0.5 0.125 0.515 0.116228 0.61 0.1162281 0.5 0.0625 0.515 0.07127195 0.515
0.116228 0.625 0.125 0.6100001 0.1337719 0.515 0.1337719 0.625 0.1875 0.61 0.178728 0.6100001 0.1337719 0.5 0.1875
0.515 0.178728 0.61 0.178728 0.5 0.125 0.515 0.1337719 0.515 0.178728 0.375 0.125 0.5 0.125 0.485 0.1337719 0.5 0.1875
0.485 0.1787281 0.485 0.1337719 0.5 0.1875 0.375 0.1875 0.39 0.178728 0.375 0.125 0.3900001 0.1337718 0.39 0.178728 0.5
0.0625 0.485 0.07127195 0.3900001 0.07127189 0.5 0.125 0.485 0.1162281 0.485 0.07127195 0.5 0.125 0.375 0.125 0.39
0.116228 0.375 0.0625 0.3900001 0.07127189 0.39 0.116228 0.39 0.008771896 0.3750001 0 0.5 0 0.485 0.05372804 0.485
0.008771896 0.5 0 0.5 0 0.5 0 0.485 0.05372804 0.375 0.0625 0.39 0.05372804 0.485 0.05372804 0.375 0 0.375 0 0.39
0.008771896 0.39 0.008771896 0.39 0.05372804 0.375 0 0.375 0.1875 0.5 0.1875 0.485 0.1962719 0.5 0.25 0.485 0.2412281
0.485 0.1962719 0.375 0.25 0.3900001 0.2412281 0.485 0.2412281 0.375 0.1875 0.3900001 0.1962719 0.3900001 0.2412281
0.61 0.1962719 0.61 0.2412281 0.5150001 0.2412281 0.625 0.25 0.625 0.5 0.5 0.5 0.625 0.6875 0.625 0.75 0.5 0.75 0.375
0.6875 0.375 0.75 0.125 0.75 0.875 0.6875 0.875 0.75 0.625 0.75 0.875 0.5 0.875 0.5625 0.625 0.5625 0.875 0.5625 0.875 0.625
0.625 0.625 0.875 0.625 0.875 0.6875 0.625 0.6875 0.375 0.5 0.375 0.5625 0.125 0.5625 0.375 0.5625 0.375 0.625 0.125 0.625
0.375 0.625 0.375 0.6875 0.125 0.6875 0.5 0.5 0.625 0.5 0.625 0.5625 0.5 0.5625 0.625 0.5625 0.625 0.625 0.5 0.625 0.625
0.625 0.625 0.6875 0.61 0.008771896 0.61 0.05372804 0.515 0.05372804 0.6100001 0.07127195 0.61 0.1162281 0.515
0.116228 0.6100001 0.1337719 0.61 0.178728 0.515 0.178728 0.485 0.1337719 0.485 0.1787281 0.39 0.178728 0.485
0.07127195 0.485 0.1162281 0.39 0.116228 0.485 0.008771896 0.485 0.05372804 0.39 0.05372804 0.5 0.625 0.5 0.6875 0.375
0.6875 0.5 0.5625 0.5 0.625 0.375 0.625 0.5 0.5 0.5 0.5625 0.375 0.5625 0.5 0.6875 0.5 0.75 0.375 0.75 0.5 0.25 0.5 0.5 0.375
0.5 0.485 0.1962719 0.485 0.2412281 0.3900001 0.2412281 0.625 0.1875 0.61 0.1962719 0.5150001 0.1962719 0.625 0.25 0.61
0.2412281 0.61 0.1962719 0.5 0.25 0.5150001 0.2412281 0.61 0.2412281 0.5 0.25 0.5 0.1875 0.5150001 0.1962719 0.625 0 0.61
0.008771896 0.515 0.008771896 0.625 0.0625 0.61 0.05372804 0.61 0.008771896 0.5 0.0625 0.515 0.05372804 0.61
0.05372804 0.5 0 0.515 0.008771896 0.515 0.05372804 0.625 0.0625 0.6100001 0.07127195 0.515 0.07127195 0.625 0.125 0.61
0.1162281 0.6100001 0.07127195 0.5 0.125 0.515 0.116228 0.61 0.1162281 0.5 0.0625 0.515 0.07127195 0.515 0.116228 0.625
0.125 0.6100001 0.1337719 0.515 0.1337719 0.625 0.1875 0.61 0.178728 0.6100001 0.1337719 0.5 0.1875 0.515 0.178728 0.61
0.178728 0.5 0.1875 0.5 0.125 0.515 0.1337719 0.375 0.125 0.5 0.125 0.485 0.1337719 0.5 0.1875 0.485 0.1787281 0.485
0.1337719 0.5 0.1875 0.375 0.1875 0.39 0.178728 0.375 0.125 0.3900001 0.1337718 0.39 0.178728 0.5 0.0625 0.485
0.07127195 0.3900001 0.07127189 0.5 0.125 0.485 0.1162281 0.485 0.07127195 0.5 0.125 0.375 0.125 0.39 0.116228 0.375
0.0625 0.3900001 0.07127189 0.39 0.116228 0.5 0 0.485 0.008771896 0.39 0.008771896 0.5 0.0625 0.485 0.05372804 0.485
0.008771896 0.375 0.0625 0.39 0.05372804 0.485 0.05372804 0.375 0 0.39 0.008771896 0.39 0.05372804 0.375 0.1875 0.5
0.1875 0.485 0.1962719 0.5 0.25 0.485 0.2412281 0.485 0.1962719 0.375 0.25 0.3900001 0.2412281 0.485 0.2412281 0.375
0.1875 0.3900001 0.1962719 0.3900001 0.2412281 0.61 0.1962719 0.61 0.2412281 0.5150001 0.2412281 0.625 0.6875 0.625
0.7486255 0.5 0.7486255 0.375 0.6875 0.375 0.75 0.125 0.75 0.625 0.6875 0.875 0.6875 0.875 0.7486255 0.875 0.5 0.875
0.5625 0.625 0.5625 0.875 0.5625 0.875 0.625 0.625 0.625 0.875 0.625 0.875 0.6875 0.625 0.6875 0.125 0.5625 0.125
0.5000001 0.375 0.5 0.375 0.5625 0.375 0.625 0.125 0.625 0.375 0.625 0.375 0.6875 0.125 0.6875 0.625 0.5625 0.5 0.5625 0.5
0.5000001 0.5 0.5625 0.625 0.5625 0.625 0.625 0.5 0.625 0.625 0.625 0.625 0.6875 0.61 0.008771896 0.61 0.05372804 0.515
0.05372804 0.6100001 0.07127195 0.61 0.1162281 0.515 0.116228 0.6100001 0.1337719 0.61 0.178728 0.515 0.178728 0.485
0.1337719 0.485 0.1787281 0.39 0.178728 0.485 0.07127195 0.485 0.1162281 0.39 0.116228 0.485 0.008771896 0.485
0.05372804 0.39 0.05372804 0.5 0.625 0.5 0.6875 0.375 0.6875 0.5 0.5625 0.5 0.625 0.375 0.625 0.375 0.5625 0.375 0.5 0.5
0.5000001 0.37625 0.7486256 0.37625 0.75 0.375 0.75 0.375 0.6875 0.5 0.6875 0.37625 0.7486256 0.5 0.6875 0.5 0.7486255
0.37625 0.7486256 0.485 0.1962719 0.485 0.2412281 0.3900001 0.2412281 0.625 0.1875 0.61 0.1962719 0.5150001 0.1962719
0.61 0.1962719 0.625 0.1875 0.625 0.25 0.625 0.25 0.625 0.25 0.61 0.2412281 0.61 0.2412281 0.625 0.25 0.5000001 0.25 0.5
0.1875 0.5150001 0.1962719 0.5000001 0.25 0.5150001 0.1962719 0.5150001 0.2412281 0.5000001 0.25 0.61 0.008771896
0.515 0.008771896 0.5023503 0.001374423 0.6226497 0.001374483 0.625 0.001374423 0.61 0.008771896 0.625 0.001374423
0.625 0.0625 0.61 0.05372804 0.5 0.0625 0.515 0.05372804 0.61 0.05372804 0.5023504 0.001374423 0.515 0.008771896 0.5

0.001374423 0.515 0.008771896 0.515 0.05372804 0.5 0.001374423 0.625 0.0625 0.6100001 0.07127195 0.515 0.07127195 0.625 0.125 0.61 0.1162281 0.6100001 0.07127195 0.5 0.125 0.515 0.116228 0.61 0.1162281 0.5 0.0625 0.515 0.07127195 0.515 0.116228 0.625 0.125 0.6100001 0.1337719 0.515 0.1337719 0.625 0.1875 0.61 0.178728 0.6100001 0.1337719 0.5 0.1875 0.515 0.178728 0.61 0.178728 0.5 0.125 0.515 0.1337719 0.515 0.178728 0.375 0.125 0.5 0.125 0.485 0.1337719 0.5 0.1875 0.485 0.1787281 0.485 0.1337719 0.5 0.1875 0.375 0.1875 0.39 0.178728 0.375 0.125 0.3900001 0.1337718 0.39 0.178728 0.5 0.0625 0.485 0.07127195 0.3900001 0.07127189 0.5 0.125 0.485 0.1162281 0.485 0.07127195 0.5 0.125 0.375 0.125 0.39 0.116228 0.375 0.0625 0.3900001 0.07127189 0.39 0.116228 0.39 0.008771896 0.3773503 0.001374423 0.4976496 0.001374423 0.4976496 0.001374423 0.5 0.001374423 0.485 0.008771896 0.5 0.001374423 0.5 0.0625 0.485 0.05372804 0.375 0.0625 0.39 0.05372804 0.485 0.05372804 0.3773504 0.001374423 0.39 0.008771896 0.37625 0.001374423 0.39 0.008771896 0.39 0.05372804 0.37625 0.001374423 0.39 0.05372804 0.375 0.0625 0.37625 0.001374423 0.375 0.0625 0.375 0 0.37625 0.001374423 0.375 0.1875 0.5 0.1875 0.485 0.1962719 0.485 0.1962719 0.5 0.1875 0.5000001 0.25 0.5000001 0.25 0.5 0.25 0.485 0.2412281 0.485 0.2412281 0.5 0.25 0.3750001 0.25 0.3900001 0.1962719 0.3900001 0.2412281 0.3750001 0.25 0.3750001 0.25 0.375 0.25 0.3900001 0.1962719</float_array>

<technique_common>

<accessor source="#Cube_013-mesh-map-0-array" count="1071" stride="2">

<param name="S" type="float"/>

<param name="T" type="float"/>

</accessor>

</technique_common>

</source>

<vertices id="Cube_013-mesh-vertices">

<input semantic="POSITION" source="#Cube_013-mesh-positions"/>

</vertices>

<triangles material="Material-material" count="60">

<input semantic="VERTEX" source="#Cube_013-mesh-vertices" offset="0"/>

<input semantic="NORMAL" source="#Cube_013-mesh-normals" offset="1"/>

<input semantic="TEXCOORD" source="#Cube_013-mesh-map-0" offset="2" set="0"/>

<p>104 1 3 19 1 4 58 1 5 62 2 6 6 2 7 46 2 8 25 2 21 41 2 22 10 2 23 70 2 24 42 2 25 41 2 26 66 2 27 46 2 28 42 2 29 101 1 57 62 1 58 66 1 59 99 1 60 66 1 61 70 1 62 91 1 63 70 1 64 25 1 65 62 1 66 58 1 67 17 1 68 14 24 171 93 24 172 89 24 173 83 1 174 91 1 175 106 1 176 61 2 177 10 2 178 49 2 179 26 2 192 39 2 193 5 2 194 69 2 195 44 2 196 39 2 197 65 2 198 49 2 199 44 2 200 102 1 228 61 1 229 65 1 230 97 1 231 65 1 232 69 1 233 93 1 234 69 1 235 26 1 236 106 1 237 25 1 238 61 1 239 89 24 240 26 24 241 5 24 242 52 1 345 201 1 346 64 1 347 43 2 348 2 2 349 33 2 350 24 2 363 18 2 364 47 2 365 47 2 366 28 2 367 24 2 368 45 2 369 33 2 370 28 2 371 63 1 399 43 1 400 45 1 401 60 1 402 45 1 403 47 1 404 47 1 405 95 1 406 60 1 407 205 1 408 11 1 409 43 1 410 104 1 516 81 1 517 19 1 518 62 2 519 17 2 520 6 2 521 25 53 534 70 53 535 41 53 536 70 54 537 66 54 538 42 54 539 66 2 540 62 2 541 46 2 542 101 1 570 104 1 571 62 1 572 99 1 573 101 1 574 66 1 575 91 1 576 99 1 577 70 1 578 62 1 579 104 1 580 58 1 581 14 24 696 30 24 697 93 24 698 83 1 699 34 1 700 91 1 701 61 2 702 25 2 703 10 2 704 26 73 717 69 73 718 39 73 719 69 74 720 65 74 721 44 74 722 65 2 723 61 2 724 49 2 725 102 1 753 106 1 754 61 1 755 97 1 756 102 1 757 65 1 758 93 1 759 97 1 760 69 1 761 106 1 762 91 1 763 25 1 764 89 24 765 93 24 766 26 24 767 52 1 870 200 1 871 201 1 872 43 2 873 11 2 874 2 2 875 24 2 888 0 2 889 18 2 890 47 54 891 45 54 892 28 54 893 45 2 894 43 2 895 33 2 896 63 1 924 64 1 925 43 1 926 60 1 927 63 1 928 45 1 929 47 1 930 18 1 931 95 1 932 205 1 933 203 1 934 11 1 935 43 87 936 64 87 937 205 87 938 64 1 939 201 1 940 205 1 941</p>

</triangles>

<triangles material="Material_001-material" count="48">

<input semantic="VERTEX" source="#Cube_013-mesh-vertices" offset="0"/>

<input semantic="NORMAL" source="#Cube_013-mesh-normals" offset="1"/>

<input semantic="TEXCOORD" source="#Cube_013-mesh-map-0" offset="2" set="0"/>

<p>124 0 0 132 0 1 121 0 2 138 0 39 142 0 40 136 0 41 146 0 42 151 0 43 145 0 44 154 0 45 158 0 46 152 0 47 162 0 48 167 0 49 161 0 50 170 0 51 174 0 52 168 0 53 178 0 54 183 0 55 176 0 56 186 0 69 190 0 70 185 0 71 126 0 168 134 0 169 123 0 170 139 0 210 143 0 211 137 0 212 147 0 213 150 0 214 144 0 215 155 0 216 159 0 217 153 0 218 163 0 219 166 0 220 160 0 221 171 0 222 175 0 223 169 0 224 179 0 225 182 0 226 177 0 227 187 0 243 191 0 244 184 0 245 75 0 342 78 0 343 72 0 344 82 0 381 86 0 382 80 0 383 90 0 384 94 0 385 88 0 386 98 0 387 103 0 388 96 0 389 107 0 390 110 0 391 105 0 392 115 0 393 119 0 394 112 0 395 122 0 396 127 0 397 120 0 398 131 0 411 135 0 412 129 0 413 124 0 513 128 0 514 132 0 515 138 0 552 140 0 553 142 0 554 146 0 555 148 0 556 151 0 557 154 0 558 156 0 559 158 0 560 162 0 561 165 0 562 167 0 563 170 0 564 172 0 565 174 0 566 178 0 567 180 0 568 183 0 569 186 0 582 188 0 583 190 0 584 126 0 693 130 0 694 134 0 695 139 0 735 141 0 736 143 0 737 147 0 738 149 0 739 150 0 740 155 0 741 157 0 742 159 0 743 163 0 744 164 0 745 166 0 746 171 0 747 173 0 748 175 0 749 179 0 750 181 0 751 182 0 752 187 0 768 189 0 769 191 0 770 75 0 867 76 0 868 78 0 869 82 0 906 85 0 907 86 0 908 90 0 909 92 0 910 94 0 911 98 0 912 100 0 913 103 0 914 107 0 915 109 0 916 110 0 917 115 0 918 117 0 919 119 0 920 122 0 921 125 0 922 127 0 923 131 0 942 133 0 943 135 0 944</p>

</triangles>

<triangles material="Material_002-material" count="249">

<input semantic="VERTEX" source="#Cube_013-mesh-vertices" offset="0"/>

<input semantic="NORMAL" source="#Cube_013-mesh-normals" offset="1"/>

<input semantic="TEXCOORD" source="#Cube_013-mesh-map-0" offset="2" set="0"/>

<p>81 3 9 8 3 10 19 3 11 12 3 12 73 3 13 34 3 14 57 3 15 79 3 16 73 3 17 54 3 18 81 3 19 79 3 20 91 1 30 73 1 31 99 1 32 99 1 33 79 1 34 101 1 35 101 1 36 81 1 37 104 1 38 57 4 72 121 4 73 116 4 74 12 5 75 124 5 76 57 5 77 87 6 78 128 6 79 12 6 80 116 7 81 132 7 82 87 7 83 136 8 84 196 8 85 138 8 86 8 9 87 53 9 88 140 9 89 111 6 90 140 6 91 53 6 92 142 10 93 111 10 94 55 10 95 53 4 96 145 4 97 111 4 98 54 11 99 146 11 100 53 11 101 114 6 102 148 6 103 54 6 104 111 12 105 151 12 106 114 12 107 54 4 108 152 4 109 114 4 110 57 13 111 154 13 112 54 13 113 116 6 114 156 6 115 57 6 116 114 14 117 158 14 118 116 14 119 42 15 120 162 15 121 161 15 122 116 11 123 162 11 124 114 11 125 116 16 126 167 16 127 165 16 128 42 7 129 167 7 130 41 7 131 111 17 132 168 17 133 46 17 134 114 18 135 170 18 136 111 18 137 114 16 138 174 16 139 172 16 140 46 19 141 174 19 142 42 19 143 176 20 144 198 20 145 178 20 146 55 21 147 111 21 148 180 21 149 46 22 150 180 22 151 111 22 152 183 23 153 46 23 154 6 23 155 41 15 156 186 15 157 185 15 158 87 11 159 186 11 160 116 11 161 10 22 162 188 22 163 87 22 164 41 7 165 190 7 166 10 7 167 51 3 180 34 3 181 83 3 182 14 3 183 74 3 184 30 3 185 59 3 186 77 3 187 74 3 188 56 3 189 83 3 190 77 3 191 93 1 201 74 1 202 97 1 203 97 1 204 77 1 205 102 1 206 102 1 207 83 1 208 106 1 209 59 25 246 123 25 247 118 25 248 14 26 249 126 26 250 59 26 251 89 27 252 130 27 253 14 27 254 89 28 255 123 28 256 134 28 257 12 4 258 137 4 259 87 4 260 51 29 261 139 29 262 12 29 263 108 6 264 141 6 265 51 6 266 87 14 267 143 14 268 108 14 269 51 4 270 144 4 271 108 4 272 56 18 273 147 18 274 51 18 275 113 6 276 149 6 277 56 6 278 108 30 279 150 30 280 113 30 281 56 4 282 153 4 283 113 4 284 59 31 285 155 31 286 56 31 287 118 27 288 157 27 289 59 27 290 118 32 291 153 32 292 159 32 293 44 15 294 163 15 295 160 15 296 118 33 297 163 33 298 113 33 299 118 34 300 166 34 301 164 34 302 44 35 303 166 35 304 39 35 305 108 17 306 169 17 307 49 17 308 113 36 309 171 36 310 108 36 311 113 16 312 175 16 313 173 16 314 49 37 315 175 37 316 44 37 317 87 17 318 177 17 319 10 17 320 108 13 321 179 13 322 87 13 323 49 22 324 181 22 325 108 22 326 10 7 327 182 7 328 49 7 329 39 15 330 187 15 331 184 15 332 89 38 333 187 38 334 118 38 335 5 27 336 189 27 337 89 27 338 39 12 339 191 12 340 5 12 341 52 3 351 202 3 352 200 3 353 3 3 354 48 3 355 21 3 356 40 3 357 50 3 358 48 3 359 38 3 360 52 3 361 50 3 362 48 1 372 95 1 373 21 1 374 60 1 375 50 1 376 63 1 377 63 1 378 52 1 379 64 1 380 40 4 414 72 4 415 71 4 416 3 29 417 76 29 418 75 29 419 76 39 420 193 39 421 78 39 422 78 40 423 193 40 424 84 40 425 82 41 426 207 41 427 206 41 428 82 42 429 202 42 430 85 42 431 67 6 432 85 6 433 37 6 434 86 43 435 67 43 436 208 43 437 37 4 438 88 4 439 67 4 440 38 18 441 90 18 442 37 18 443 68 6 444 92 6 445 38 6 446 67 44 447 94 44 448 68 44 449 38 4 450 96 4 451 68 4 452 40 18 453 98 18 454 38 18 455 71 6 456 100 6 457 40 6 458 68 30 459 103 30 460 71 30 461 28 15 462 107 15 463 105 15 464 71 36 465 107 36 466 68 36 467 71 16 468 110

16 469 109 16 470 28 35 471 110 35 472 24 35 473 67 17 474 112 17 475 33 17 476 68 36 477 115 36 478 67 36 479 68 16 480 119 16 481 117 16 482 33 35 483 119 35 484 28 35 485 210 45 486 2 45 487 204 45 488 120 46 489 209 46 490 122 46 491 122 5 492 208 5 493 125 5 494 33 22 495 125 22 496 67 22 497 2 47 498 210 47 499 212 47 500 24 15 501 131 15 502 129 15 503 84 48 504 133 48 505 131 48 506 133 49 507 195 49 508 135 49 509 0 50 510 24 50 511 129 50 512 81 3 522 53 3 523 8 3 524 12 51 525 57 51 526 73 51 527 57 52 528 54 52 529 79 52 530 54 3 531 53 3 532 81 3 533 91 1 543 34 1 544 73 1 545 99 1 546 73 1 547 79 1 548 101 1 549 79 1 550 81 1 551 57 17 585 124 17 586 121 17 587 12 42 588 128 42 589 124 42 590 87 55 591 132 55 592 128 55 593 116 56 594 121 56 595 132 56 596 136 57 597 197 57 598 196 57 599 140 58 600 138 58 601 196 58 602 196 59 603 8 59 604 140 59 605 111 55 606 142 55 607 140 55 608 55 60 609 197 60 610 136 60 611 136 14 612 142 14 613 55 14 614 53 17 615 146 17 616 145 17 617 54 42 618 148 42 619 146 42 620 114 55 621 151 55 622 148 55 623 111 12 624 145 12 625 151 12 626 54 17 627 154 17 628 152 17 629 57 5 630 156 5 631 154 5 632 116 55 633 158 55 634 156 55 635 114 12 636 152 12 637 158 12 638 42 61 639 114 61 640 162 61 641 116 62 642 165 62 643 162 62 644 116 63 645 41 63 646 167 63 647 42 64 648 161 64 649 167 64 650 111 65 651 170 65 652 168 65 653 114 62 654 172 62 655 170 62 656 114 63 657 42 63 658 174 63 659 46 64 660 168 64 661 174 64 662 176 57 663 199 57 664 198 57 665 180 66 666 178 66 667 198 66 668 198 67 669 55 67 670 180 67 671 46 6 672 183 6 673 180 6 674 6 68 675 199 68 676 176 68 677 176 12 678 183 12 679 6 12 680 41 61 681 116 61 682 186 61 683 87 69 684 188 69 685 186 69 686 10 6 687 190 6 688 188 6 689 41 70 690 185 70 691 190 70 692 51 3 705 12 3 706 34 3 707 14 71 708 59 71 709 74 71 710 59 72 711 56 72 712 77 72 713 56 3 714 51 3 715 83 3 716 93 1 726 30 1 727 74 1 728 97 1 729 74 1 730 77 1 731 102 1 732 77 1 733 83 1 734 59 75 771 126 75 772 123 75 773 14 76 774 130 76 775 126 76 776 89 16 777 134 16 778 130 16 779 89 30 780 118 30 781 123 30 782 12 17 783 139 17 784 137 17 785 51 77 786 141 77 787 139 77 788 108 55 789 143 55 790 141 55 791 87 78 792 137 78 793 143 78 794 51 17 795 147 17 796 144 17 797 56 79 798 149 79 799 147 79 800 113 55 801 150 55 802 149 55 803 108 80 804 144 80 805 150 80 806 56 17 807 155 17 808 153 17 809 59 79 810 157 79 811 155 79 812 118 16 813 159 16 814 157 16 815 118 78 816 113 78 817 153 78 818 44 61 819 113 61 820 163 61 821 118 69 822 164 69 823 163 69 824 118 81 825 39 81 826 166 81 827 44 28 828 160 28 829 166 28 830 108 65 831 171 65 832 169 65 833 113 69 834 173 69 835 171 69 836 113 63 837 44 63 838 175 63 839 49 82 840 169 82 841 175 82 842 87 65 843 179 65 844 177 65 845 108 33 846 181 33 847 179 33 848 49 6 849 182 6 850 181 6 851 10 83 852 177 83 853 182 83 854 39 84 855 118 84 856 187 84 857 89 76 858 189 76 859 187 76 860 5 27 861 191 27 862 189 27 863 39 85 864 184 85 865 191 85 866 52 3 876 37 3 877 202 3 878 3 86 879 40 86 880 48 86 881 40 52 882 38 52 883 50 52 884 38 3 885 37 3 886 52 3 887 48 1 897 60 1 898 95 1 899 60 1 900 48 1 901 50 1 902 63 1 903 50 1 904 52 1 905 40 17 945 75 17 946 72 17 947 75 9 948 40 9 949 3 9 950 3 88 951 192 88 952 76 88 953 76 27 954 192 27 955 193 27 956 71 14 957 72 14 958 84 14 959 72 89 960 78 89 961 84 89 962 82 46 963 80 46 964 207 46 965 206 90 966 202 90 967 82 90 968 202 91 969 37 91 970 85 91 971 67 55 972 86 55 973 85 55 974 207 92 975 80 92 976 208 92 977 80 19 978 86 19 979 208 19 980 37 17 981 90 17 982 88 17 983 38 79 984 92 79 985 90 79 986 68 55 987 94 55 988 92 55 989 67 64 990 88 64 991 94 64 992 38 17 993 98 17 994 96 17 995 40 79 996 100 79 997 98 79 998 71 55 999 103 55 1000 100 55 1001 68 80 1002 96 80 1003 103 80 1004 28 61 1005 68 61 1006 107 61 1007 71 69 1008 109 69 1009 107 69 1010 71 63 1011 24 63 1012 110 63 1013 28 82 1014 105 82 1015 110 82 1016 67 65 1017 115 65 1018 112 65 1019 68 69 1020 117 69 1021 115 69 1022 68 63 1023 28 63 1024 119 63 1025 33 93 1026 112 93 1027 119 93 1028 120 41 1029 211 41 1030 209 41 1031 209 94 1032 208 94 1033 122 94 1034 208 95 1035 67 95 1036 125 95 1037 33 6 1038 127 6 1039 125 6 1040 211 96 1041 120 96 1042 212 96 1043 120 89 1044 127 89 1045 212 89 1046 127 97 1047 33 97 1048 212 97 1049 33 98 1050 2 98 1051 212 98 1052 24 61 1053 71 61 1054 131 61 1055 131 13 1056 71 13 1057 84 13 1058 84 99 1059 194 99 1060 133 99 1061 133 100 1062 194 100 1063 195 100 1064 129 101 1065 135 101 1066 195 101 1067 195 102 1068 0 102 1069 129 102 1070</p>

</triangles>

</mesh>

</geometry>

<geometry id="Cube_012-mesh" name="Cube.012">

<mesh>

<source id="Cube_012-mesh-positions">

<float_array id="Cube_012-mesh-positions-array" count="564">-0.002881348 -0.1549686 -0.1 -0.002881348 -0.4969686 -0.1 -0.002881348 -0.1549686 0.1 -0.002881348 -0.4969686 0.1 -0.002881348 0.5290315 -0.1 -0.002881348 -0.1549685 -0.1 -0.002881348 -0.1549685 0.1 -0.002881348 0.1870314 -0.1 0.005818665 -0.4969686 -0.1 -0.002881348 0.1870314 0.1 -0.002881348 0.5290315 0.1 0.005818665 -0.4969686 0.1 0.005818665 -0.1549685 -0.1 0.005818665 -0.1549686 -0.1 0.005818665 -0.1549685 0.1 0.005818665 -0.1549686 0.1 -0.002881348 -0.2404685 -0.1 0.005818665 0.1870314 -0.1 0.005818665 0.5290315 -0.1 -0.002881348 -0.3259686 -0.1 0.005818665 0.5290315 0.1 -0.002881348 -0.4114686 -0.1 0.005818665 0.1870314 0.1 -0.002881348 -0.4114686 0.1 -0.002881348 -0.3259686 0.1 -0.002881348 0.4435315 -0.1 -0.002881348 -0.2404686 0.1 -0.002881348 0.1015314 -0.1 -0.002881348 0.01603144 -0.1 0.005818665 -0.4114686 -0.1 -

0.002881348 0.3580315 -0.1 0.005818665 -0.3259686 -0.1 -0.002881348 -0.06946861 -0.1 0.005818665 -0.2404686 -0.1 0.005818665 -0.2404685 0.1 -0.002881348 0.2725315 -0.1 0.005818665 -0.3259686 0.1 -0.002881348 0.2725315 0.1 0.005818665 -0.4114686 0.1 -0.002881348 -0.06946861 0.1 -0.002881348 0.01603138 0.1 -0.002881348 -0.4969686 0 -0.002881348 -0.1549685 0 -0.002881348 0.3580315 0.1 -0.002881348 0.1015313 0.1 0.005818665 -0.1549685 0 0.005818665 -0.4969686 0 -0.002881348 0.4435314 0.1 0.005818665 -0.2404686 0 0.005818665 0.2725315 -0.1 0.005818665 -0.06946861 -0.1 0.005818665 -0.3259686 0 0.005818665 -0.4114686 0 0.005818665 0.3580315 -0.1 0.005818665 0.01603138 -0.1 -0.002881348 -0.4114686 0 -0.002881348 -0.3259686 0 0.005818665 0.4435314 -0.1 0.005818665 0.1015313 -0.1 -0.002881348 -0.2404686 0 -9.21667e-4 -0.2284685 0.01200002 0.005818665 0.1015314 0.1 0.005818665 0.4435315 0.1 -9.21667e-4 -0.2284685 0.08799999 -9.21667e-4 -0.1669685 0.08799999 0.005818665 0.3580315 0.1 -9.21667e-4 -0.1669685 0.01200002 0.005818665 0.01603144 0.1 -9.21667e-4 -0.4849686 0.01200002 0.005818665 -0.06946861 0.1 -9.21667e-4 -0.4849686 0.08799999 0.005818665 0.2725315 0.1 -0.002881348 -0.1549686 0 -9.21667e-4 -0.4234687 0.08799999 -9.21667e-4 -0.4234687 0.01200002 -0.002881348 0.1870314 0 -9.21667e-4 -0.3994686 0.01200002 -0.002881348 0.5290315 0 -9.21667e-4 -0.3994686 0.08799999 0.005818665 0.1870314 0 -9.21667e-4 -0.3379687 0.08799999 0.005818665 0.5290315 0 -9.21667e-4 -0.3379687 0.01200002 0.005818665 -0.1549686 0 -9.21667e-4 -0.3139686 0.01200002 0.005818665 0.4435314 0 -9.21667e-4 -0.3139686 0.08799999 0.005818665 0.1015313 0 -9.21667e-4 -0.2524687 0.08799999 0.005818665 0.01603138 0 0.005818665 0.3580315 0 -9.21667e-4 -0.2524687 0.01200002 0.005818665 -0.06946861 0 -9.21667e-4 -0.3139686 -0.08799999 0.005818665 0.2725315 0 -9.21667e-4 -0.3139686 -0.01200002 -0.002881348 0.2725315 0 -9.21667e-4 -0.2524686 -0.01200002 -9.21667e-4 -0.2524686 -0.08799999 -0.002881348 -0.06946861 0 -9.21667e-4 -0.3994686 -0.08799999 -0.002881348 0.3580315 0 -0.002881348 0.01603138 0 -9.21667e-4 -0.3994686 -0.01200002 -0.002881348 0.1015313 0 -9.21667e-4 -0.3379686 -0.01200002 -0.002881348 0.4435314 0 -9.21667e-4 -0.3379686 -0.08799999 -9.21667e-4 -0.4849686 -0.08799999 -9.21667e-4 0.1135314 0.01200002 -9.21667e-4 -0.4849686 -0.01200002 -9.21667e-4 0.4555315 0.01200002 -9.21667e-4 0.1135314 0.08799999 -9.21667e-4 -0.4234687 -0.01200002 -9.21667e-4 0.4555315 0.08799999 -9.21667e-4 -0.4234687 -0.08799999 -9.21667e-4 0.1750314 0.08799999 -9.21667e-4 -0.2284685 -0.08799999 -9.21667e-4 0.5170316 0.08799999 -9.21667e-4 -0.2284685 -0.01200002 -9.21667e-4 0.1750314 0.01200002 -9.21667e-4 -0.1669685 -0.01200002 -9.21667e-4 0.5170316 0.01200002 -9.21667e-4 -0.1669685 -0.08799999 -9.21667e-4 -0.1429686 0.01200002 -9.21667e-4 0.1990314 0.01200002 -9.21667e-4 -0.1429686 0.08799999 -9.21667e-4 0.1990314 0.08799999 -9.21667e-4 -0.08146864 0.08799999 -9.21667e-4 0.2605314 0.08799999 -9.21667e-4 -0.08146864 0.01200002 -9.21667e-4 0.2605314 0.01200002 -9.21667e-4 0.2845315 0.01200002 -9.21667e-4 -0.05746859 0.01200002 -9.21667e-4 -0.05746859 0.08799999 -9.21667e-4 0.2845315 0.08799999 -9.21667e-4 0.00403136 0.08799999 -9.21667e-4 0.3460314 0.08799999 -9.21667e-4 0.3460314 0.01200002 -9.21667e-4 0.00403136 0.01200002 -9.21667e-4 0.0280314 0.01200002 -9.21667e-4 0.3700315 0.01200002 -9.21667e-4 0.0280314 0.08799999 -9.21667e-4 0.3700315 0.08799999 -9.21667e-4 0.08953136 0.08799999 -9.21667e-4 0.4315314 0.08799999 -9.21667e-4 0.08953136 0.01200002 -9.21667e-4 0.4315314 0.01200002 -9.21667e-4 0.3700315 -0.08799999 -9.21667e-4 0.0280314 -0.08799999 -9.21667e-4 0.0280314 -0.01200002 -9.21667e-4 0.3700315 -0.01200002 -9.21667e-4 0.4315316 -0.01200002 -9.21667e-4 0.08953142 -0.01200002 -9.21667e-4 0.4315316 -0.08799999 -9.21667e-4 0.08953142 -0.08799999 -9.21667e-4 -0.05746859 -0.08799999 -9.21667e-4 0.2845315 -0.08799999 -9.21667e-4 -0.05746859 -0.01200002 -9.21667e-4 0.2845315 -0.01200002 -9.21667e-4 0.004031419 -0.01200002 -9.21667e-4 0.3460315 -0.01200002 -9.21667e-4 0.004031419 -0.08799999 -9.21667e-4 0.3460315 -0.08799999 -9.21667e-4 -0.1429686 -0.08799999 -9.21667e-4 0.1990314 -0.08799999 -9.21667e-4 -0.1429686 -0.01200002 -9.21667e-4 0.1990314 -0.01200002 -9.21667e-4 -0.08146864 -0.01200002 -9.21667e-4 0.2605314 -0.01200002 -9.21667e-4 0.2605314 -0.08799999 -9.21667e-4 -0.08146864 -0.08799999 -9.21667e-4 0.4555315 -0.08799999 -9.21667e-4 0.1135314 -0.08799999 -9.21667e-4 0.1135314 -0.01200002 -9.21667e-4 0.4555315 -0.01200002 -9.21667e-4 0.1750314 -0.01200002 -9.21667e-4 0.5170316 -0.01200002 -9.21667e-4 0.1750314 -0.08799999 -9.21667e-4 0.5170316 -0.08799999 -0.002881348 -0.1549686 0.09999996 -0.002881348 -0.1549686 0 -0.002881348 -0.1549686 0 -0.002881348 -0.1549686 -0.09999996 -0.002881348 -0.1549685 0.09999996 -0.002881348 -0.1549685 0 -0.002881348 -0.1549685 0 -0.002881348 -0.1549685 -0.09999996</float_array>

<technique_common>

<accessor source="#Cube_012-mesh-positions-array" count="188" stride="3">

<param name="X" type="float"/>

<param name="Y" type="float"/>

<param name="Z" type="float"/>

</accessor>

</technique_common>

</source>

<source id="Cube_012-mesh-normals">

<float_array id="Cube_012-mesh-normals-array" count="276">-1 0 0 1 0 0 0 0 -1 0 0 1 -0.9869264 0.1611714 0 -0.9869264 0 -0.1611716 -0.9869264 -0.1611714 0 -0.9869265 0 0.1611714 -0.9869263 0.1611726 0 -0.9869265 0 -0.1611714 -0.9869264 0 0.1611714 -0.9869265 0 -0.1611714 -0.9869265 0 0.1611714 -0.9869265 0 -0.1611714 -0.9869265 0 0.1611714 -0.9869263 0.1611722 0 -0.9869264 -0.1611722 0 -0.9869264 0.1611714 0 -0.9869264 0 0.1611716 -0.9869263 0.1611726 0 -0.9869264 -0.1611714 0 -0.9869266 0.1611707 0 -0.9869264 0 -0.1611714 -0.9869263 -0.1611722 0 -0.9869264 0 0.1611713 -0.9869265 0 -0.1611714 -0.9869265 0 0.1611715 -0.9869265 0 -0.1611713 -0.9869264 0 0.1611714 -0.9869265 0 -0.1611714 -0.9869261 -0.1611738 0 -0.9869265 0 0.1611715 -0.9869265 0 -0.1611714 -0.9869264 0 0.1611716 -0.9869265 0 -0.1611715 0 -1 0 -0.9869264 -0.1611722 0 -0.9869264 0.1611718 0 -0.9869264 0 -0.1611715 -0.9869265 0 0.1611714 -0.9869264 0.1611718 0 -0.9869264 0 -0.1611716 -0.9869264 0 -0.1611714 -0.9869263 -0.1611722 0 -0.9869265 0 0.1611714 -1.00163e-6 0 1 -1.00163e-6 0 1 1.00163e-6 0 -1 1.00163e-6 0 -1 -0.9869265 -0.1611714 0 -0.9869264 0 0.1611714 -0.9869263 0.1611726 0 -0.9863939 0.164399 0 -0.9869264 0 0.1611714 -0.9869329 0.1611319 0 -0.9869264 0.1611716 0 -0.9869264 0 -0.1611714 -0.9869265 -0.1611715 0 -0.9869265 0 0.1611715 -0.9869265 0.1611714 0 -0.9869264 0 -0.1611714 -0.9869265 0 0.1611713 -0.9869264 0 -0.1611715 -0.9869265 0 0.1611715 5.00803e-7 0 1 1.50243e-6 0 1 -5.00803e-7 0 -1 -1.50243e-6 0 -1 -0.9869266 0.1611707 0 -0.9869264 0 -0.1611713 -0.9869264 0 -0.1611715 -0.9869265 0 0.1611714 -0.9869264 0 -0.1611716 -0.9869265 0 0.1611713 -0.9869263 -0.1611724 -1.9149e-7 -0.9869265 0 0.1611714 -0.9869264 0 0.1611715 -0.9869266 0.1611708 1.91488e-7 -0.9869264 0 0.1611715 -1.00163e-6 0 1 -0.9869265 0 -0.1611714 -0.9863939 -0.164399 0 -0.9869263 0 0.1611722 -0.9996447 -0.02665716 0 -0.9869264 0.1611719 0 -0.9869264 0 0.1611716 -0.9869264 0 0.1611715 -0.9869263 0.1611718 0 -0.9869329 -0.1611319 0 -0.9869263 -0.1611722 0 -0.9869264 0 0.1611723 -0.9996877 -0.02499216 0</float_array>

<technique_common>

<accessor source="#Cube_012-mesh-normals-array" count="92" stride="3">

<param name="X" type="float"/>

<param name="Y" type="float"/>

<param name="Z" type="float"/>

</accessor>

</technique_common>

</source>

<source id="Cube_012-mesh-map-0">

<float_array id="Cube_012-mesh-map-0-array" count="2088">0.61 0.1962719 0.5150001 0.2412281 0.5150001 0.1962719 0.5 0.6875 0.625 0.75 0.5 0.75 0.375 0.6875 0.125 0.75 0.125 0.6875 0.625 0.6875 0.875 0.75 0.625 0.75 0.875 0.5 0.625 0.5625 0.625 0.5 0.875 0.5625 0.625 0.625 0.625 0.5625 0.875 0.625 0.625 0.6875 0.625 0.625 0.375 0.5 0.125 0.5625 0.125 0.5 0.375 0.5625 0.125 0.625 0.125 0.5625 0.375 0.625 0.125 0.6875 0.125 0.625 0.5 0.5 0.625 0.5625 0.5 0.5625 0.5 0.5625 0.625 0.625 0.5 0.625 0.5 0.625 0.625 0.6875 0.5 0.6875 0.61 0.008771896 0.515 0.05372804 0.515 0.008771896 0.6100001 0.07127195 0.515 0.116228 0.515 0.07127195 0.6100001 0.1337719 0.515 0.178728 0.515 0.1337719 0.485 0.1337719 0.39 0.178728 0.3900001 0.1337718 0.485 0.07127195 0.39 0.116228 0.3900001 0.07127189 0.485 0.008771896 0.39 0.05372804 0.39 0.008771896 0.5 0.625 0.375 0.6875 0.375 0.625 0.5 0.5625 0.375 0.625 0.375 0.5625 0.5 0.5 0.375 0.5625 0.375 0.5 0.375 0.6875 0.5 0.75 0.375 0.75 0.485 0.1962719 0.3900001 0.2412281 0.3900001 0.1962719 0.625 0.1875 0.5150001 0.1962719 0.5 0.1875 0.625 0.25 0.61 0.1962719 0.625 0.1875 0.5 0.25 0.61 0.2412281 0.625 0.25 0.5 0.1875 0.5150001 0.2412281 0.5 0.25 0.515 0.008771896 0.6249999 0 0.61 0.008771896 0.625 0.0625 0.61 0.05372804 0.61 0.008771896 0.5 0.0625 0.61 0.05372804 0.625 0.0625 0.5 0 0.515 0.008771896 0.515 0.05372804 0.625 0.0625 0.515 0.07127195 0.5 0.0625 0.625 0.125 0.6100001 0.07127195 0.625 0.0625 0.5 0.125 0.61 0.1162281 0.625 0.125 0.5 0.0625 0.515 0.116228 0.5 0.125 0.625 0.125 0.515 0.1337719 0.5 0.125 0.625 0.1875 0.6100001 0.1337719 0.625 0.125 0.5 0.1875 0.61 0.178728 0.625 0.1875 0.5 0.125 0.515 0.178728 0.5 0.1875 0.375 0.125 0.485 0.1337719 0.3900001 0.1337718 0.5 0.1875 0.485 0.1337719 0.5 0.125 0.5 0.1875 0.39 0.178728 0.485 0.1787281 0.375 0.125 0.39 0.178728 0.375 0.1875 0.5 0.0625 0.3900001 0.07127189 0.375 0.0625 0.5 0.125 0.485 0.07127195 0.5 0.0625 0.5 0.125 0.39 0.116228 0.485 0.1162281 0.375

0.0625 0.39 0.116228 0.375 0.125 0.39 0.008771896 0.5 0 0.485 0.008771896 0.5 0.0625 0.485 0.05372804 0.485 0.008771896
0.375 0.0625 0.485 0.05372804 0.5 0.0625 0.375 0 0.39 0.008771896 0.39 0.05372804 0.375 0.1875 0.485 0.1962719 0.3900001
0.1962719 0.5 0.25 0.485 0.1962719 0.5 0.1875 0.375 0.25 0.485 0.2412281 0.5 0.25 0.375 0.1875 0.3900001 0.2412281 0.375
0.25 0.61 0.1962719 0.5150001 0.2412281 0.5150001 0.1962719 0.625 0.6875 0.5 0.75 0.5 0.6875 0.375 0.6875 0.125 0.75
0.125 0.6875 0.875 0.6875 0.625 0.75 0.625 0.6875 0.875 0.5 0.625 0.5625 0.625 0.5 0.875 0.5625 0.625 0.625 0.625 0.5625
0.875 0.625 0.625 0.6875 0.625 0.625 0.375 0.5 0.125 0.5625 0.125 0.5 0.375 0.5625 0.125 0.625 0.125 0.5625 0.375 0.625
0.125 0.6875 0.125 0.625 0.5 0.5 0.625 0.5625 0.5 0.5625 0.5 0.5625 0.625 0.625 0.5 0.625 0.5 0.625 0.625 0.6875 0.5 0.6875
0.61 0.008771896 0.515 0.05372804 0.515 0.008771896 0.6100001 0.07127195 0.515 0.116228 0.515 0.07127195 0.6100001
0.1337719 0.515 0.178728 0.515 0.1337719 0.485 0.1337719 0.39 0.178728 0.3900001 0.1337718 0.485 0.07127195 0.39
0.116228 0.3900001 0.07127189 0.485 0.008771896 0.39 0.05372804 0.39 0.008771896 0.5 0.625 0.375 0.6875 0.375 0.625 0.5
0.5625 0.375 0.625 0.375 0.5625 0.5 0.5 0.375 0.5625 0.375 0.5 0.5 0.6875 0.375 0.75 0.375 0.6875 0.485 0.1962719 0.3900001
0.2412281 0.3900001 0.1962719 0.625 0.1875 0.5150001 0.1962719 0.5 0.1875 0.625 0.25 0.61 0.1962719 0.625 0.1875 0.5
0.25 0.61 0.2412281 0.625 0.25 0.5 0.25 0.5150001 0.1962719 0.5150001 0.2412281 0.625 0 0.515 0.008771896 0.5 0 0.625
0.0625 0.61 0.008771896 0.625 0 0.5 0.0625 0.61 0.05372804 0.625 0.0625 0.5 0 0.515 0.05372804 0.5 0.0625 0.625 0.0625
0.515 0.07127195 0.5 0.0625 0.625 0.125 0.6100001 0.07127195 0.625 0.0625 0.5 0.125 0.61 0.1162281 0.625 0.125 0.5 0.0625
0.515 0.116228 0.5 0.125 0.625 0.125 0.515 0.1337719 0.5 0.125 0.625 0.1875 0.6100001 0.1337719 0.625 0.125 0.5 0.1875
0.61 0.178728 0.625 0.1875 0.5 0.1875 0.515 0.1337719 0.515 0.178728 0.375 0.125 0.485 0.1337719 0.3900001 0.1337718 0.5
0.1875 0.485 0.1337719 0.5 0.125 0.5 0.1875 0.39 0.178728 0.485 0.1787281 0.375 0.125 0.39 0.178728 0.375 0.1875 0.5
0.0625 0.3900001 0.07127189 0.375 0.0625 0.5 0.125 0.485 0.07127195 0.5 0.0625 0.5 0.125 0.39 0.116228 0.485 0.1162281
0.375 0.0625 0.39 0.116228 0.375 0.125 0.5 0 0.39 0.008771896 0.375 0 0.5 0.0625 0.485 0.008771896 0.5 0 0.375 0.0625 0.485
0.05372804 0.5 0.0625 0.375 0 0.39 0.05372804 0.375 0.0625 0.375 0.1875 0.485 0.1962719 0.3900001 0.1962719 0.5 0.25
0.485 0.1962719 0.5 0.1875 0.375 0.25 0.485 0.2412281 0.5 0.25 0.375 0.1875 0.3900001 0.2412281 0.375 0.25 0.61 0.1962719
0.5150001 0.2412281 0.5150001 0.1962719 0.625 0.6875 0.5 0.75 0.5 0.6875 0.625 0.75 0.5 1 0.5 0.75 0.375 0.6875 0.125 0.75
0.125 0.6875 0.875 0.6875 0.625 0.75 0.625 0.6875 0.875 0.5 0.625 0.5625 0.625 0.5000001 0.875 0.5625 0.625 0.625 0.625
0.5625 0.875 0.625 0.625 0.6875 0.625 0.625 0.125 0.5625 0.375 0.5 0.375 0.5625 0.375 0.5625 0.125 0.625 0.125 0.5625 0.375
0.625 0.125 0.6875 0.125 0.625 0.625 0.5625 0.5 0.5000001 0.625 0.5000001 0.5 0.5625 0.625 0.625 0.5 0.625 0.5 0.625 0.625
0.6875 0.5 0.6875 0.61 0.008771896 0.515 0.05372804 0.515 0.008771896 0.6100001 0.07127195 0.515 0.116228 0.515
0.07127195 0.6100001 0.1337719 0.515 0.178728 0.515 0.1337719 0.485 0.1337719 0.39 0.178728 0.3900001 0.1337718 0.485
0.07127195 0.39 0.116228 0.3900001 0.07127189 0.485 0.008771896 0.39 0.05372804 0.39 0.008771896 0.5 0.625 0.375
0.6875 0.375 0.625 0.5 0.5625 0.375 0.625 0.375 0.5625 0.375 0.5625 0.5 0.5000001 0.5 0.5625 0.5 0.75 0.375 1 0.375 0.75 0.5
0.6875 0.375 0.75 0.375 0.6875 0.485 0.1962719 0.3900001 0.2412281 0.3900001 0.1962719 0.625 0.1875 0.5150001
0.1962719 0.5 0.1875 0.625 0.25 0.61 0.2412281 0.61 0.1962719 0.61 0.2412281 0.5000001 0.25 0.5150001 0.2412281
0.5000001 0.25 0.5 0.1875 0.5150001 0.1962719 0.625 0 0.515 0.008771896 0.5 0 0.625 0 0.61 0.05372804 0.61 0.008771896
0.5 0.0625 0.61 0.05372804 0.625 0.0625 0.5 0 0.515 0.05372804 0.5 0.0625 0.625 0.0625 0.515 0.07127195 0.5 0.0625 0.625
0.125 0.6100001 0.07127195 0.625 0.0625 0.5 0.125 0.61 0.1162281 0.625 0.125 0.5 0.0625 0.515 0.116228 0.5 0.125 0.625
0.125 0.515 0.1337719 0.5 0.125 0.625 0.1875 0.6100001 0.1337719 0.625 0.125 0.5 0.1875 0.61 0.178728 0.625 0.1875 0.5
0.125 0.515 0.178728 0.5 0.1875 0.375 0.125 0.485 0.1337719 0.3900001 0.1337718 0.5 0.1875 0.485 0.1337719 0.5 0.125 0.5
0.1875 0.39 0.178728 0.485 0.1787281 0.375 0.125 0.39 0.178728 0.375 0.1875 0.5 0.0625 0.3900001 0.07127189 0.375 0.0625
0.5 0.125 0.485 0.07127195 0.5 0.0625 0.5 0.125 0.39 0.116228 0.485 0.1162281 0.375 0.0625 0.39 0.116228 0.375 0.125 0.5 0
0.39 0.008771896 0.375 0 0.5 0 0.485 0.05372804 0.485 0.008771896 0.375 0.0625 0.485 0.05372804 0.5 0.0625 0.375 0 0.39
0.05372804 0.375 0.0625 0.375 0.1875 0.485 0.1962719 0.3900001 0.1962719 0.5000001 0.25 0.485 0.2412281 0.485
0.1962719 0.485 0.2412281 0.3750001 0.25 0.3900001 0.2412281 0.375 0.25 0.375 0.1875 0.3900001 0.1962719 0.61
0.1962719 0.61 0.2412281 0.5150001 0.2412281 0.5 0.6875 0.625 0.6875 0.625 0.75 0.375 0.6875 0.375 0.75 0.125 0.75 0.625
0.6875 0.875 0.6875 0.875 0.75 0.875 0.5 0.875 0.5625 0.625 0.5625 0.875 0.5625 0.875 0.625 0.625 0.625 0.875 0.625 0.875
0.6875 0.625 0.6875 0.375 0.5 0.375 0.5625 0.125 0.5625 0.375 0.5625 0.375 0.625 0.125 0.625 0.375 0.625 0.375 0.6875 0.125
0.6875 0.5 0.5 0.625 0.5 0.625 0.5625 0.5 0.5625 0.625 0.5625 0.625 0.625 0.5 0.625 0.625 0.625 0.625 0.6875 0.61
0.008771896 0.61 0.05372804 0.515 0.05372804 0.6100001 0.07127195 0.61 0.1162281 0.515 0.116228 0.6100001 0.1337719
0.61 0.178728 0.515 0.178728 0.485 0.1337719 0.485 0.1787281 0.39 0.178728 0.485 0.07127195 0.485 0.1162281 0.39
0.116228 0.485 0.008771896 0.485 0.05372804 0.39 0.05372804 0.5 0.625 0.5 0.6875 0.375 0.6875 0.5 0.5625 0.5 0.625 0.375
0.625 0.5 0.5 0.5 0.5625 0.375 0.5625 0.375 0.6875 0.5 0.6875 0.5 0.75 0.485 0.1962719 0.485 0.2412281 0.3900001 0.2412281
0.625 0.1875 0.61 0.1962719 0.5150001 0.1962719 0.625 0.25 0.61 0.2412281 0.61 0.1962719 0.5 0.25 0.5150001 0.2412281
0.61 0.2412281 0.5 0.1875 0.5150001 0.1962719 0.5150001 0.2412281 0.515 0.008771896 0.5000001 0 0.6249999 0 0.625 0
0.625 0 0.61 0.008771896 0.625 0 0.625 0.0625 0.61 0.008771896 0.5 0.0625 0.515 0.05372804 0.61 0.05372804 0.515
0.05372804 0.5 0.0625 0.5 0 0.5 0 0.5 0 0.515 0.008771896 0.625 0.0625 0.6100001 0.07127195 0.515 0.07127195 0.625 0.125
0.61 0.1162281 0.6100001 0.07127195 0.5 0.125 0.515 0.116228 0.61 0.1162281 0.5 0.0625 0.515 0.07127195 0.515 0.116228
0.625 0.125 0.6100001 0.1337719 0.515 0.1337719 0.625 0.1875 0.61 0.178728 0.6100001 0.1337719 0.5 0.1875 0.515
0.178728 0.61 0.178728 0.5 0.125 0.515 0.1337719 0.515 0.178728 0.375 0.125 0.5 0.125 0.485 0.1337719 0.5 0.1875 0.485
0.1787281 0.485 0.1337719 0.5 0.1875 0.375 0.1875 0.39 0.178728 0.375 0.125 0.3900001 0.1337718 0.39 0.178728 0.5 0.0625
0.485 0.07127195 0.3900001 0.07127189 0.5 0.125 0.485 0.1162281 0.485 0.07127195 0.5 0.125 0.375 0.125 0.39 0.116228
0.375 0.0625 0.3900001 0.07127189 0.39 0.116228 0.39 0.008771896 0.3750001 0 0.5 0 0.5 0 0.5 0 0.485 0.008771896 0.5 0 0.5
0.0625 0.485 0.008771896 0.375 0.0625 0.39 0.05372804 0.485 0.05372804 0.39 0.05372804 0.375 0.0625 0.375 0 0.375 0
0.375 0 0.39 0.008771896 0.375 0.1875 0.5 0.1875 0.485 0.1962719 0.5 0.25 0.485 0.2412281 0.485 0.1962719 0.375 0.25

0.3900001 0.2412281 0.485 0.2412281 0.375 0.1875 0.3900001 0.1962719 0.3900001 0.2412281 0.61 0.1962719 0.61
0.2412281 0.5150001 0.2412281 0.625 0.6875 0.625 0.75 0.5 0.75 0.375 0.6875 0.375 0.75 0.125 0.75 0.875 0.6875 0.875 0.75
0.625 0.75 0.875 0.5 0.875 0.5625 0.625 0.5625 0.875 0.5625 0.875 0.625 0.625 0.625 0.875 0.625 0.875 0.6875 0.625 0.6875
0.375 0.5 0.375 0.5625 0.125 0.5625 0.375 0.5625 0.375 0.625 0.125 0.625 0.375 0.625 0.375 0.6875 0.125 0.6875 0.5 0.5 0.625
0.5 0.625 0.5625 0.5 0.5625 0.625 0.5625 0.625 0.625 0.5 0.625 0.625 0.625 0.625 0.6875 0.61 0.008771896 0.61 0.05372804
0.515 0.05372804 0.6100001 0.07127195 0.61 0.1162281 0.515 0.116228 0.6100001 0.1337719 0.61 0.178728 0.515 0.178728
0.485 0.1337719 0.485 0.1787281 0.39 0.178728 0.485 0.07127195 0.485 0.1162281 0.39 0.116228 0.485 0.008771896 0.485
0.05372804 0.39 0.05372804 0.5 0.625 0.5 0.6875 0.375 0.6875 0.5 0.5625 0.5 0.625 0.375 0.625 0.5 0.5 0.5 0.5625 0.375
0.5625 0.5 0.6875 0.5 0.75 0.375 0.75 0.485 0.1962719 0.485 0.2412281 0.3900001 0.2412281 0.625 0.1875 0.61 0.1962719
0.5150001 0.1962719 0.625 0.25 0.61 0.2412281 0.61 0.1962719 0.5 0.25 0.5150001 0.2412281 0.61 0.2412281 0.5 0.25 0.5
0.1875 0.5150001 0.1962719 0.625 0 0.61 0.008771896 0.515 0.008771896 0.625 0.0625 0.61 0.05372804 0.61 0.008771896 0.5
0.0625 0.515 0.05372804 0.61 0.05372804 0.5 0 0.515 0.008771896 0.515 0.05372804 0.625 0.0625 0.6100001 0.07127195
0.515 0.07127195 0.625 0.125 0.61 0.1162281 0.6100001 0.07127195 0.5 0.125 0.515 0.116228 0.61 0.1162281 0.5 0.0625
0.515 0.07127195 0.515 0.116228 0.625 0.125 0.6100001 0.1337719 0.515 0.1337719 0.625 0.1875 0.61 0.178728 0.6100001
0.1337719 0.5 0.1875 0.515 0.178728 0.61 0.178728 0.5 0.1875 0.5 0.125 0.515 0.1337719 0.375 0.125 0.5 0.125 0.485
0.1337719 0.5 0.1875 0.485 0.1787281 0.485 0.1337719 0.5 0.1875 0.375 0.1875 0.39 0.178728 0.375 0.125 0.3900001
0.1337718 0.39 0.178728 0.5 0.0625 0.485 0.07127195 0.3900001 0.07127189 0.5 0.125 0.485 0.1162281 0.485 0.07127195 0.5
0.125 0.375 0.125 0.39 0.116228 0.375 0.0625 0.3900001 0.07127189 0.39 0.116228 0.5 0 0.485 0.008771896 0.39 0.008771896
0.5 0.0625 0.485 0.05372804 0.485 0.008771896 0.375 0.0625 0.39 0.05372804 0.485 0.05372804 0.375 0 0.39 0.008771896
0.39 0.05372804 0.375 0.1875 0.5 0.1875 0.485 0.1962719 0.5 0.25 0.485 0.2412281 0.485 0.1962719 0.375 0.25 0.3900001
0.2412281 0.485 0.2412281 0.375 0.1875 0.3900001 0.1962719 0.3900001 0.2412281 0.61 0.1962719 0.61 0.2412281
0.5150001 0.2412281 0.625 0.6875 0.625 0.75 0.5 0.75 0.625 0.75 0.625 1 0.5 1 0.375 0.6875 0.375 0.75 0.125 0.75 0.875
0.6875 0.875 0.75 0.625 0.75 0.875 0.5 0.875 0.5625 0.625 0.5625 0.875 0.5625 0.875 0.625 0.625 0.625 0.875 0.625 0.875
0.6875 0.625 0.6875 0.125 0.5625 0.125 0.5000001 0.375 0.5 0.375 0.5625 0.375 0.625 0.125 0.625 0.375 0.625 0.375 0.6875
0.125 0.6875 0.625 0.5625 0.5 0.5625 0.5 0.5000001 0.5 0.5625 0.625 0.5625 0.625 0.625 0.5 0.625 0.625 0.625 0.625 0.6875
0.61 0.008771896 0.61 0.05372804 0.515 0.05372804 0.6100001 0.07127195 0.61 0.1162281 0.515 0.116228 0.6100001
0.1337719 0.61 0.178728 0.515 0.178728 0.485 0.1337719 0.485 0.1787281 0.39 0.178728 0.485 0.07127195 0.485 0.1162281
0.39 0.116228 0.485 0.008771896 0.485 0.05372804 0.39 0.05372804 0.5 0.625 0.5 0.6875 0.375 0.6875 0.5 0.5625 0.5 0.625
0.375 0.625 0.375 0.5625 0.375 0.5 0.5 0.5000001 0.5 0.75 0.5 1 0.375 1 0.5 0.6875 0.5 0.75 0.375 0.75 0.485 0.1962719 0.485
0.2412281 0.3900001 0.2412281 0.625 0.1875 0.61 0.1962719 0.5150001 0.1962719 0.61 0.1962719 0.625 0.1875 0.625 0.25
0.625 0.25 0.625 0.25 0.61 0.2412281 0.61 0.2412281 0.625 0.25 0.5000001 0.25 0.5150001 0.1962719 0.5150001 0.2412281
0.5000001 0.25 0.5000001 0.25 0.5000001 0.25 0.5150001 0.1962719 0.625 0 0.61 0.008771896 0.515 0.008771896 0.625 0
0.625 0.0625 0.61 0.05372804 0.5 0.0625 0.515 0.05372804 0.61 0.05372804 0.5 0 0.515 0.008771896 0.515 0.05372804 0.625
0.0625 0.6100001 0.07127195 0.515 0.07127195 0.625 0.125 0.61 0.1162281 0.6100001 0.07127195 0.5 0.125 0.515 0.116228
0.61 0.1162281 0.5 0.0625 0.515 0.07127195 0.515 0.116228 0.625 0.125 0.6100001 0.1337719 0.515 0.1337719 0.625 0.1875
0.61 0.178728 0.6100001 0.1337719 0.5 0.1875 0.515 0.178728 0.61 0.178728 0.5 0.125 0.515 0.1337719 0.515 0.178728 0.375
0.125 0.5 0.125 0.485 0.1337719 0.5 0.1875 0.485 0.1787281 0.485 0.1337719 0.5 0.1875 0.375 0.1875 0.39 0.178728 0.375
0.125 0.3900001 0.1337718 0.39 0.178728 0.5 0.0625 0.485 0.07127195 0.3900001 0.07127189 0.5 0.125 0.485 0.1162281
0.485 0.07127195 0.5 0.125 0.375 0.125 0.39 0.116228 0.375 0.0625 0.3900001 0.07127189 0.39 0.116228 0.5 0 0.485
0.008771896 0.39 0.008771896 0.5 0 0.5 0.0625 0.485 0.05372804 0.375 0.0625 0.39 0.05372804 0.485 0.05372804 0.375 0
0.39 0.008771896 0.39 0.05372804 0.375 0.1875 0.5 0.1875 0.485 0.1962719 0.485 0.1962719 0.5 0.1875 0.5000001 0.25
0.5000001 0.25 0.5 0.25 0.485 0.2412281 0.485 0.2412281 0.5 0.25 0.3750001 0.25 0.3900001 0.1962719 0.3900001 0.2412281
0.3750001 0.25 0.3750001 0.25 0.375 0.25 0.3900001 0.1962719</float_array>

<technique_common>

<accessor source="#Cube_012-mesh-map-0-array" count="1044" stride="2">

<param name="S" type="float"/>

<param name="T" type="float"/>

</accessor>

</technique_common>

</source>

<vertices id="Cube_012-mesh-vertices">

<input semantic="POSITION" source="#Cube_012-mesh-positions"/>

</vertices>

<triangles material="Material-material" count="58">

<input semantic="VERTEX" source="#Cube_012-mesh-vertices" offset="0"/>

<input semantic="NORMAL" source="#Cube_012-mesh-normals" offset="1"/>

<input semantic="TEXCOORD" source="#Cube_012-mesh-map-0" offset="2" set="0"/>

<p>92 1 3 14 1 4 45 1 5 50 2 6 5 2 7 32 2 8 17 2 21 27 2 22 7 2 23 58 2 24 28 2 25 27 2 26 54 2 27 32 2 28 28 2 29 89 1 57 50 1 58 54 1 59 87 1 60 54 1 61 58 1 62 79 1 63 58 1 64 17 1 65 50 1 66 45 1 67 12 1 68 71 1 171 79 1 172 94 1 173 49 2 174 7 2 175 35 2 176 18 2 189 25 2 190 4 2 191 57 2 192 30 2 193 25 2 194 53 2 195 35 2 196 30 2 197 90 1 225 49 1 226 53 1 227 85 1 228 53 1 229 57 1 230 81 1 231 57 1 232 18 1 233 94 1 234 17 1 235 49 1 236 38 1 339 46 1 340 52 1 341 11 35 342 41 35 343 46 35 344 29 2 345 1 2 346 21 2 347 16 2 360 13 2 361 33 2 362 33 2 363 19 2 364 16 2 365 31 2 366 21 2 367 19 2 368 51 1 396 29 1 397 31 1 398 48 1 399 31 1 400 33 1 401 33 1 402 83 1 403 48 1 404 46 35 405 1 35 406 8 35 407 52 1 408 8 1 409 29 1 410 92 1 513 69 1 514 14 1 515 50 2 516 12 2 517 5 2 518 17 47 531 58 47 532 27 47 533 58 48 534 54 48 535 28 48 536 54 2 537 50 2 538 32 2 539 89 1 567 92 1 568 50 1 569 87 1 570 89 1 571 54 1 572 79 1 573 87 1 574 58 1 575 50 1 576 92 1 577 45 1 578 71 1 693 22 1 694 79 1 695 49 2 696 17 2 697 7 2 698 18 66 711 57 66 712 25 66 713 57 67 714 53 67 715 30 67 716 53 2 717 49 2 718 35 2 719 90 1 747 94 1 748 49 1 749 85 1 750 90 1 751 53 1 752 81 1 753 85 1 754 57 1 755 94 1 756 79 1 757 17 1 758 38 1 861 11 1 862 46 1 863 11 35 864 3 35 865 41 35 866 29 2 867 8 2 868 1 2 869 16 2 882 0 2 883 13 2 884 33 48 885 31 48 886 19 48 887 31 2 888 29 2 889 21 2 890 51 1 918 52 1 919 29 1 920 48 1 921 51 1 922 31 1 923 33 1 924 13 1 925 83 1 926 46 35 927 41 35 928 1 35 929 52 1 930 46 1 931 8 1 932</p>

</triangles>

<triangles material="Material_001-material" count="48">

<input semantic="VERTEX" source="#Cube_012-mesh-vertices" offset="0"/>

<input semantic="NORMAL" source="#Cube_012-mesh-normals" offset="1"/>

<input semantic="TEXCOORD" source="#Cube_012-mesh-map-0" offset="2" set="0"/>

<p>112 0 0 120 0 1 109 0 2 126 0 39 130 0 40 124 0 41 134 0 42 139 0 43 133 0 44 142 0 45 146 0 46 140 0 47 150 0 48 155 0 49 149 0 50 158 0 51 162 0 52 156 0 53 166 0 54 171 0 55 164 0 56 174 0 69 178 0 70 173 0 71 114 0 168 122 0 169 111 0 170 127 0 207 131 0 208 125 0 209 135 0 210 138 0 211 132 0 212 143 0 213 147 0 214 141 0 215 151 0 216 154 0 217 148 0 218 159 0 219 163 0 220 157 0 221 167 0 222 170 0 223 165 0 224 175 0 237 179 0 238 172 0 239 63 0 336 66 0 337 60 0 338 70 0 378 74 0 379 68 0 380 78 0 381 82 0 382 76 0 383 86 0 384 91 0 385 84 0 386 95 0 387 98 0 388 93 0 389 103 0 390 107 0 391 100 0 392 110 0 393 115 0 394 108 0 395 119 0 411 123 0 412 117 0 413 112 0 510 116 0 511 120 0 512 126 0 549 128 0 550 130 0 551 134 0 552 136 0 553 139 0 554 142 0 555 144 0 556 146 0 557 150 0 558 153 0 559 155 0 560 158 0 561 160 0 562 162 0 563 166 0 564 168 0 565 171 0 566 174 0 579 176 0 580 178 0 581 114 0 690 118 0 691 122 0 692 127 0 729 129 0 730 131 0 731 135 0 732 137 0 733 138 0 734 143 0 735 145 0 736 147 0 737 151 0 738 152 0 739 154 0 740 159 0 741 161 0 742 163 0 743 167 0 744 169 0 745 170 0 746 175 0 759 177 0 760 179 0 761 63 0 858 64 0 859 66 0 860 70 0 900 73 0 901 74 0 902 78 0 903 80 0 904 82 0 905 86 0 906 88 0 907 91 0 908 95 0 909 97 0 910 98 0 911 103 0 912 105 0 913 107 0 914 110 0 915 113 0 916 115 0 917 119 0 933 121 0 934 123 0 935</p>

</triangles>

<triangles material="Material_002-material" count="242">

<input semantic="VERTEX" source="#Cube_012-mesh-vertices" offset="0"/>

<input semantic="NORMAL" source="#Cube_012-mesh-normals" offset="1"/>

<input semantic="TEXCOORD" source="#Cube_012-mesh-map-0" offset="2" set="0"/>

<p>69 3 9 6 3 10 14 3 11 9 3 12 61 3 13 22 3 14 44 3 15 67 3 16 61 3 17 40 3 18 69 3 19 67 3 20 79 1 30 61 1 31 87 1 32
87 1 33 67 1 34 89 1 35 89 1 36 69 1 37 92 1 38 44 4 72 109 4 73 104 4 74 9 5 75 112 5 76 44 5 77 75 6 78 116 6 79 9 6 80 104 7
81 120 7 82 75 7 83 124 8 84 184 8 85 126 8 86 39 9 87 128 9 88 126 9 89 99 6 90 128 6 91 39 6 92 42 10 93 124 10 94 130 10
95 39 4 96 133 4 97 99 4 98 40 11 99 134 11 100 39 11 101 102 6 102 136 6 103 40 6 104 99 12 105 139 12 106 102 12 107 40 4
108 140 4 109 102 4 110 44 13 111 142 13 112 40 13 113 104 6 114 144 6 115 44 6 116 102 14 117 146 14 118 104 14 119 28
15 120 150 15 121 149 15 122 104 11 123 150 11 124 102 11 125 104 16 126 155 16 127 153 16 128 28 7 129 155 7 130 27 7
131 99 17 132 156 17 133 32 17 134 102 9 135 158 9 136 99 9 137 102 16 138 162 16 139 160 16 140 32 18 141 162 18 142 28
18 143 164 19 144 186 19 145 166 19 146 99 13 147 168 13 148 166 13 149 32 20 150 168 20 151 99 20 152 5 12 153 164 12
154 171 12 155 27 15 156 174 15 157 173 15 158 75 11 159 174 11 160 104 11 161 7 20 162 176 20 163 75 20 164 27 7 165 178
7 166 7 7 167 37 3 177 22 3 178 71 3 179 10 3 180 62 3 181 20 3 182 47 3 183 65 3 184 62 3 185 43 3 186 71 3 187 65 3 188 81
1 198 62 1 199 85 1 200 85 1 201 65 1 202 90 1 203 90 1 204 71 1 205 94 1 206 47 21 240 111 21 241 106 21 242 10 22 243 114
22 244 47 22 245 77 23 246 118 23 247 10 23 248 77 24 249 111 24 250 122 24 251 9 4 252 125 4 253 75 4 254 37 25 255 127
25 256 9 25 257 96 6 258 129 6 259 37 6 260 75 14 261 131 14 262 96 14 263 37 4 264 132 4 265 96 4 266 43 9 267 135 9 268
37 9 269 101 6 270 137 6 271 43 6 272 96 26 273 138 26 274 101 26 275 43 4 276 141 4 277 101 4 278 47 27 279 143 27 280 43
27 281 106 23 282 145 23 283 47 23 284 106 28 285 141 28 286 147 28 287 30 15 288 151 15 289 148 15 290 106 29 291 151
29 292 101 29 293 106 30 294 154 30 295 152 30 296 30 31 297 154 31 298 25 31 299 96 17 300 157 17 301 35 17 302 101 32
303 159 32 304 96 32 305 101 16 306 163 16 307 161 16 308 35 33 309 163 33 310 30 33 311 75 17 312 165 17 313 7 17 314 96
13 315 167 13 316 75 13 317 35 20 318 169 20 319 96 20 320 7 7 321 170 7 322 35 7 323 25 15 324 175 15 325 172 15 326 77
34 327 175 34 328 106 34 329 4 23 330 177 23 331 77 23 332 25 12 333 179 12 334 4 12 335 23 3 348 11 3 349 38 3 350 2 3
351 34 3 352 15 3 353 26 3 354 36 3 355 34 3 356 24 3 357 38 3 358 36 3 359 34 1 369 83 1 370 15 1 371 48 1 372 36 1 373 51
1 374 51 1 375 38 1 376 52 1 377 26 4 414 60 4 415 59 4 416 2 25 417 64 25 418 63 25 419 64 36 420 181 36 421 66 36 422 72
14 423 59 14 424 60 14 425 3 37 426 68 37 427 41 37 428 3 38 429 73 38 430 70 38 431 55 6 432 73 6 433 23 6 434 41 39 435
74 39 436 55 39 437 23 4 438 76 4 439 55 4 440 24 9 441 78 9 442 23 9 443 56 6 444 80 6 445 24 6 446 55 39 447 82 39 448 56
39 449 24 4 450 84 4 451 56 4 452 26 9 453 86 9 454 24 9 455 59 6 456 88 6 457 26 6 458 56 26 459 91 26 460 59 26 461 19 15
462 95 15 463 93 15 464 59 32 465 95 32 466 56 32 467 59 16 468 98 16 469 97 16 470 19 31 471 98 31 472 16 31 473 55 17
474 100 17 475 21 17 476 56 32 477 103 32 478 55 32 479 56 16 480 107 16 481 105 16 482 21 31 483 107 31 484 19 31 485 41
40 486 108 40 487 1 40 488 41 41 489 113 41 490 110 41 491 21 20 492 113 20 493 55 20 494 1 12 495 115 12 496 21 12 497
16 15 498 119 15 499 117 15 500 72 42 501 121 42 502 119 42 503 121 43 504 183 43 505 123 43 506 0 44 507 16 44 508 117
44 509 69 3 519 39 3 520 6 3 521 9 45 522 44 45 523 61 45 524 44 46 525 40 46 526 67 46 527 40 3 528 39 3 529 69 3 530 79 1
540 22 1 541 61 1 542 87 1 543 61 1 544 67 1 545 89 1 546 67 1 547 69 1 548 44 17 582 112 17 583 109 17 584 9 38 585 116 38
586 112 38 587 75 49 588 120 49 589 116 49 590 104 50 591 109 50 592 120 50 593 124 51 594 185 51 595 184 51 596 184 52
597 6 52 598 126 52 599 6 29 600 39 29 601 126 29 602 99 49 603 130 49 604 128 49 605 130 53 606 99 53 607 42 53 608 42
54 609 185 54 610 124 54 611 39 17 612 134 17 613 133 17 614 40 38 615 136 38 616 134 38 617 102 49 618 139 49 619 136
49 620 99 12 621 133 12 622 139 12 623 40 17 624 142 17 625 140 17 626 44 5 627 144 5 628 142 5 629 104 49 630 146 49 631
144 49 632 102 12 633 140 12 634 146 12 635 28 55 636 102 55 637 150 55 638 104 56 639 153 56 640 150 56 641 104 57 642
27 57 643 155 57 644 28 58 645 149 58 646 155 58 647 99 59 648 158 59 649 156 59 650 102 56 651 160 56 652 158 56 653
102 57 654 28 57 655 162 57 656 32 58 657 156 58 658 162 58 659 164 51 660 187 51 661 186 51 662 186 54 663 42 54 664
166 54 665 42 60 666 99 60 667 166 60 668 32 6 669 171 6 670 168 6 671 171 61 672 32 61 673 5 61 674 5 52 675 187 52 676
164 52 677 27 55 678 104 55 679 174 55 680 75 62 681 176 62 682 174 62 683 7 6 684 178 6 685 176 6 686 27 63 687 173 63
688 178 63 689 37 3 699 9 3 700 22 3 701 10 64 702 47 64 703 62 64 704 47 65 705 43 65 706 65 65 707 43 3 708 37 3 709 71 3
710 81 1 720 20 1 721 62 1 722 85 1 723 62 1 724 65 1 725 90 1 726 65 1 727 71 1 728 47 68 762 114 68 763 111 68 764 10 69
765 118 69 766 114 69 767 77 16 768 122 16 769 118 16 770 77 26 771 106 26 772 111 26 773 9 17 774 127 17 775 125 17 776
37 70 777 129 70 778 127 70 779 96 49 780 131 49 781 129 49 782 75 71 783 125 71 784 131 71 785 37 17 786 135 17 787 132
17 788 43 72 789 137 72 790 135 72 791 101 49 792 138 49 793 137 49 794 96 73 795 132 73 796 138 73 797 43 17 798 143 17
799 141 17 800 47 72 801 145 72 802 143 72 803 106 16 804 147 16 805 145 16 806 106 71 807 101 71 808 141 71 809 30 55
810 101 55 811 151 55 812 106 62 813 152 62 814 151 62 815 106 74 816 25 74 817 154 74 818 30 24 819 148 24 820 154 24
821 96 59 822 159 59 823 157 59 824 101 62 825 161 62 826 159 62 827 101 57 828 30 57 829 163 57 830 35 75 831 157 75
832 163 75 833 75 59 834 167 59 835 165 59 836 96 29 837 169 29 838 167 29 839 35 6 840 170 6 841 169 6 842 7 76 843 165
76 844 170 76 845 25 77 846 106 77 847 175 77 848 77 69 849 177 69 850 175 69 851 4 23 852 179 23 853 177 23 854 25 78
855 172 78 856 179 78 857 23 3 870 3 3 871 11 3 872 2 79 873 26 79 874 34 79 875 26 46 876 24 46 877 36 46 878 24 3 879 23
3 880 38 3 881 34 1 891 48 1 892 83 1 893 48 1 894 34 1 895 36 1 896 51 1 897 36 1 898 38 1 899 26 17 936 63 17 937 60 17
938 63 80 939 26 80 940 2 80 941 2 81 942 180 81 943 64 81 944 64 23 945 180 23 946 181 23 947 60 82 948 66 82 949 181 82
950 181 83 951 72 83 952 60 83 953 3 84 954 70 84 955 68 84 956 3 9 957 23 9 958 73 9 959 55 49 960 74 49 961 73 49 962 41
85 963 68 85 964 74 85 965 23 17 966 78 17 967 76 17 968 24 72 969 80 72 970 78 72 971 56 49 972 82 49 973 80 49 974 55 58
975 76 58 976 82 58 977 24 17 978 86 17 979 84 17 980 26 72 981 88 72 982 86 72 983 59 49 984 91 49 985 88 49 986 56 73
987 84 73 988 91 73 989 19 55 990 56 55 991 95 55 992 59 62 993 97 62 994 95 62 995 59 57 996 16 57 997 98 57 998 19 75
999 93 75 1000 98 75 1001 55 59 1002 103 59 1003 100 59 1004 56 62 1005 105 62 1006 103 62 1007 56 57 1008 19 57 1009
107 57 1010 21 86 1011 100 86 1012 107 86 1013 41 87 1014 110 87 1015 108 87 1016 41 32 1017 55 32 1018 113 32 1019 21
6 1020 115 6 1021 113 6 1022 1 86 1023 108 86 1024 115 86 1025 16 55 1026 59 55 1027 119 55 1028 119 13 1029 59 13 1030

72 13 1031 72 88 1032 182 88 1033 121 88 1034 121 89 1035 182 89 1036 183 89 1037 117 90 1038 123 90 1039 183 90 1040 183 91 1041 0 91 1042 117 91 1043</p>

</triangles>

</mesh>

</geometry>

<geometry id="Cube_005-mesh" name="Cube.005">

<mesh>

<source id="Cube_005-mesh-positions">

<float_array id="Cube_005-mesh-positions-array" count="165">-0.1858198 0.4433824 -0.1012217 0.1562936 0.1032627 -0.1002218 0.1562936 -0.09673732 -0.1002218 -0.1858198 0.1013824 -0.1012217 -0.1858198 0.4433824 0.09877824 0.1562936 0.1032627 0.09977823 0.1562936 -0.09673732 0.09977823 -0.1872063 0.1032627 -0.1002218 -0.1858198 0.4433825 -0.1012217 -0.1872063 -0.09673732 -0.1002218 -0.1872063 0.1032627 0.09977823 -0.1858198 0.4433825 0.09877824 -0.1872063 -0.09673732 0.09977823 -0.1771197 0.1013824 -0.1012217 -0.1872063 0.1042131 0.09977811 -0.1872063 -0.09578686 0.09977811 -0.1872063 0.1042131 -0.1002219 -0.1872063 -0.09578686 -0.1002219 -0.1872063 0.1012626 -0.1002216 -0.1771197 0.4433825 -0.1012217 -0.1771197 0.4433824 -0.1012217 -0.1872063 0.1012626 0.09977835 -0.1771197 0.4433825 0.09877824 -0.1785063 0.1012626 -0.1002216 -0.1771197 0.4433824 0.09877824 -0.1785063 0.1012626 0.09977835 -0.1872063 0.1012626 -2.21659e-4 -0.1785063 0.1012626 -2.21659e-4 -0.1872063 -0.09273737 -0.1002217 -0.1872063 -0.09273737 0.09977835 -0.1785063 -0.09273737 -0.1002217 -0.1785063 -0.09273737 0.09977835 -0.1872063 -0.09273737 -2.21719e-4 -0.1785063 -0.09273737 -2.21719e-4 -0.1858198 0.4433825 -0.001221716 -0.1771197 0.4433825 -0.001221716 -0.1858198 0.4433824 -0.001221716 -0.1771197 0.4433824 -0.001221716 -0.1858198 0.4433825 0.09877818 -0.1858198 0.4433825 -0.001221656 -0.1858198 0.4433825 -0.001221776 -0.1858198 0.4433825 -0.1012217 -0.1771197 0.1032627 0.09877824 -0.1771197 0.1032627 -0.001221716 -0.1858198 0.1032627 0.09877824 -0.1771197 0.1013824 -0.1002218 -0.1858198 0.1013824 -0.1002218 -0.1771197 0.1032627 -0.1002218 -0.1855127 0.1032627 0.09689795 -0.1855127 0.1032627 6.5852e-4 -0.1858198 0.1032627 -0.001221716 -0.1855127 0.1032627 -0.003102064 -0.1856564 0.1023824 -0.1002218 -0.1855127 0.1032627 -0.09934151 -0.1856564 0.1032627 -0.1002218</float_array>

<technique_common>

<accessor source="#Cube_005-mesh-positions-array" count="55" stride="3">

<param name="X" type="float"/>

<param name="Y" type="float"/>

<param name="Z" type="float"/>

</accessor>

</technique_common>

</source>

<source id="Cube_005-mesh-normals">

<float_array id="Cube_005-mesh-normals-array" count="42">1 0 0 0 0 -1 0 0 1 -0.9977492 0.06705826 0 -1 0 0 -0.9977491 0.06705826 0 0 -1 0 -0.9977491 -0.06705826 0 -0.9977491 -0.06705826 0 0 1 -3.34528e-6 0 1 0 0 1 1.35564e-6 8.59208e-6 0 -1 -1.46927e-6 0 -1</float_array>

<technique_common>

<accessor source="#Cube_005-mesh-normals-array" count="14" stride="3">

<param name="X" type="float"/>

<param name="Y" type="float"/>

<param name="Z" type="float"/>

</accessor>

</technique_common>

</source>

<source id="Cube_005-mesh-map-0">

<float_array id="Cube_005-mesh-map-0-array" count="342">0.5 0.75 0.625 0.75 0.5 0.75 0.125 0.75 0.375 0.75 0.125 0.75 0.625 0.75 0.875 0.75 0.625 0.75 0.375 0.75 0.5 0.75 0.375 0.75 0.625 0 0.5000001 0 0.5 0 0.625 0 0.625 0 0.625 0 0.5 0 0.5 0 0.5 0 0.5 0 0.375 0 0.375 0 0.5 0 0.5 0 0.5 0 0.375 0 0.375 0 0.375 0 0.375 1 0.37625 0.75 0.37625 1 0.5 0.25 0.625 0.25 0.625 0.25 0.375 0.25 0.5 0.25 0.5 0.25 0.867659 0.5 0.8739908 0.5 0.875 0.5 0.375 0.75 0.375 1 0.375 0.75 0.375 0.5 0.125 0.75 0.125 0.75 0.625 0.5 0.375 0.75 0.375 0.5 0.375 0.25 0.375 0.2510092 0.375 0.257341 1 0 0 1 0 0 0.5 0.75 0.5 1 0.5 0.75 0.375 0.75 0.375 1 0.375 0.75 0.5 0.25 0.5 0.5 0.5 0.25 0.375 0.25 0.375 0.5 0.375 0.25 0.5 0.75 0.625 0.75 0.625 0.75 0.125 0.75 0.375 0.75 0.375 0.75 0.625 0.75 0.875 0.75 0.875 0.75 0.375 0.75 0.5 0.75 0.5 0.75 0.625 0 0.6249999 0 0.5000001 0 0.5 0 0.5 0 0.375 0 0.375 1 0.375 0.75 0.37625 0.75 0.5 0.25 0.5000001 0.25 0.625 0.25 0.375 0.25 0.3750001 0.25 0.5 0.25 0.8737674 0.5 0.8738719 0.5 0.875 0.5 0.625 0.75 0.625 0.75 0.867659 0.5 0.625 0.75 0.867659 0.5 0.867659 0.5 0.867659 0.5 0.867659 0.5 0.625 0.75 0.8737674 0.5 0.875 0.5 0.8737674 0.5 0.875 0.5 0.875 0.5 0.8739908 0.5 0.8739908 0.5 0.8737674 0.5 0.875 0.5 0.8737674 0.5 0.8737674 0.5 0.875 0.5 0.8737674 0.5 0.8739908 0.5 0.875 0.5 0.8739908 0.5 0.8737674 0.5 0.875 0.5 0.625 0.75 0.867659 0.5 0.875 0.5 0.375 0.75 0.375 1 0.375 1 0.375 0.5 0.375 0.5 0.125 0.75 0.625 0.5 0.625 0.75 0.375 0.75 0.375 0.257341 0.375 0.257341 0.375 0.5 0.375 0.5 0.375 0.5 0.375 0.257341 0.375 0.5 0.375 0.25 0.375 0.257341 0.375 0.25 0.375 0.251128 0.375 0.251128 0.375 0.25 0.375 0.251128 0.375 0.2510092 0.375 0.25 0.375 0.25 0.375 0.2510092 1 0 1 1 0 1 0.5 0.75 0.5 1 0.5 1 0.375 0.75 0.375 1 0.375 1 0.5 0.25 0.5 0.5 0.5 0.5 0.375 0.25 0.375 0.5 0.375 0.5</float_array>

<technique_common>

<accessor source="#Cube_005-mesh-map-0-array" count="171" stride="2">

<param name="S" type="float"/>

<param name="T" type="float"/>

</accessor>

</technique_common>

</source>

<vertices id="Cube_005-mesh-vertices">

<input semantic="POSITION" source="#Cube_005-mesh-positions"/>

</vertices>

<triangles material="Material-material" count="43">

<input semantic="VERTEX" source="#Cube_005-mesh-vertices" offset="0"/>

<input semantic="NORMAL" source="#Cube_005-mesh-normals" offset="1"/>

<input semantic="TEXCOORD" source="#Cube_005-mesh-map-0" offset="2" set="0"/>

<p>35 0 0 24 0 1 37 0 2 8 1 3 20 1 4 0 1 5 19 0 9 37 0 10 20 0 11 3 6 30 45 6 31 46 6 32 42 9 39 44 9 40 10 9 41 5 2 42 12 2 43 6 2 44 2 6 45 12 6 46 9 6 47 1 0 48 6 0 49 2 0 50 9 1 51 46 1 52 45 1 53 15 0 54 16 0 55 14 0 56 25 6 57 26 6 58 27 6 59 27 6 60 18 6 61 23 6 62 29 10 63 33 10 64 32 10 65 32 10 66 30 10 67 28 10 68 35 0 69 22 0 70 24 0 71 8 1 72 19 1 73 20 1 74 19 0 78 35 0 79 37 0 80 3 6 87 13 6 88 45 6 89 53 10 96 54 10 97 7 10 98 5 10 99 1 10 100 43 10 101 1 10 102 47 10 103 43 10 104 43 10 105 42 10 106 5 10 107 53 10 108 7 10 109 51 10 110 7 10 111 10 10 112 50 10 113 50 10 114 51 10 115 7 10 116 48 10 117 49 10 118 10 10 119 49 10 120 50 10 121 10 10 122 44 10 123 48 10 124 10 10 125 5 11 126 42 11 127 10 11 128 5 2 129 10 2 130 12 2 131 2 6 132 6 6 133 12 6 134 1 0 135 5 0 136 6 0 137 45 1 138 47 1 139 1 1 140 1 1 141 2 1 142 45 1 143 2 1 144 9 1 145 45 1 146 7 1 147 54 1 148 52 1 149 7 12 150 52 12 151 46 12 152 9 13 153 7 13 154 46 13 155 15 0 156 17 0 157 16 0 158 25 6 159 21 6 160 26 6 161 27 6 162 26 6 163 18 6 164 29 10 165 31 10 166 33 10 167 32 10 168 33 10 169 30 10 170</p>

</triangles>

<triangles material="Material_002-material" count="14">

<input semantic="VERTEX" source="#Cube_005-mesh-vertices" offset="0"/>

<input semantic="NORMAL" source="#Cube_005-mesh-normals" offset="1"/>

<input semantic="TEXCOORD" source="#Cube_005-mesh-map-0" offset="2" set="0"/>

<p>22 2 6 4 2 7 24 2 8 4 3 12 39 3 13 36 3 14 4 4 15 11 4 16 38 4 17 39 4 18 34 4 19 36 4 20 36 5 21 41 5 22 0 5 23 36 4 24 34 4 25 40 4 26 41 4 27 8 4 28 0 4 29 34 7 33 38 7 34 11 7 35 8 8 36 40 8 37 34 8 38 22 2 75 11 2 76 4 2 77 4 4 81 38 4 82 39 4 83 36 4 84 40 4 85 41 4 86 34 4 90 39 4 91 38 4 92 8 4 93 41 4 94 40 4 95</p>

</triangles>

</mesh>

</geometry>

</library_geometries>

<library_visual_scenes>

<visual_scene id="Scene" name="Scene">

<node id="Top_Solar_Panel" name="Top Solar Panel" type="NODE">

<matrix sid="transform">-4.37114e-8 4.37114e-8 1 0.12 1 1.91069e-15 4.37114e-8 0.08 0 1 -4.37114e-8 2.75 0 0 0 1</matrix>

<instance_geometry url="#Cube_013-mesh" name="Top Solar Panel">

<bind_material>

<technique_common>

<instance_material symbol="Material-material" target="#Material-material">

<bind_vertex_input semantic="UVMap" input_semantic="TEXCOORD" input_set="0"/>

```
            </instance_material>
            <instance_material symbol="Material_001-material" target="#Material_001-material">
              <bind_vertex_input semantic="UVMap" input_semantic="TEXCOORD" input_set="0"/>
            </instance_material>
            <instance_material symbol="Material_002-material" target="#Material_002-material">
              <bind_vertex_input semantic="UVMap" input_semantic="TEXCOORD" input_set="0"/>
            </instance_material>
          </technique_common>
        </bind_material>
      </instance_geometry>
              <extra type="attach_point">
              <technique profile="AGI">
              <solar_panel group="-y Panels" efficiency="30" />
              </technique>
              </extra>
    </node>
    <node id="Bottom_Solar_Panel" name="Bottom Solar Panel" type="NODE">
      <matrix sid="transform">-4.37114e-8 4.37114e-8 1 0.121 1 1.91069e-15 4.37114e-8 0.079 0 1 -4.37114e-8 1.525 0 0 0
1</matrix>
      <instance_geometry url="#Cube_012-mesh" name="Bottom Solar Panel">
        <bind_material>
          <technique_common>
            <instance_material symbol="Material-material" target="#Material-material">
              <bind_vertex_input semantic="UVMap" input_semantic="TEXCOORD" input_set="0"/>
            </instance_material>
            <instance_material symbol="Material_001-material" target="#Material_001-material">
              <bind_vertex_input semantic="UVMap" input_semantic="TEXCOORD" input_set="0"/>
```

```xml
          </instance_material>
          <instance_material symbol="Material_002-material" target="#Material_002-material">
            <bind_vertex_input semantic="UVMap" input_semantic="TEXCOORD" input_set="0"/>
          </instance_material>
        </technique_common>
      </bind_material>
    </instance_geometry>
            <extra type="attach_point">
            <technique profile="AGI">
            <solar_panel group="+y Panels" efficiency="30" />
            </technique>
            </extra>
  </node>
  <node id="Cubesat_Body" name="Cubesat Body" type="NODE">
    <matrix sid="transform">-4.37114e-8 4.37114e-8 1 0.1204499 1 1.91069e-15 4.37114e-8 0.2635089 0 1 -4.37114e-8 2.151649 0 0 0 1</matrix>
    <instance_geometry url="#Cube_005-mesh" name="Cubesat Body">
      <bind_material>
        <technique_common>
          <instance_material symbol="Material-material" target="#Material-material">
            <bind_vertex_input semantic="UVMap" input_semantic="TEXCOORD" input_set="0"/>
          </instance_material>
          <instance_material symbol="Material_001-material" target="#Material_001-material">
            <bind_vertex_input semantic="UVMap" input_semantic="TEXCOORD" input_set="0"/>
          </instance_material>
          <instance_material symbol="Material_002-material" target="#Material_002-material">
            <bind_vertex_input semantic="UVMap" input_semantic="TEXCOORD" input_set="0"/>
```

```
          </instance_material>
        </technique_common>
      </bind_material>
    </instance_geometry>
  </node>
  </visual_scene>
 </library_visual_scenes>
 <scene>
  <instance_visual_scene url="#Scene"/>
 </scene>
</COLLADA>
```